Master's Thesis

Master in Biomedicine

May 2021

EXPLORING CHANGES IN LONG NON-CODING RNAS DURING NEONATAL HYPOXIA-ISCHEMIA USING A PIGLET MODEL

Name: Benedicte Grebstad Tune
Course code: MABIO5900
Candidate number: 505

60 ECTS

Faculty of Health Sciences
OSLO METROPOLITAN UNIVERSITY
STORBYUNIVERSITETET

EXPLORING CHANGES IN LONG NON-CODING RNAS DURING NEONATAL HYPOXIA-ISCHEMIA USING A PIGLET MODEL

By

Benedicte Grebstad Tune

A thesis submitted for the degree of

Master in Biomedicine, 60 ECTS

Oslo Metropolitan University (OsloMet)

Faculty of Health Sciences

Department of Life Science and Health

Conducted at the Department of Pediatric Research,

Oslo University Hospital, Rikshospitalet, Oslo

Supervisor: Dr. Lars Oliver Baumbusch, MSc, PhD

May 2021

OSLOMET

OSLO METROPOLITAN UNIVERSITY
STORBYUNIVERSITETET

Oslo University Hospital

Acknowledgments

The work presented in this thesis was conducted at the Department of Pediatric Research (PFI) at Oslo University Hospital, Rikshospitalet, from August 2020 until May 2021. This project is the culmination of my master´s degree in Biomedicine at Oslo Metropolitan University, and was supervised by Lars O. Baumbusch.

First and foremost I would like to express my sincerest gratitude to my supervisor Lars O. Baumbusch for believing in me and giving me this opportunity. You have introduced me to a research field I have developed great interest in. I have really appreciated your guidance and enthusiasm during this entire process. Your feedback and knowledge has been invaluable, and I have truly enjoyed our scientific discussions. I could not have asked for a better supervisor!

I would also like to thank Rønnaug Solberg for inviting me to participate in one of her piglet studies and for providing me a broad insight to the piglet model. I am also grateful for your support and feedback during the writing process, and for always being available and answering my never-ending questions regarding hypoxia-ischemia. I have deeply appreciated our conversations and your shared knowledge.

I am also very grateful for all the help and support from Weronika when investigating and performing new techniques and methods. I would like to thank Monica and Sofie for introducing me to the lab, and for always being available and answering my many questions. The advice and constructive feedback from Monica during this project has been extremely helpful. And Thomas Brüning from the Department of Pathology, for taking the time to teach me how to perform cryostat sectioning. I would also like to acknowledge the rest of the department and thank them for making me feel welcome at your lab.

Finally, I wish to thank my better half, family, and friends for their unconditional support, patience and encouragement throughout this process.

Abstract

Background: Despite major advances in research and clinical care during the last decade, hypoxic-ischemic encephalopathy (HIE) remains one of the leading causes worldwide of death and disability in children under five years of age. The disorder is caused by oxygen deprivation (hypoxia) and decreased blood flow (ischemia) (HI) to the brain during the birth process. However, not only oxygen deficiency, but also excess oxygen supply (hyperoxia) during the reoxygenation period can increase oxidative stress and contribute to increased morbidity or various life-long disabilities. Consequently, early and reliable biomarkers to detect the severity and predict the overall outcome of neonatal HI are highly demanded. Long non-coding RNAs (lncRNAs) are non-protein-coding RNA transcripts with key regulatory properties. Changes in their expression indicate a variety of diseases, conditions, and biological processes, including cancer, oxidative stress, and hypoxia. ***Aim of study:*** This thesis intended to explore specific lncRNAs as potential markers for the severity of neonatal hypoxia-ischemia using a neonatal piglet model. ***Material and methods:*** A total of 42 newborn piglets were randomized into four study arms: 1. hypoxia-normoxic reoxygenation, 2. hypoxia-3 minutes of hyperoxic reoxygenation, 3. hypoxia-30 minutes of hyperoxic reoxygenation, and 4. sham-operated control. The identified lncRNAs BDNF-AS, H19, MALAT1, ANRIL, TUG1, PANDA, and related target genes were investigated by qPCR to determine the RNA expression alterations in the cortex, hippocampus, white matter, and cerebellum after exposure to severe hypoxia versus control. BDNF-AS, H19, MALAT1, and ANRIL were chosen for å more detailed analysis to estimate the time-dependent effect of hyperoxic exposure versus normoxic reoxygenation in the cortex. The results of BDNF-AS and H19 were validated by a second, independent method (Droplet Digital PCR, ddPCR). ***Results:*** A significant increase of BDNF-AS, H19, MALAT1, and ANRIL was observed in various brain regions of piglets exposed to severe hypoxia compared to the control. A so far unknown, striking enhancement in BDNF-AS expression levels in piglets exposed to short or long periods of hyperoxic reoxygenation emerged from this study, indicating an increased level of hyperoxic and oxidative stress when resuscitated with supplementary oxygen. ***Conclusion:*** The lncRNAs BDNF-AS, H19, MALAT1, ANRIL, TUG1, and PANDA were differentially expressed in a newborn piglet model of hypoxia-ischemia. Specific changes in the expression of BDNF-AS could be related to both deficiency and excess of oxygen, suggesting further studies to verify the potential use of this lncRNA as a biomarker for oxidative stress damage and the severity of perinatal hypoxia-ischemia in the future.

Sammendrag

Bakgrunn: Til tross for store fremskritt innen forskning og klinisk behandling det siste tiåret, er hypoksisk-iskemisk encefalopati (HIE) fortsatt en av de verdensledende årsakene til død og nedsatt funksjonsevne i barn under fem år. Lidelsen er forårsaket av oksygenmangel (hypoksi) og nedsatt blodtilførsel til hjernen (iskemi) (HI) under fødsel. Imidlertid kan ikke bare oksygenmangel, men også overflødig oksygentilførsel (hyperoksi) ved reoksygenering øke oksidativt stress og bidra til økt morbiditet eller ulike livslange funksjonsnedsettelser. Derfor er det et sterkt behov for tidlige og pålitelige biomarkører som kan si noe om alvorligheten og forutsi utfallet av neonatal hypoksisk-iskemi. Lange ikke-kodende RNA (lncRNA) er ikke-protein-kodende RNA transkripter med nøkkelregulerende egenskaper. Endringer i deres uttrykk indikerer en rekke sykdommer, tilstander og biologiske prosesser, inkludert kreft, oksidativt stress og hypoksi. **Problemstilling:** Formålet med denne oppgaven var å utforske spesifikke lncRNA som potensielle markører for å si noe om alvorlighetsgraden som følge av neonatal hypoksisk-iskemi ved bruk av en nyfødt grisemodell. ***Materialer og metoder:*** Totalt 42 nyfødte griser ble randomisert i fire studiearmer: 1. Hypoksi-normoksisk reoksygenering, 2. hypoksi-3 minutter med hyperoksisk reoksygenering, 3. hyperoksi-30 minutter med hyperoksisk reoksygenering, og 4. kontrollgruppe. De identifiserte lncRNAene BDNF-AS, H19, MALAT1, ANRIL, TUG1, PANDA og relaterte målgener ble undersøkt vha qPCR for å bestemme endringer i RNA ekspresjon i cortex, hippocampus, hvit substans og cerebellum etter eksponering av alvorlig hypoksi versus kontroll. Videre ble BDNF-AS, H19, MALAT1 og ANRIL valgt for en mer detaljert analyse for å estimere den tidsavhengige effekten av hyperoksisk reoksygenering versus normoksisk reoksygenering i cortex. Resultatene fra BDNF-AS og H19 ble validert vha en uavhengig metode (Dråpe digital PCR, ddPCR). ***Resultater:*** En signifikant økning av BDNF-AS, H19, MALAT1 og ANRIL ble observert i forskjellige hjerneregioner hos nyfødte griser etter eksponering av alvorlig hypoksi sammenliknet med kontrollen. En hittil ukjent, men slående økning av BDNF-AS ekspresjon i nyfødte griser utsatt for korte eller lange perioder med hyperoksisk reoksygenering kom frem i denne studien, hvilket indikerer et økt nivå av hyperoksisk- og oksidativt stress når supplerende oksygen blir benyttet ved gjenopplivning. Konklusjon: lncRNAene BDNF-AS, H19, MALAT1, ANRIL, TUG1 og PANDA var ulike uttrykt i den neonatale hypoksisk-iskemiske grisemodellen. Spesifikke endringer i uttrykket av BDNF-AS kan være relatert til både mangel på og overskudd av oksygen. Derfor bør ytterligere studier verifisere den potensielle bruken av denne lncRNAen som en biomarkør for oksidativ stresskade og alvorlighetsgraden av perinatal hypoksisk-iskemi i fremtiden.

Abbreviations

General Abbreviations	
ABS	Absolute quantification
ALS	Amyotrophic lateral sclerosis
ANOVA	Analysis of variance
AS	Alzheimer´s disease
asRNA	antisense RNA
BE	Base excess
Cb	Cerebellum
cDNA	Complementary DNA
CNS	Central nervous system
CNV	Copy number variation
Cx	Cortex
ddPCR	Droplet digital PCR
DNA	Deoxyribonucleic acid
FELASA	Federation of European Laboratory Animals Science Association
FOTS	Norwegian Food Safety Authority
FP	Forward primer
GEX	Gene expression
H/R	Hypoxia-reoxygenation
HAL	Hypoxia-associated lncRNA
Hc	Hippocampus
HGP	Human Genome Project
HI	Hypoxia-ischemia
HIBD	Hypoxia/ischemia-induced brain damage
HIE	Hypoxia-ischemia encephalopathy
HIF	Hypoxia inducible factor
HRE	Hypoxia-response elements
HUVEC	Human umbilical vein endothelial cells
I/R	Ischemia-reperfusion
IGF2	Insulin-like growth factor 2
ILCOR	International Liaison Committee on Resuscitation
IQ	Interquartile range
lncRNA	Long non-coding RNA
MABP	Mean arterial blood pressure
miRNA	micro RNA
mmHg	Millimetre of mercury (blood pressure)
mRNA	messenger RNA
MS	Multiple Sclerosis
NARA	The National Animal Research Authority
ncRNA	non-coding RNA

NE	Normalized expression
NF-YA	Nuclear Transcription Factor Y subunit α
NFW	Nuclease free water
ng	Nanogram
nM	Nano molar
NRNA	Negative RNA control
NRT	Negative reverse transcription control
nt	Nucleotide
NTC	Negative template control
OS	Oxidative stress
PCR	Polymerase chain reaction
PD	Parkinson's disease
PFC	Prefrontal cortex
PNS	Peripheral nervous system
PRC	Polycomb repressive complex
PRC1	Polycomb repressive complexes 1
PRC2	Polycomb repressive complexes 2
qPCR	Quantitative PCR
RBP	RNA-binding proteins
RED	Rare event detection
RIN^{e}	RNA integrity number
RNA	Ribonucleic acid
RNase	Ribonuclease
ROS	Reactive oxygen species
RP	Reverse primer
RQ	Relative quantity
RT	Room temperature
SD	Standard deviation
TH	Therapeutic hypothermia
WHO	World Health Organization
Wm	White Matter

Housekeeping genes, target genes and lncRNA	
ANRIL	Antisense Non-coding RNA in the INK4 Locus
BACE1-AS	Beta-secretase 1-antisense
BC200	Brain cytoplasmic 200
BDNF	Brain-derived neurotrophic factor
BDNF-AS	BDNF-antisense
H19	H19 Imprinted Maternally Expressed Transcript
HIF1α	Hypoxia-inducible factor subunit 1α
HIF1β	Hypoxia-inducible factor 1 subunit β
HOTAIR	HOX antisense intergenic RNA
LincRNA-p21	Long intergenic non-coding RNA-p21
MALAT1	Metastasis Associated Lung Adenocarcinoma Transcript 1
p53	Tumor suppressor gene 53
PANDA	p21-associated ncRNA DNA damage-activated
RPLP0	Ribosomal protein, large, P0
TBP	TATA-Box binding protein
TNFα	Tumor necrosis factor α
TUG1	Taurine Upregulated gene 1
VEGF	Vascular endothelial growth factor
VEGFA	Vascular endothelial growth factor A

Content

1. Introduction

Hypoxic-ischemic encephalopathy (HIE) is worldwide one of the leading causes of death and lifelong impairment in children under five years of age, according to the World Health Organization (WHO) (1). However, despite this dramatic status, only a few preventive measures and therapeutic approaches are available today. Reliable and early biomarkers are highly demanded to detect the severity and predict the outcome of neonatal hypoxia-ischemia (HI). The Department of Pediatric Research at Oslo University Hospital (OUS) has over the last 30 years studied the effects of hypoxia and reoxygenation, oxidative stress, and subsequent damages in neonates, and their research has made a strong contribution to this field (2, 3). This thesis is a continuation and extension to these approaches investigating the lncRNAs as potential markers for oxidative stress and the severity of hypoxic-ischemic encephalopathy using one of the established model systems.

1.1 Hypoxic-Ischemic Encephalopathy

Hypoxia is a term for depleted of adequate oxygen (O_2) in organs and tissues of an organism, resulting in insufficient O_2 supply to sustain cellular function due to a supply-demand imbalance (4). Hypoxia can lead to ischemia, characterized by decreased blood supply to organs, and especially the brain. Hypoxic-ischemic encephalopathy (HIE), describes a brain damage caused by decreased delivery of oxygen and decreased blood flow to the brain (Figure 1-1). HIE is estimated to affect about 1 to 8 per 1000 live births in developed countries (5). The surviving newborns may obtain lifelong complications and disabilities, such as cerebral palsy, epilepsy, and motor and learning impairments (6). Additionally, an increased risk of clinical manifestations in adulthood such as social and cognitive deficits, behavior problems and depression, may occur (7).

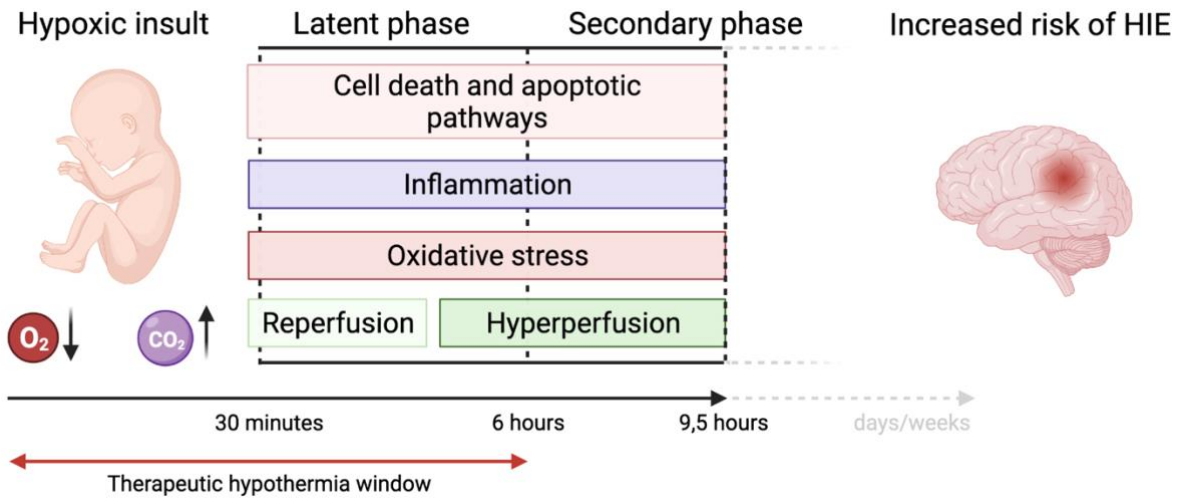

Figure 1-1. Simplified schematic overview of the latent and secondary phase following hypoxia-ischemia (HI) up to 9,5 hours after HI-insult, reflecting the time of the neonatal HI piglet model used in the study. HIE, hypoxic-ischemic encephalopathy. Modified from Kleuskens et al. (2021) (8) Made with BioRender.com.

1.1.1 Reactive oxygen species and oxidative stress accumulation

HI initiates a number of biochemical processes, with oxidative stress being one of the most common causes, that can damage organs of the neonate (9, 10). Oxidative stress is a result of excess reactive oxygen species (ROS) generated and accumulated in tissues and cells outnumbering to antioxidant defense systems. Multiple processes are dependent on low-level ROS; however, increased production can lead to harmful effects on DNA, RNA, and proteins, causing induction of several diseases (11). These conditions includes both chronic and degenerative diseases, accelerating aging processes of the body, and causing acute pathologies. Oxidative stress has also been linked to neurological disorders such as Parkinson's disease, Alzheimer's disease, amyotrophic lateral sclerosis (ALS), multiple sclerosis (MS), depression and, memory loss (12).

The antioxidant defense protecting the organism against oxidative stress is immature in term newborns and especially in preterm newborns (13). Also, brain tissue has been reported to be particularly sensitive to oxidative stress, compared to other tissues such as the liver (14). Hence, the risk of HI-induced oxidative stress in newborns is higher than in adults and can lead to more serious short and long-term consequences.

1.1.2 The effect of hyperoxic injury to the newborn

Oxygen is an essential but dangerous molecule and the right balance of oxygen supply is crucial, not only for infants. Both, too little and too much oxygen may harm cellular structures, cells, organs, and an entire organism. Newborns are to some extent protected against hypoxia, due to the hypoxic environment during development and growth (15). However, this is different during hyperoxia, illustrating a state of excess supply of oxygen to organs and tissues. Like for hypoxia, hyperoxia may cause accumulation of ROS and oxidative stress. The use of 100% O_2 for resuscitation of critical newborns was common practice for many years, despite the lack of evidence to support its use and that a harmful effect of 100% O_2 for newborn resuscitation had been hypothesized. For decades, several animal models have been involved to demonstrate its damaging effect, and an increase in neonatal mortality has been reported when resuscitating newborns with supplementary oxygen (3, 16-21). It was not until 2010 that decade's worth of research made a breakthrough, and International Liaison Committee on Resuscitation (ILCOR) changed its recommendations. Since then an initial 21% O_2 has been recommended to term infants who need assisted ventilation. However, if chest compressions are necessary, resuscitation with 100% O_2 is still recommended (22, 23). Despite extensive research on this matter, there are still many unanswered questions regarding the best practice concerning percentage and duration of oxygen supply during neonatal resuscitation (24).

1.1.3 Treatment of hypoxic-ischemic encephalopathy

Therapeutic hypothermia (TH), a mild hypothermia reducing the brain temperature by around 2-5°C, is so far the only current standard treatment for moderate HI and has greatly improved the prognosis. However, the treatment has several drawbacks. It is not only expensive and requires a multidisciplinary team, but should be initiated within 6 h post-insult and is only effective in moderate cases of HI (25-27). This emphasizes the need for new therapeutic approaches.

1.2 Regulation of gene expression in response to hypoxia

Through evolution, cells have developed strategies to endure low oxygen environments. One of these approaches is the hypoxic response, aiming to maintain homeostasis through regulation of cellular activities (28). The hypoxic condition activates several transcription factors. Among these are Hypoxia-inducible factor 1 (HIF1), Vascular Endothelial Growth

Factors (VEGFs), Brain-derived neurotrophic factor (BDNF), tumor suppressor gene p53, and others.

Hypoxia-inducible factor 1 (HIF1) is one of the key transcription factors controlling the cellular response to hypoxia. It is a heterodimeric factor consisting of the continually expressed β subunit (HIF1β) and the oxygen-sensitive α subunit (HIF1α) (29). HIF1-α is stable in normoxic conditions where it is continuously synthesized and degraded. However, under hypoxic conditions, HIF1α is stabilized and its degradation is inhibited, resulting in translocation of HIF1α to the nucleus, followed by dimerization with HIF1β and binding to hypoxia-responsive elements in the promoters of hypoxia-regulated genes. This initiation step activates the expression of HIFs downstream targets (30). Moreover, while HIF1α protein expression is elevated in response to hypoxia, the HIF1α mRNA level is constitutively expressed in many cell types, whereas in some others its gene expression is up-regulated (31, 32). HIF1α is also required in embryonic and fetal development (15).

Vascular Endothelial Growth Factors (VEGFs) are major transcriptional targets for HIF1. They are primarily responsible for angiogenesis and may also promote cell proliferation. VEGFA, a founding member of the VEGFs, has been demonstrated to play an important role in various biological processes and is activated under hypoxic stress by HIF1α-binding to a hypoxia response element (HRE) in the 5´-region (33). Studies have shown an increased expression of VEGFA in various cancers (34). The up-regulation of VEGF mRNA in response to hypoxia has been demonstrated in various animal studies (35, 36). Aly et al. discovered in their work that VEGF protein levels in neonatal cord blood increased after perinatal hypoxia-ischemia and that a further increase was associated with the development of HIE later on (37).

Brain-derived neurotrophic factor (BDNF) is a highly conserved member of the neurotrophic family (38) and it is the most abundant neurotrophin in the brain. High levels of expression have been observed in the hippocampus, cerebellum, and cerebral cortex of humans and rodents, with hippocampal neurons exhibiting the highest level in rodents (39, 40). The molecule is essential for the growth, production, differentiation, maintenance, and regeneration of different types of neurons in the central nervous system (CNS) (38, 41). BDNF is also involved in the antioxidant response, protecting against ROS (42). Many external and

internal causes, such as ischemia, hypoxia, brain damage, influence its expression (43). The neurotrophic superfamily plays a critical role in neural repair following injury (44). In animal models, *in-vitro* and *in-vivo* studies have shown that BDNF activates the protective mechanisms against myocardial ischemia through survival-signaling pathways (among these the VEGFA) to mediate angiogenesis (45, 46). BDNF-related signaling pathways have also been reported to induce major cellular regeneration in the CNS and peripheral nervous system (PNS) against hypoxia followed by reoxygenation (H/R) (47, 48). Previous research has also shown that neurotrophic factors, such as BDNF, may prevent the death of damaged adult neurons in the hippocampal formation, cortex, and basal forebrain (49, 50). Taken together, these findings indicate that BDNF plays an essential role in the developing and adult nervous systems, and only strict regulated to preserves normal activity (51). Several animal studies have also reported a protective role for BDNF in the neonatal brain after hypoxic-ischemic injury (52-54).

Hypoxia also activates the **tumor suppressor gene p53**. Due to its intricate and precise regulatory control over cellular functions, p53 is known as the "guardian of the genome" (55, 56). The protein levels of p53 are low in absence of stress but increased when a cell is subjected to stress signals, such as DNA damage and nutritional deprivation, causing p53 to bind to p53-binding elements in target genes triggering their expression. Via its target genes, p53 controls a variety of cellular responses, such as cell cycle arrest, senescence, apoptosis, autophagy, DNA repair, metabolism, invasion, and migration of cells, and oxidative stress modulation (57-61). Additionally, the tumor suppressor is involved in processes that include reproduction, growth, ischemia, tissue injuries, and neurodegeneration (57-63). Hypoxia-induced stress may also activate p53, and hypoxia and HIF-pathways are closely linked to p53; however, reports are contradictory and changes in p53 expression remains somehow unclear suggesting a cell type- and context dependent expression. One study demonstrated that while p53 protein levels accumulated, p53 mRNA and mRNA and protein levels of its endogenous downstream effectors' genes were not affected by hypoxic stress (64). Others reported that hypoxia and HIF signaling had a both negative and positive effects on p53 levels and activities (65).

The tumor necrosis factor α (TNFα) is a part of the TNF superfamily, regulating several pathways involved in cell proliferation, differentiation, survival and death. Being one of the most important proinflammatory cytokines, it plays an essential part in the human physiology and pathology making it a promising therapeutic target (66). TNFα is activated by HI-induced injury along with other proinflammatory cytokines, causing aggravated injury by inducing neuronal cell apoptosis, increase toxic nitric oxide levels and inhibiting neurogenesis (67). Several studies have reported increased TNFα mRNA and protein levels following hypoxia and ischemia (68-71), and inflammation has been stated as one of the main causes of hypoxic-ischemic injury (72, 73).

1.3 Non-coding RNA

In the 1970s, it was believed that the human genome contained about 35 000-100 000 protein-coding genes in the 1970s. When the Human Genome Project (HGP) was finalized, researchers were surprised by the discovery that the human genome only consisted of around 21 000 protein-coding genes, which is only about 1,5% of the entire genome (74). Consequently, the remaining part of the human sequence consisting of non-coding elements, was determined as "junk-DNA" and supposed to enclose no biological function (75). The development of second-generation sequencing technology has led to the discovery of numerous RNA transcripts with similar regulatory properties like protein-encoding mRNAs. They are; however, not translated into proteins (76). Non-coding transcripts are divided into regulatory and housekeeping ncRNAs. The latter include ribosomes, metastasis, small nuclei, and small nucleolar RNA, whereas regulatory ncRNAs are further divided into two classes based on their nucleotide length. LncRNAs are transcripts > 200 nt long without protein-coding potential. They are transcribed from the intergenic and intronic regions of the genome primarily by RNA polymerase II, 5'methyl-capped, and polyadenylated in the same manner like mRNAs (77). Despite not being protein-coding, studies have shown that lncRNAs can modulate gene expression transcriptional, posttranscriptional, translational, and posttranslational levels via interaction with DNA, RNA, RNA-binding proteins (RBPs), and chromatin modifiers (78). There are currently 17 957 human lncRNAs and 48 684 human lncRNA transcripts annotated in the GENCODE project (79).

1.3.1 Role of lncRNAs in response to hypoxia

LncRNAs have been implicated in a range of developmental processes and diseases and have been shown to regulate gene expression for several biological processes and conditions, including apoptosis, inflammatory response, and angiogenesis (80). They also play key roles in response to hypoxia and oxidative stress, and several hypoxia-associated lncRNAs (HALs) have been identified (81). The lncRNAs are regulated by hypoxia-inducible factors (HIFs) under hypoxic conditions via hypoxia response elements (HREs) in their promoters (82). LncRNAs regulate many cell functions influencing the response to oxidative stress, in a negative or positive direction (80, 83). Several lncRNAs are expressed in the developing and adult CNS, and studies have revealed a key role in brain damage, altering expression and influencing the pathological outcome (84-86). LncRNAs are expressed in various types of tissues, although, in a tissue-specific manner (87, 88). Taking together, the disease-, developmental-, tissue-, and time-specific expression predisposes lncRNAs as potential biomarkers for a range of conditions and illnesses, including HI.

1.3.2 Long non-coding RNAs associated with hypoxia and oxidative stress

Despite recent research efforts about lncRNA in association with hypoxia oxidative stress, a systematic investigation about lncRNA during neonatal HI is still missing. In particular, it is difficult to choose the cardinal candidates among the various lncRNA suggested to play a major role in oxidative stress, many discovered in relation to cancer (76, 80, 83, 89, 90). Following extensive literature and bioinformatic research, a number of the best well-known and some of special interest have been selected for further and detailed investigations for this thesis (Table 1-1).

Table 1-1. Summary of selected lncRNAs associated with hypoxia and/or oxidative stress.

LncRNA	Associated mRNAs	Association with pathology	References
BDNF-AS	BDNF	Hypoxic and oxidative stress	(86)
H19	HIF1α	Oxidative stress, imprinting	(91, 92)
MALAT1	HIF1α	Hypoxic and oxidative stress, angiogenesis, DNA damage	(93-95)
ANRIL	HIF1α	Oxidative stress, cellular senescence, angiogenesis, apoptosis, inflammation	(81, 96)
TUG1	p53, HIF1α	Neurodegenerative diseases, apoptosis, immune response	(97)
PANDA	p53	DNA damage, cellular senescence	(98)

Abbreviations: BDNF, Brain-derived neurotrophic factor; HIF1α, Hypoxia-inducible factor α; p53, Tumor suppressor gene p53; BDNF-AS, Brain-derived neurotrophic factor antisense; H19, H19 Imprinted Maternally Expressed Transcript; MALAT1, metastasis-associated lung adenocarcinoma transcript 1; ANRIL, Antisense Noncoding RNA in the INK4 Locus; TUG1, Taurine Upregulated gene 1; PANDA, p21-associated ncRNA DNA damage-activated.

Brain-derived neurotrophic factor antisense (BDNF-AS) is the antisense RNA (asRNA) (non-coding strand complementary to the coding sequence) of BDNF (99), both located at chromosome 11 (Figure 1-2). These asRNAs can bind to the coding strand of mRNAs, and either targets them for destruction or prevent them from being expressed (100). BDNF-AS is expressed in several adult human tissues, as demonstrated by Pruunsild et al. (2007), with elevated levels in the brain, kidney, spinal cord, and testis. The same study revealed that BDNF and BDNF-AS transcripts form double-strand RNA duplexes in vivo, suggesting that BDNF-AS transcripts could have an important role in the regulation of BDNF expression in humans (101). Furthermore, a recent study identified a possible role of BDNF-AS in the pathogenesis of HI-induced neonatal brain injury and its underlying molecular mechanism. The work promoted that BDNF-AS may be a viable target for the treatment of hypoxia/ischemia-induced brain damage (HIBD) due to BDNF-AS knockdown improving brain function by reducing the infarct size and improving the neurological function (86).

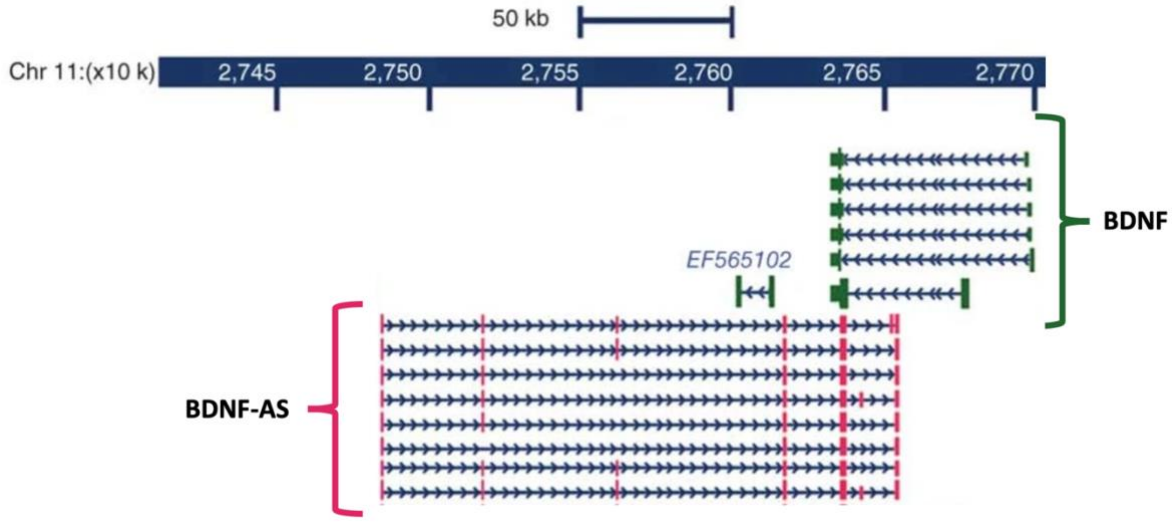

Figure 1-2. The genomic location of BDNF and its antisense RNA BDNF-AS transcripts on chromosome 11 (102). Modified from Modarresi et al. (2012) (103).

The **H19** transcripts originate from the H19/IGF2 genomic imprinted cluster on chromosome 11p15.5. H19 is paternally imprinted, and transcribed from the maternally inherited chromosome, while IGF2 is transcribed from the paternally inherited chromosome, implying that H19 is involved in embryonic growth and development (91). The lncRNA has been confirmed as being critical in tumor development (104) and given contradictory roles in cancer (105), representing both an oncogene and tumor suppressor features at the same time. H19 is also a HAL, and upon hypoxia, the lncRNA is directly or indirectly regulated by HIF1 causing its up-regulation (104, 106, 107). One of the most damaging factors in ischemic stroke has been reported as ROS, causing oxidative stress. Circulating H19 was significantly higher in patients with ischemic stroke, as well as ischemic rats and cells. Studies have shown that H19 knock-down reduced infarct volume and brain edema in brain tissue and plasma 24 hours post-stroke and decreased brain tissue loss and neurological deficits 14 days post-stroke (108). A recent study verified that H19 presented pro-apoptotic and proliferative effects in kidney cells during H/R treatment (109). H19 was elevated after HI, and H19 inhibition attenuated HI induced neuronal apoptosis *in-vivo* and *in-vitro* (110).

Metastasis Associated Lung Adenocarcinoma Transcript 1 (MALAT1) is a highly abundant and conserved lncRNA. The widely studied transcript is involved in several cancer types, as well as pathological and biological processes (93). Surprisingly, MALAT1 knock-out mice did not reveal

any phenotypical or histological irregularities (111). Others have suggested this is due to MALAT1 only be activated under certain conditions related to stress and not under normal physiological conditions (112), or that other lncRNAs are compensating for its loss of functions (113). Moreover, in cancer cells, MALAT1 has been found to regulate pathways involved in stress responses, including hypoxia and DNA damage (114), and elevated MALAT1 expression has been linked to poor overall survival in several cancers (113). However, the roles of MALAT1 extend far and wide and do not limit themselves to cancer. MALAT1 expression has been shown to increase in hippocampal neurons due to hypoxia-induced brain damage (94) and to modify pathology in rats following traumatic brain injury (115). Additionally, MALAT1 has been reported to regulate pathology following ischemia (116), increase in response to hypoxic and oxidative stress (94), and regulate angiogenesis via the hypoxia-induced VEGF (95). Therefore, a role in hypoxic-ischemic encephalopathy has been suggested (117). Also, MALAT1 is involved in neuronal diseases like Parkinson's disease (PD), Alzheimer´s disease (AD), and MS (112, 118).

The antisense non-coding RNA in the INK4 locus (ANRIL) is a hypoxia-associated lncRNA activated by HIF1a in (96). The lncRNA mediates gene silencing of the INKfb-ARF-INK4 locus and regulates gene expression by binding to polycomb repressive complexes 1 (PRC1) and 2 (PRC2), which is functioning as transcriptional repressors of gene expression (119). Silencing of ANRIL has led to inhibition of viability, migration, and invasion of gastric cancer cells (120). Altered expression or mutations in ANRIL has been linked to several pathological processes such as hypoxia, oxidative stress, angiogenesis, inflammation, and apoptosis (81). Increased expression of ANRIL in ischemic stroke injured rats resulted in VEGF activation, promoting angiogenesis and inflammatory processes. ANRIL was also increased in plasma obtained from patients who suffering an ischemic stroke, cerebral ischemic animals, and oxygen-glucose-deprived cells (121). A recent study suggested that circulating ANRIL is inversely correlated with the severity of ischemic stroke (122).

Taurine Upregulated gene 1 (TUG1) was first discovered being a taurine-regulated transcript in mouse retinal cells, participating in retinal development and photoreceptor formation. The lncRNA is one of the most conserved lncRNAs between humans and mice (123). However, the TUG1 has not yet been reported in pigs. Studies from the past decade have identified and

suggested several and broad roles for TUG1. The lncRNA is a direct transcriptional target for p53 and has been shown to regulate HIF1α (124), and has been shown to have crucial regulatory roles in biological processes associated with several types of cancer (125). A meta-analysis on TUG1 in cancer reported an inverse relationship between these two, further a correlation of increased TUG1 expression with more advanced clinicopathological characteristics and poor prognosis (126). TUG1 has also been listed as potential therapeutic target for cerebral ischemia/reperfusion injury (127). Furthermore, recent studies have demonstrated that TUG1 can regulate gene expression through several mechanisms, including acting as a miRNA sponge and interacting with transcription-silencing PRC1 and PRC2 (128, 129). Overexpression of TUG1 has been reported to exert protective effects through modulation of apoptosis, immune responses, and oxidative stress (97). A study demonstrated that TUG1 was attenuated in both ischemia-reperfusion (I/R)-injured mice and H/R human kidney cells (130).

The **P21 Associated ncRNA DNA damage Activated (PANDA)** lncRNA is located and transcribed from the p21 locus, upstream from the p21 transcriptional start site and p53 response element. The lncRNA is involved in the DNA damage response in a p53-manner, and upon its activation it regulates apoptosis by inhibiting the function of the transcription factor Nuclear Transcription Factor Y subunit α (NF-YA) (98). PANDA has been reported as up-regulated in cancer (131, 132), but whether the lncRNA plays a role in hypoxia-ischemia is yet to be determined.

1.4 The piglet model of Neonatal Hypoxia-Ischemia

1.4.1 Choice of animal model

To understand the mechanisms, processes, and outcome of a disease, it is of great advantage to use an animal model that is very similar to the humans. The genomes of humans and pigs are strikingly similar, and several genes are conserved across the two organisms (133). The neonatal brain development of newborn piglets has large likeness with newborn babies' brain development, making newborn piglets an ideal model for neonatal hypoxia-ischemia research. The size, respiratory system, and peak brain spurt (134) of a newborn piglet are highly equal to those of a human newborn at the time of birth. Human infants and newborn

piglets also have, among other close relationships, comparable gene order and DNA methylation patterns (133, 135-137). Character and distribution of gray matter, white matter, and brain gyri, a ridge on the cerebral cortex, is comparable equal in both organisms (138, 139). Furthermore, the monitoring, instrumentation, and outcome assessment are similar to those used in neonatal clinical care. Hence, the adaption of this model into neonatal care is of a high degree (140).

1.4.2 Brain regions analyzed

In this thesis, samples from the prefrontal cortex, hippocampus, white matter, and the cerebellum from the piglet brain were studied (Figure 1-3).

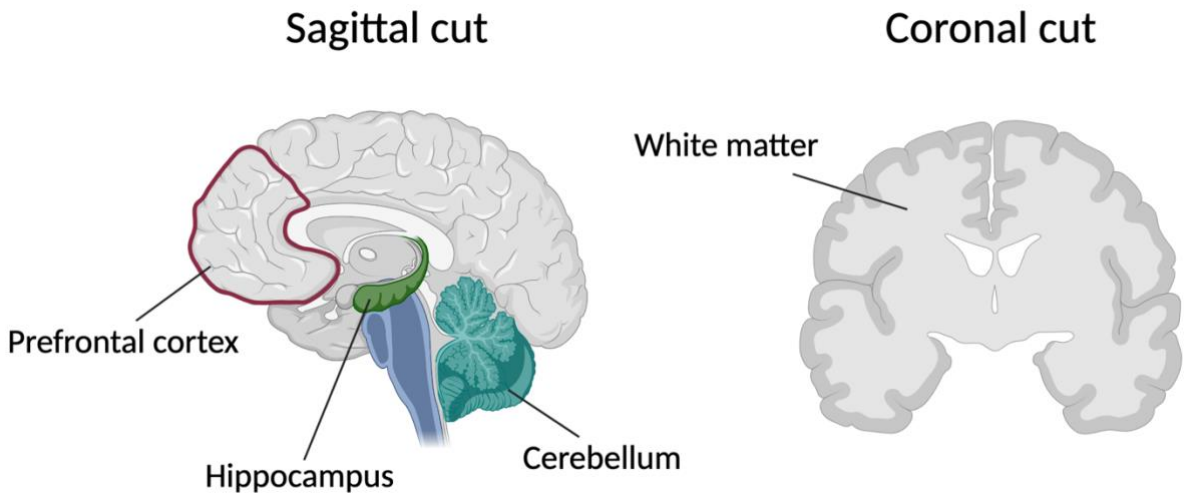

Figure 1-3. A simplified view of the brain regions used in the study, displaying the sagittal cut of the prefrontal cortex, hippocampus, and cerebellum, and the coronal cut of white matter. Created with BioRender.com

The **prefrontal cortex (PFC)** is the largest area of the human brain, accounting for about 29% of the entire cerebral cortex (141). Despite several studies on this area of the brain, its exact function remains enigmatic (142). However, it is a critical component of the human species´ increasingly complex, and evolved behavior, mediating intellectual or executive functions. PFC mediated complex processes including attention, planning, decision-making, emotion, and personality. It is also thought to be responsible for our intelligence, reasoning, and rationality (143). The prefrontal cortex is a key component of a large-scale neurocognitive network in which complex behaviors are organized (143). Further in this thesis, the prefrontal cortex will be mentioned as the cortex.

The **hippocampus** is one of the most extensively studied parts of the brain and a part of the larger structure known as the hippocampal formation. This structure is essential for the generation and regulation of several brain functions, such as memory and learning, and is highly vulnerable to neurological disorders (144). It is also vulnerable and is particularly susceptible to hypoxia-ischemia. Initially, damage to the hippocampus in neonates may have no apparent cognitive or behavioral consequences. However, difficulties with memory might develop later in life. A study conducted by Cooper et al. (2015) found that neonates treated for acute respiratory failure have severe hippocampal atrophy due to the associated hypoxia, and as a result, they show deficient memory later in life (145).

White matter is any nervous tissue that is largely made up of nerve fibers (axons), connecting neurons in different brain regions into functional circuits. It is found in all mammals and is, along with gray matter, spread throughout the human CNS. Many axons are insulated with myelin, a fatty substance giving the structure a relatively light appearance and thereby its name (146). Damage to the myelin can result in impaired sensory, motor, and cognitive functions (147). Major ROS development in the prenatal brain can lead to white matter injury and was demonstrated in prenatal rodents exposed to chronic hypoxia accompanied by room air. Further, when exposed to postnatal hyperoxia, white matter injury was intensified (148).

Cerebellum, also known as the “little brain”, is a highly organized structure that contains more neurons than the entire cerebral cortex. It is thus an important part of the CNS, with major connections to and from the spinal cord, brainstem, and sensorimotor areas of the cerebral cortex (149). Since the structure does not reach its mature configuration until several months after birth (150), it is vulnerable to developmental abnormalities (151). Hypoxia and ischemia in the developing brain can damage the cerebellum (152).

1.5 Gene expression measurements

1.5.1 Quantitative real-time PCR

Quantitative real-time PCR (qPCR) is referred to as the “golden standard” when measuring gene expression (153) due to its high sensitivity and accuracy. The method is based on logarithmic amplification in cyclically repeated stages, and is dependent on a nearly 100%

amplicon efficiency, meaning that the PCR products doubles with each cycle. Reference genes or standard curves are also required to measure accurate relative or absolute gene expression, and a difference in amplicon efficiency between target gene and standards can significantly affect the accuracy (154).

1.5.2 Droplet digital PCR

Droplet digital polymerase chain reaction (ddPCR) is a relatively novel method and referred to as the third generation of PCR and enables absolute quantification of nucleic acids (155, 156). The method is based on water-in-oil emulsions, where samples are partitioned into approximately 20 000 droplets per sample before amplification and analyzing. The samples contain either fluorescently labeled probes or EvaGreen intercalating dyes, which are analyzed and determined as positive or negative values by the detection software (156). The positive droplets contain at least one copy of the template, while negative droplets do not (Figure 1-4).

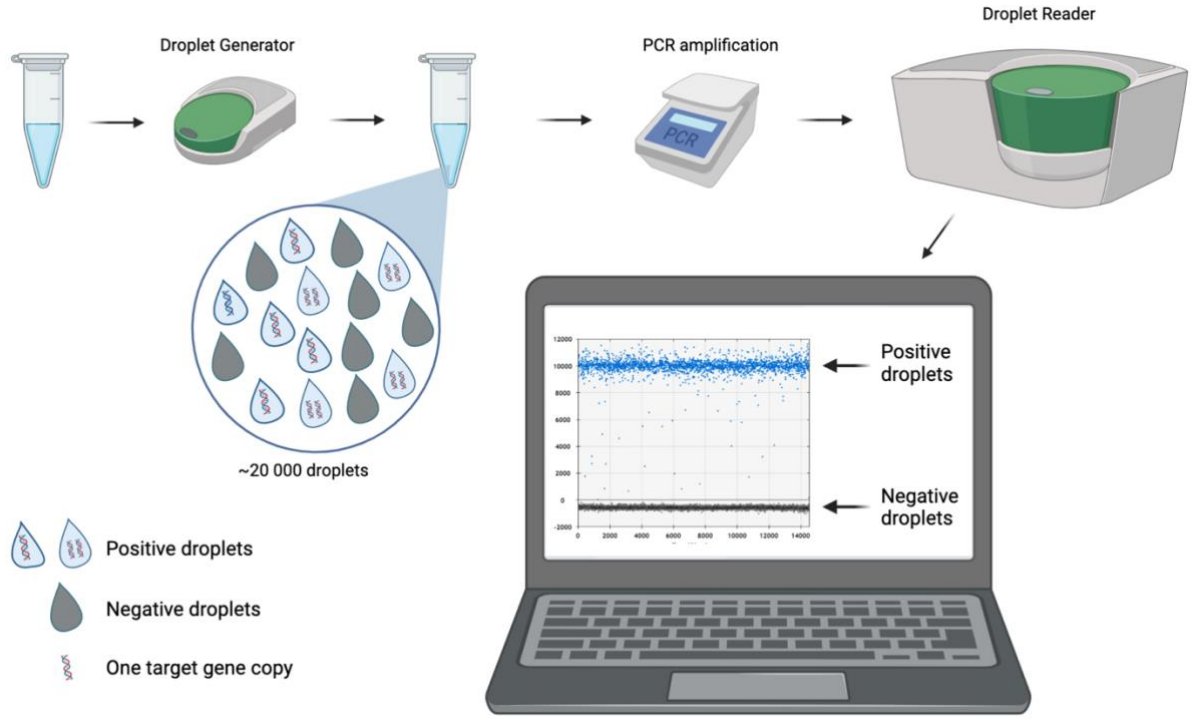

Figure 1-4. Simplified workflow of droplet digital PCR (ddPCR). Made using BioRender.com

Moreover, the positive samples are fitted to a probability distribution (Poisson distribution) by the software, which used Poisson statistics (157) to measure the absolute concentration of the target sequence based on the ratio of positive droplets and the total number of droplets. The sample partitioning is the key aspect of the technology, enabling measurement of

thousands of amplification events within one sample. The combination of major sample partitioning, Poisson statistics and end-point analysis enables direct and independent quantification of nucleic acids without the use of standard curves and reference genes. Additionally, the sample variability is estimated using Poisson statistics. One of the major benefits of ddPCR compared to the well-established qPCR method is its ability to quantify low abundant targets with small-expression differences, despite the presence of inhibitors (155). Furthermore, ddPCR also offers a greater advantage in terms of sensitivity, precision, and reproducibility, making the ddPCR method a powerful tool in gene expression analysis (158, 159).

2. Aim and objectives

Reliable early diagnostic markers for the severity and overall outcome of neonatal hypoxia-ischemia are crucial for improved intervention strategies and treatment. To fulfill this aim, several strategies were followed.

2.1 Aim of study

The overall aim of this study was to explore specific lncRNAs as potential markers for the severity of neonatal hypoxia-ischemia.

2.2 Objectives

1. Identify lncRNAs involved in hypoxia and oxidative stress
2. Adapt different methods to assess selected lncRNAs in a piglet model of neonatal hypoxia-ischemia
3. Examine changes in lncRNA expression during normoxic-reoxygenation
4. Perform comparative analysis of individual lncRNA in various sections of the piglet brain
5. Explore expression differences of selected lncRNAs during hyperoxia

3. Materials and methods

3.1 The neonatal hypoxia-ischemia piglet model

Newborn Noroc pigs (N=42) were treated with a well-developed model of neonatal hypoxia-ischemia at facilities of OUS. Piglets of good general condition between 12-36 hours of age and 1,8–2,2 kg were included to the study. Due to their anatomical and physiological similarity to newborn babies, piglets are well suited to investigate the aim of this study (140).

Approval for the pig studies is provided by The National Animal Research Authority, NARA (FOTS No. 17447, 13638, 8289). The animals were cared for and handled per the European Guidelines for Use of Experimental Animals by a certified FELASA (Federation of European Laboratory Animals Science Association) fellow and pediatrician with extensive experience with piglet models.

3.1.1 Anesthesia and surgical preparation

The piglets were placed in an incubator with a thermoneutral temperature (26-32°C) and a 50% humidity, before being gently transferred to the operating room. The temperatures of the piglets were continuously monitored and maintained (38,5-39,5°C). Anesthesia was induced by a dose of fentanyl (0,05 mg/kg) and pentobarbital (15 mg/kg) intravenously through a cannula in the ear. The piglets were orally intubated, ventilated, and surgically prepared as described by Benterud et al (160). Infusion of fentanyl (0,05 mg/kg/hour) and benelyte were continuously given throughout the procedure. Additional doses of pentobarbital were given if necessary (2,5 mg/kg). The piglets were then stabilized for one hour before proceeding with the experimental protocol.

3.1.2 Experimental protocol

After stabilization, the piglets were block randomized into four study arms: Hypoxia (8% O_2) and normoxic reoxygenation (21% O_2), hypoxia and 30 minutes of hyperoxic reoxygenation (100% O_2), hypoxia and 3 minutes of reoxygenation, and a sham-operated control group (Figure 3-1). Animals included in the control group went through the same procedures and observation times but were not exposed to hypoxia.

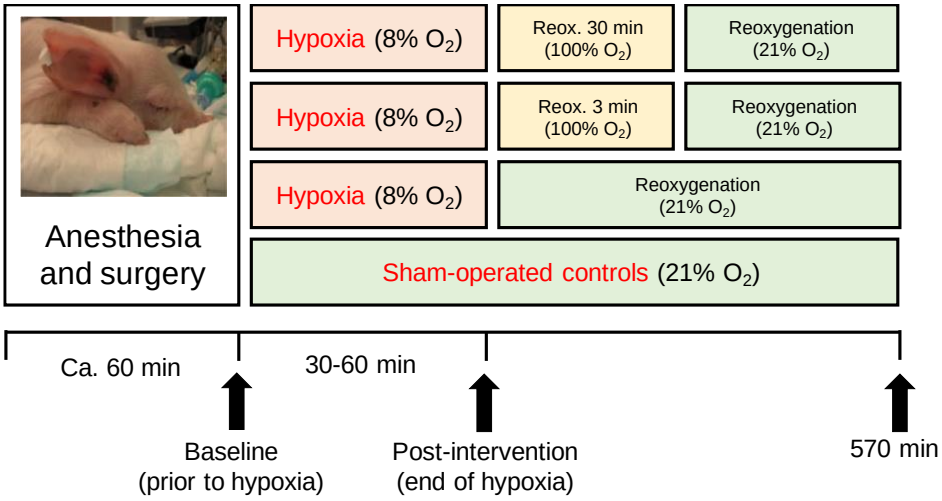

Figure 3-1. A schematic overview of the four study arms in the neonatal hypoxia-ischemia piglet model.

Hypoxia was mimicked by ventilation of 8% O_2 in N_2 until base excess (BE) reached -20 mM or the mean arterial blood pressure (MABP) decreased to 20 mmHg before the piglets were reoxygenated. The normoxic group was reoxygenated with 21% O_2 (n=11). The hyperoxic groups were reoxygenated with either 30 (n=10) or 3 (n=10) minutes of 100% O_2 followed by 21% O_2 for the remaining time of the experiment. The control group (n=11) received 21% O_2 the entire experiment. All the piglets were observed for 9,5 hours after the end of hypoxia. Blood gas measurements, pulse, oxygen saturation, blood pressure, and temperature were continuously surveilled. Additionally, the pigs' anesthesia and analgesia were assessed continuously. If shivering, an increase in blood pressure and/or pulse, or increased tone assessed by passive movements were observed, an additional bolus of fentanyl and pentobarbital were given. At the end of the experiment, urine and spinal fluid were collected through bladder- and spinal puncture. The piglets were then euthanized with an overdose of pentobarbital (150mg/kg) intravenously. The brain was immediately removed and tissue specimens from the right half of the brain, including the prefrontal cortex, hippocampus, white matter, and cerebellum, were frozen in liquid nitrogen and stored at -80°C until further analysis. The left half was placed in 4% buffered formalin. Tissue specimens from the heart, lunge, lever, kidney, the distal end of the small intestine (terminale ileum), retina, and the choroid were also collected, frozen in liquid nitrogen, and stored at -80°C. These were; however, not used in this study. Piglets 15, 34, 37 and 41 died before the experiment was

finalized, and were therefore excluded. Piglets 04, 14 and 18 were excluded due to abnormalities observed in their organs.

3.2 RNA isolation

RNA molecules are highly susceptible to degradation from RNases, which can be found in tissue samples, your surroundings, or on the human body (161). To minimize RNase contamination and degradation, precautions were made. Gloves were worn at all times during RNA isolation and changed regularly. Pipette tips, chemicals, and reagents used were RNase free and lab work was done in an RNase-free environment in a fume cupboard.

Total RNA was isolated using the E.Z.N.A® Total RNA kit II – Animal Tissue Protocol (Omega Bio-tek, Inc) according to the manufacturer's instructions (Appendix A), with the following modifications: 2-Mercaptoethanol was not added to RNA Solve reagent, and DNase I Digestion was added to optimize DNA removal. RNA was isolated in the cortex, hippocampus, white matter, and cerebellum from the normoxic and control group. RNA was isolated only from the cortex in the hyperoxic groups. Samples were assessed for RNA quality, then stored at 80°C until further use.

3.2.1 RNA quality assessments

RNA quality assessments were performed to ensure acceptable RNA quality for downstream gene expression analysis. A summary of data from RNA quality assessments from each group is presented in Table 4-1, and a complete overview is presented in (Appendix D)

Estimated RNA purity and concentrations were measured using the Nanodrop® ND-1000 Spectrophotometer (NanoDrop Technologies, Inc.). 1 µl of RNA was measured twice for each sample, and purity was assessed based on the following: A260/A280 = 1,8-2,2 and A260/230 above 1,7. RNA integrity was measured using the RNA ScreenTape assay (Agilent) on the Agilent 4200 TapeStation system according to the manufacturer's instructions (Appendix A). Total RNA degradation was assessed using the RNA integrity number (RIN^e) on a scale from 1-10, indicating strong degradation to highly intact RNA, respectively (Figure 3-1). RIN^e-value of 5 was considered as the lowest acceptable value.

3.3 cDNA synthesis

In order to perform a gene expression analysis by qPCR, RNA was copied into cDNA using the High Capacity cDNA reverse transcription kit (Applied Biosystems). 20 µl of isolated RNA (1000 ng) was added to 20 µl of cDNA mix (Table 3-1) before performing the reversed transcription reaction on a PTC-100™ Programmable Thermo Controller (MJ Research, Inc.)(
Table 3-2). cDNA was diluted in NFW to 10 ng/ul before performing gene expression analysis by qPCR.

Table 3-1. Master mix and RNA template volumes in the reverse transcriptase PCR.

cDNA mix	**1x (µl)**
10x RT buffer	4,0
25x dNTP mix (100mM)	1,6
10x RT Random primers	4,0
Multiscribe Reverse Transcriptase	1,0
Nuclease free water	9,4
Total volume	20,0

Table 3-2. Reverse transcription reaction thermocycler program.

	Step 1	**Step 2**	**Step 3**	**Step 4**
Temperature (°C)	25	37°C	85°C	4°C
Time	10 min	120 min	1. sec	∞

3.4 Quantitative real-time polymerase chain reaction

The quantitative real-time polymerase chain reaction (qPCR) method is based on logarithmic amplification and undergoes cyclically repeated reactions through three different temperature stages. The method is considered to be the most reliable and accurate method for measuring gene expression (162). SYBR Green (Applied Biosystems) was used as a fluorescent dye for quantification.

Primers were purchased from Life Technologies AS, see appendix B for sequences. All primers were dissolved in NFW at a concentration of 100 µM and stored in -20°C. Prior to use, primer mixes consisting of 10 µM forward- and reverse-primers were made for each primer pair. Every 20 µl reaction contained 16 µl PCR Master mix and 4 µl cDNA (40 ng) (Table 3-3). Pre-qPCR work was performed in an RNase-free environment in a laminar flow cabinet. The reactions were pipetted in a MicroAmp® Optical 96-Well Reaction Plate (Applied Biosystems), sealed with AB-1170 Optically Clear Adhesive Seal Sheets (Thermo Scientific, USA), and

centrifuged 2x20 seconds in RT before loaded to the PCR-instrument. Reactions were performed on ViiA 7 by Life Technologies (Applied Biosystems).

For each gene analyzed, no template control (NTC), negative reverse transcriptase control (NRT), and negative RNA control (NRNA) were included for all tissues. A melting curve analysis was performed to confirm the presence of a single target in the reaction.

Table 3-3. Master mix and cDNA template volumes in RT-qPCR.

PCR Master Mix	**1x (µl)**
Power SYBR Green	10,0
Primer mix	0,8
Nuclease free water	5,2
cDNA template	4,0
Total	**20,0**

3.5 Digital droplet PCR

20 µl of each reaction mix (Table 3-4) and 70 µl of Droplet Generation Oil for EvaGreen® was transferred to the sample- and oil wells in a DG8™ Cartridge for QX200™ Droplet Generator (BioRad) respectively, before covering with Droplet Generator DG8™ Gasket (BioRad). Samples were converted to droplets with the QX200 Droplet Generator (BioRad). 40 µl droplets with ~5 µl of air were then transferred to 96-Well ddPCR Plate, Semi skirted (BioRad), heat-sealed with Pierceable Foil Heat Seal (BioRad) in a PX1 plate sealer in 180°C for 5 seconds before thermal cycling (Table 3-5) on Veriti™ 96-well Thermal Cycler (Applied Biosystems). PCR lid was heated to 105°C and sample volume was set to 40 µl. The 96-well plate was analyzed on QX200 Droplet Reader with QuantaSoft Software.

Table 3-4. Components for ddPCR reaction mix per reaction

Components	**1x (µl)**
2x QX200 ddPCR EvaGreen Supermix	10
Forward primer (200 nM)	4
Reverse primer (200 nM)	4
cDNA template	2
Total volume	20

Table 3-5. Thermocycler program for EvaGreen Supermix prior to ddPCR.

Cycling Step	Temp (°C)	Time	Ramp rate	# of cycles
Enzyme activation	95	5 min	50%	1
Denaturation	95	30 sec		40
Annealing/Extension	60	1 min		
Signal Stabilization	4	5 min		1
	90	5 min		
Hold	4	∞		

3.6 Gene expression analysis

3.6.1 Quantitative real-time PCR

Gene expression studies were made using ViiA 7 RUO Software, and absolute gene expression was calculated in Microsoft Excel using normalized Ct-values and the $2^{-\Delta Ct}$ method before performing statistical analysis.

3.6.2 Digital Droplet PCR

Values from ddPCR were obtained from Quantasoft Software, and relative normalized expression was calculated in Microsoft Excel using equation 1 and 2 before performing statistical analysis.

$$Relative\ Quantity\ (RQ) = \frac{Treatment\ group\ (copies/ul)}{Control\ group\ (copies/ul)} \quad \textbf{(1)}$$

$$Normalized\ expression\ (NE) = \frac{RQ\ of\ Treatment\ group}{RQ\ of\ reference\ gene} \quad \textbf{(2)}$$

3.6.3 Statistical Analysis

Statistical analyses were performed by GraphPad Prism 8 (GraphPad Prism Software Inc.). Normal distribution was evaluated using the Shapiro-Wilk normality test and evaluation of the QQ-plots before further analysis of the data. If normal distribution criteria were not met, the data were log2 transformed in an attempt to achieve normal distribution. If normal distribution was still not met, a non-parametric test, Mann-Whitney or Kruskal Wallis, were applied on non-transformed data and expressed as mean ± interquartile range (IQ). Unpaired t-test or Analysis of variance (ANOVA) were applied to normally distributed data and expressed as mean ± standard deviation (SD). Results with $P<.05$ were accepted as statistically significant. Comprehensive data from statistical analysis are shown in Appendix D.

4. Results

4.1 RNA quality assessments

High RNA quality is important for downstream gene expression analysis. To ensure acceptable RNA quality for the experiments, NanoDrop (NanoDrop Technologies, Inc.), and RNA Screen Tape assay (Agilent) measurements were performed. Comprehensive data from RNA quality assessments are shown in appendix D.

4.1.1 NanoDrop

Estimated mRNA concentrations and purity were measured using the NanoDrop instrument. RNA from H1_Rox-21O_2(n') and the control group were measured in samples from cortex, hippocampus, white matter and cerebellum (n=71). H2_Rox-100O_2(30') and H3_Rox-100O_2(3') samples were only measured in samples from the cortex (n=20). We observed high variation of the RNA concentrations between the samples from the same brain region. All samples, except for one in cortex and some in white matter, were within the acceptable ratio for purity; A260/A280 = 1,8-2,2 and A260/230 above 1,7 (Table 4-1).

Table 4-1. Estimated RNA concentrations and purity-ratios in treatment groups of a neonatal hypoxia-ischemia piglet model, measured by NanoDrop. Data is expressed as mean ± SD.

Tissue	Treatment group	ng/ul mean	260/280 mean	260/230 mean
Cortex	H1_Rox-21O_2(n')	195 ± 66,7	2,04 ± 0,06	2,04 ± 0,28
	H2_Rox-100O_2(30')	201 ± 68,5	2,06 ± 0,03	1,93 ± 0,45
	H3_Rox-100O_2(3')	218 ± 58,4	2,04 ± 0,02	2,00 ± 0,07
	Control	281 ± 94,0	2,07 ± 0,04	2,16 ± 0,21
Hippocampus	H1_Rox-21O_2(n')	187 ± 73,0	2,05 ± 0,04	2,09 ± 0,32
	Control	179 ± 60,9	2,03 ± 0,03	2,14 ± 0,24
White Matter	H1_Rox-21O_2(n')	156 ± 71,2	2,09 ± 0,03	1,75 ± 0,64
	Control	167 ± 57,2	2,10 ± 0,03	2,05 ± 0,49
Cerebellum	H1_Rox-21O_2(n')	266 ± 78,8	2,03 ± 0,08	2,00 ± 0,39
	Control	358 ± 134	2,02 ± 0,07	2,13 ± 0,27

4.1.2 RNA ScreenTape Analysis

RNA integrity number (RIN^e) serves as an objective assessment of total RNA degradation. RIN^e is calculated at a scale from 1-10, with the lower value indicating strong degradation and higher value indicating highly intact RNA. A RIN^e-value of 5 is considered as lowest acceptable value. RNA integrity was measured by RNA ScreenTape assay (Agilent). RNA samples from the cortex of the piglets in H1_Rox-21O2(n'), H2_Rox-100O2(30'), H3_Rox-100O2(3') and the

sham-operated control group were analyzed (Figure 4-1). A total of six samples from the cortex were excluded from downstream gene expression analysis due to low (below 5) RIN^e value: P06, P35 and P13 from H1_Rox-21O_2(n'), P06 and P42 from H2_Rox-100O_2(30'), P28 and P29 from H3_Rox-100O_2(3').

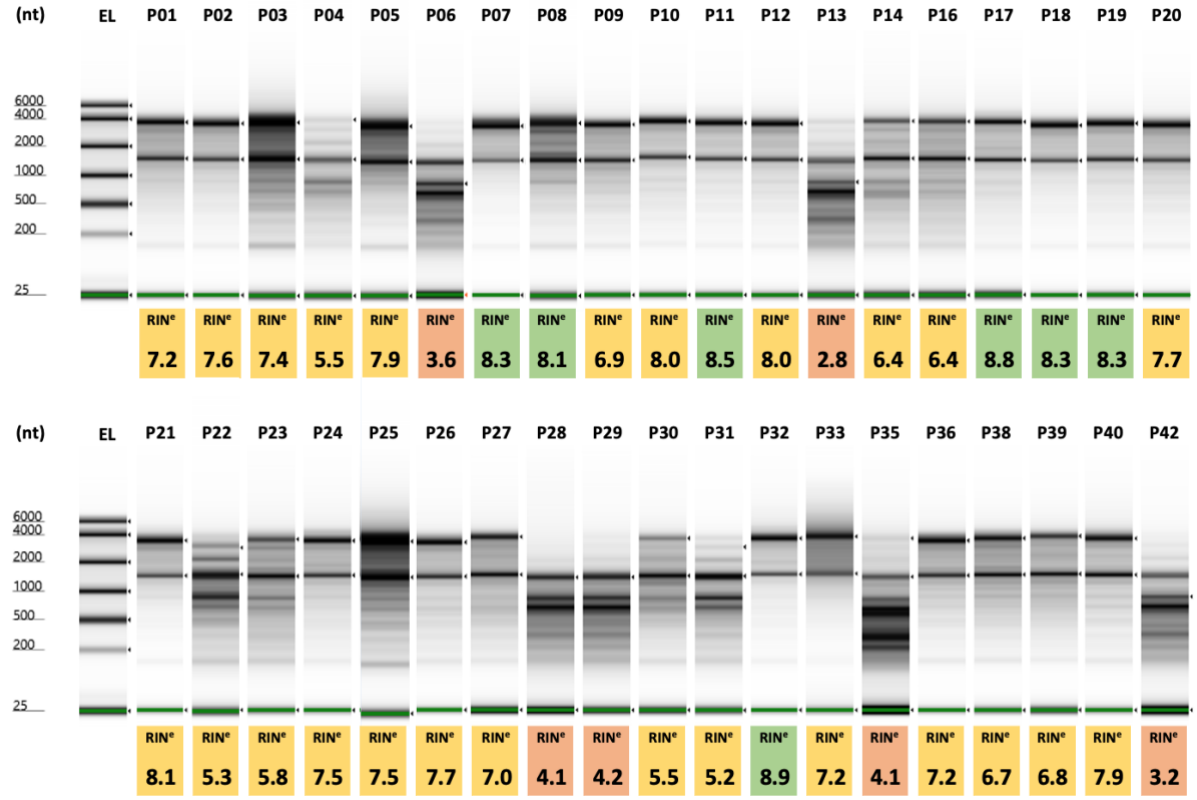

Figure 4-1. RNA integrity gel bands with RNA integrity number (RIN^e) results from the cortex of a neonatal hypoxia-ischemia piglet model, analyzed by RNA ScreenTape device. One gel band represents one piglet. Samples with RIN^e value below 5 were excluded. EL, Electronic RNA ladder; nt, nucleotide; P, piglet; red, RIN^e below 5; yellow, RIN^e between 5 and 8; green, RIN^e above 8.

4.2 Gene expression after hypoxic exposure and normoxic reoxygenation

Piglets from our neonatal hypoxia-ischemia model were divided into four different groups: Hypoxia 8% O_2 followed by 21% O_2 reoxygenation (H1_Rox-21O_2), hypoxia 8% O_2 followed by 30 minutes of 100% O_2 reoxygenation (H2_Rox-100O_2(30')), hypoxia 8% O_2 followed by 3 minutes of 100% O_2 reoxygenation (H3_Rox-100O_2(3')) and the sham-operated control group. All data were analyzed for normal distribution using the Shapiro-Wilk algorithm performing appropriate statistical tests. Log2-transformation was applied to non-normal distributed data in order to obtain normal distribution. If not met, the untransformed data was applied a non-parametric t-test Mann Whitney or Kruskal Wallis. Normal distributed data were analyzed by a parametric unpaired t-test or ANOVA. Comprehensive data and figures from the statistical

analysis´ are shown in appendix D. Piglet nr. 20 did not have a cerebellum sample, and was therefore not included in the cerebellum analysis.

4.2.1 Protein-coding gene expression

Five protein-coding genes associated with hypoxia or oxidative stress were studied using a piglet model of hypoxia-ischemia to examine the potential impact of hypoxia to different regions of the brain: cortex, hippocampus, white matter, and cerebellum. The protein-coding genes were examined in H1_Rox-21O_2 (normoxic reoxygenation) and the sham-operated control group. Ct-values were normalized to the endogenous control RLP0, and absolute gene expression was measured using the $2^{-\Delta Ct}$ method. See Table 4-2 for P-values from the statistical tests.

Vascular endothelial growth factor A (VEGFA) was determined as significantly up-regulated in the cortex (n=6), hippocampus (n=8), and cerebellum (n=7) relative to the control group (n=7). A similar tendency, although not significant, was seen in white matter (n=8) (Figure 4-2). Brain derived neurotrophic factor (BDNF) appears to increase in the cortex, hippocampus and white matter; however, the up-regulation was determined being significantly changed only in the cortex samples. In the cerebellum samples, BDNF was expressed approximately equally between the treated and control group (Figure 4-2).

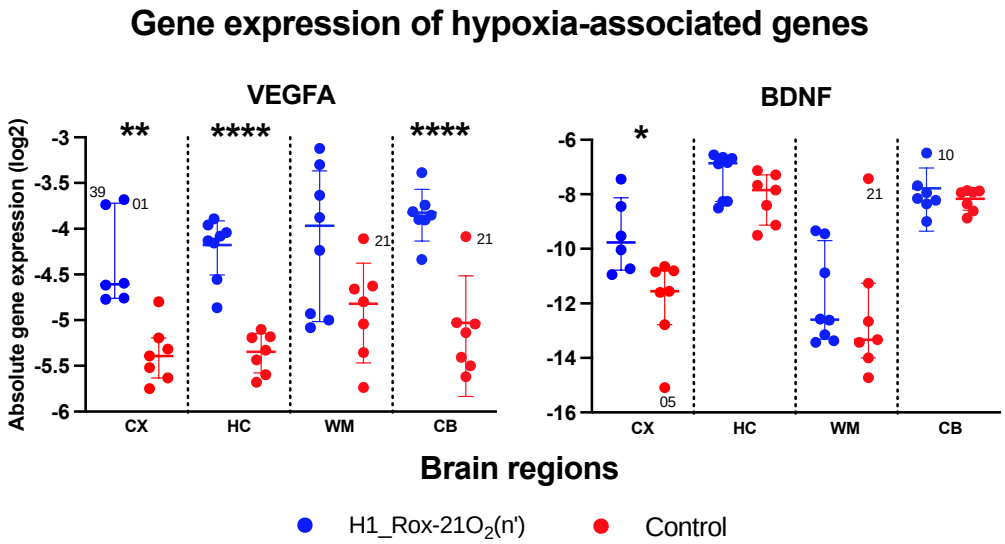

Figure 4-2. Absolute gene expression of the hypoxia-regulated genes VEGFA and BDNF in the four brain regions (CX: cortex; HC: Hippocampus; WM: white matter; CB: cerebellum) in a neonatal hypoxia-ischemia piglet model. H1_Rox-21O2(n´) (n=6) was treated with hypoxia (8% O_2) followed by normoxic reoxygenation (21% O2) and sham-operated control (n=7) was treated with 21% O2 the entire procedure. Data was normalized endogenous control RLP0, and is shown on a logarithmic scale. Each value represents one piglet. Values are expressed as either mean ± SD (VEGFA: HC, WM, CB; BDNF: CB) or median ± IQ-range

(VEGFA: CX; BDNF: CX, HC, WM). P<.05=; P<.01=**; P<.0001=****. VEGFA, Vascular endothelial growth factor A; BDNF, Brain derived neurotrophic factor;*

Moreover, Hypoxia-inducible factor alpha (HIF1α) was expressed rather similar in both groups, and across samples from the cortex, hippocampus and white matter. The HIF1α expression in cerebellum was elevated compared to the other brain regions (Figure 4-3). Tumor suppressor gene p53 expression was not significantly up- nor down-regulated in neither of the brain regions. Tumor necrosis factor α (TNFα) was determined as significantly up-regulated only in the samples from the cerebellum. We also observed a high with-in group variability (Figure 4-3).

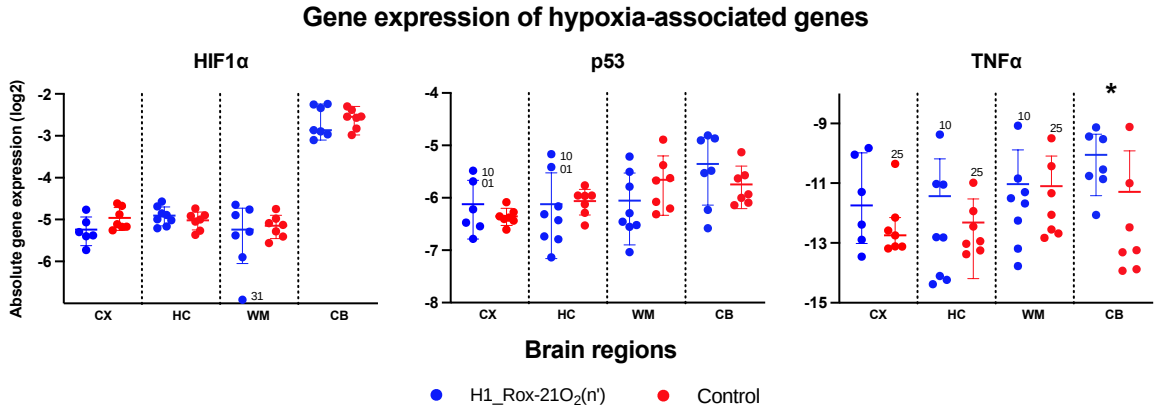

Figure 4-3. Absolute gene expression of the hypoxia-regulated genes HIF1α, p53 and TNFα in four different brain regions (CX: cortex; HC: Hippocampus; WM: white matter; CB: cerebellum) in a neonatal hypoxia-ischemia piglet model. H1_Rox-21O2(n´) (n=6) was treated with hypoxia (8% O_2) followed by normoxic reoxygenation (21% O2) and sham-operated control (n=7) was treated with 21% O2 the entire procedure. Data was normalized endogenous control RLP0, and is shown on a logarithmic scale. Each value represents one piglet. Values are expressed as either mean ± SD (p53, TNFα: HC, WM, CB; HIF1α: CX, HC, WM) or median ± IQ-range (p53, TNFα: CX; HIF1α: CB). P<.05=. HIF1α, Hypoxia-inducible factor α; p53, Tumor suppressor gene p53; TNFα, Tumor necrosis factor α.*

4.2.2 Long non-coding RNA expression

Forward and reverse primers for 10 different lncRNAs were selected for analysis on qPCR to study the potential impact of hypoxia on lncRNA expression in different regions of the brain, including cortex, hippocampus, white matter and cerebellum. HOTAIR and LincRNA-p21 were excluded from the study due to unsuccessful attempts to achieve appropriate primer efficiency, and BACE1-AS and BC200 were excluded due to inconsistent template amplification. Thus, six lncRNAs associated with hypoxia were analyzed on qPCR in a piglet model of neonatal hypoxia-ischemia. Ct-values from qPCR were normalized to the endogenous control TBP, absolute gene expression was calculated using the $2^{-\Delta Ct}$ method, and is presented on a logarithmic scale.

4.2.2.1 Normoxic reoxygenation

The lncRNAs were first studied after hypoxic exposure followed by normoxic reoxygenation. BDNF-AS, H19, MALAT1, and ANRIL were analyzed in samples from the cortex, hippocampus, white matter, and cerebellum. TUG1 and PANDA were only analyzed in hippocampus and cortex samples.

In the cortex samples, gene expression of BDNF-AS (Figure 4-4) was up-regulated in the hypoxia group in comparison to the control group in cortex. Although a similar tendency could be observed for samples from the cerebellum, the difference was determined as non-significant. BDNF-AS gene expression in samples taken from the hippocampus and white matter presented were not changed in relation to the appearance in samples present in the control group. The lncRNA H19 (Figure 4-4) was determined and we observed a significant increase in samples from cortex and white matter, with a similar tendency in hippocampus; however, the differences were not significant (**Error! Reference source not found.**). In samples extracted from the cerebellum, H19 was neither up- nor down-regulated.

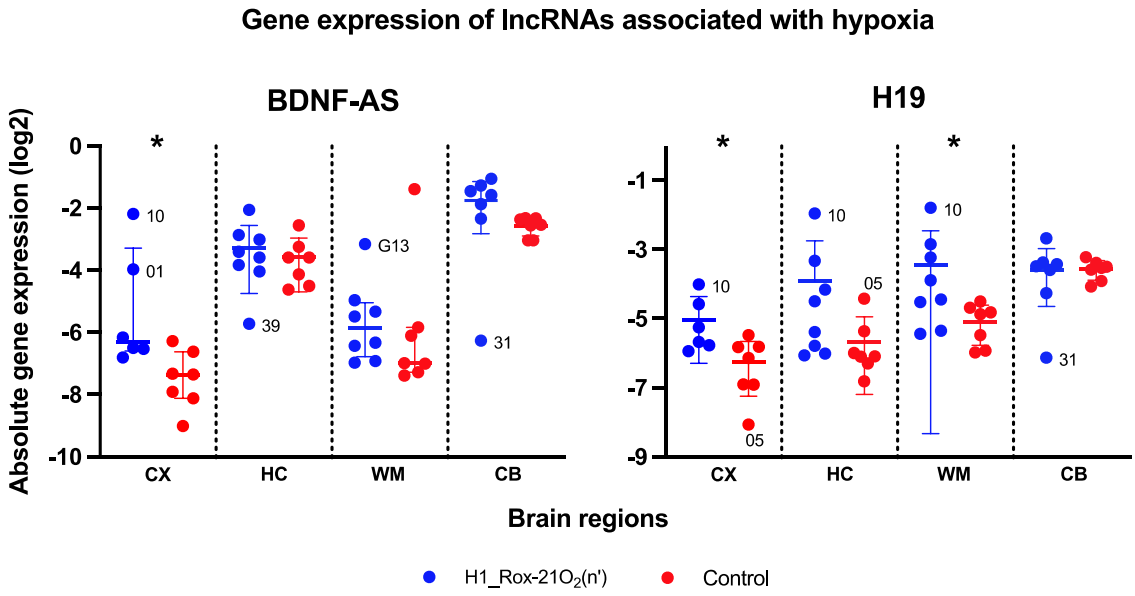

Figure 4-4. Absolute gene expression of hypoxia-associated lncRNAs BDNF-AS and H19 in different brain regions (CX: cortex; HC: Hippocampus; WM: white matter; CB: cerebellum) of a neonatal hypoxia-ischemia piglet model. H1_Rox-21O2(n´) (n=6) was treated with hypoxia (8% O_2) followed by normoxic reoxygenation (21% O_2) and sham-operated control (n=7) was treated with 21% O_2 the entire procedure. Data was normalized endogenous control TBP, and is shown on a logarithmic scale as $2^{-\Delta Ct}$. Each value represents one piglet. Values are expressed as either mean ± SD (BDNF-AS: HC, CB; H19) or median ± IQ-range (BDNF-AS: CX, WM). P<.05=. BDNF-AS, Brain derived neurotrophic factor antisense; H19, H19 Imprinted Maternally Expressed Transcript.*

MALAT1 and ANRIL (Figure 4-5) were determined as significantly up-regulated in hippocampus and cerebellum, respectively (**Error! Reference source not found.**). Gene expression in the other brain regions were determined as being non-significant. TUG1 (Figure 4-5) expression was significantly down-regulated in samples taken from the hippocampus region and a similar tendency was revealed for the expression in samples extracted from the cortex, although not significant. Gene expression in the hypoxia samples of PANDA (Figure 4-5) was neither up- nor down-regulated relative to samples from the control group. In addition, melt curve analysis of PANDA displayed multiple peaks.

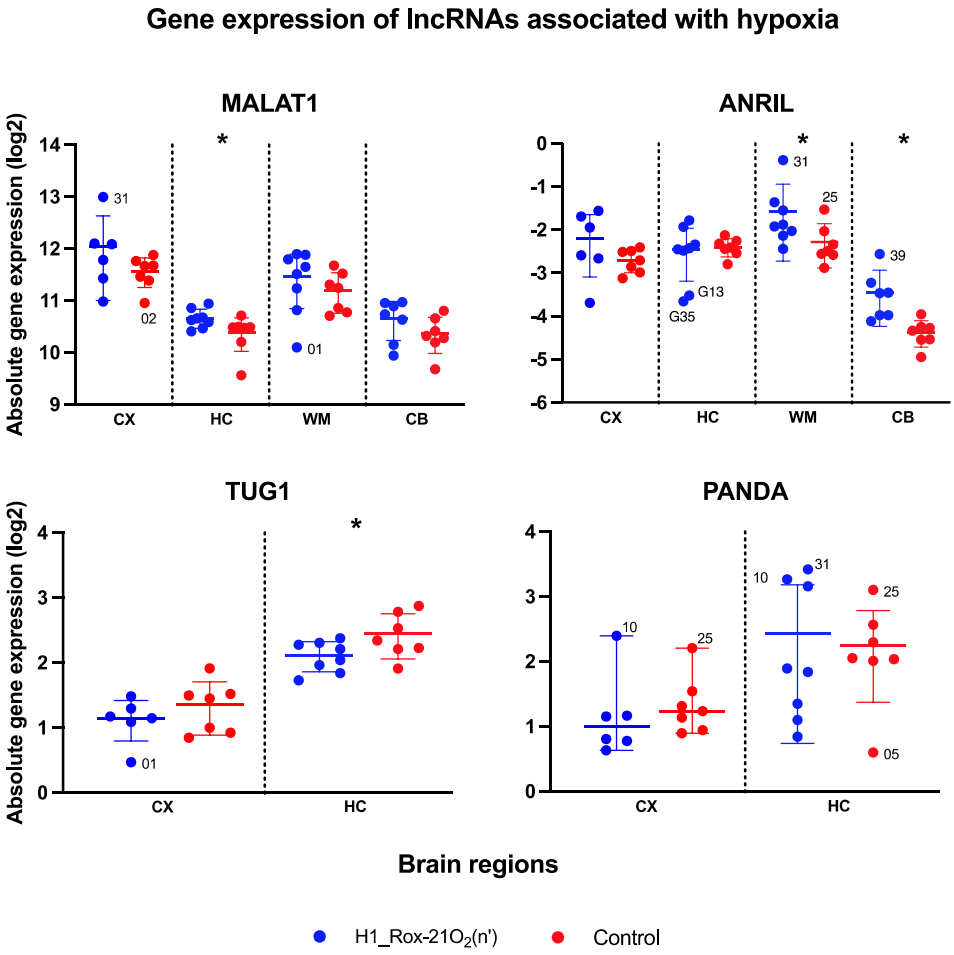

Figure 4-5. Absolute gene expression of the hypoxia-associated lncRNAs MALAT1, ANRIL, TUG1 and PANDA in different brain regions (CX: cortex; HC: Hippocampus; WM: white matter; CB: cerebellum) of a neonatal hypoxia-ischemia piglet model. H1_Rox-21O2(n´) (n=6) was treated with hypoxia (8% O2) followed by normoxic reoxygenation (21% O_2) and sham-operated control (n=7) was treated with 21% O_2 the entire procedure. Data was normalized endogenous control TBP, and is shown on a logarithmic scale as $2^{-\Delta Ct}$. Each value represents one piglet. Values are expressed as either mean ± SD (MALAT1; ANRIL; TUG1; PANDA: HC) or median ± IQ-range (PANDA: CX). P<.05=. MALAT1, metastasis associated lung adenocarcinoma transcript 1; ANRIL, Antisense Noncoding RNA in the INK4 Locus; TUG1, Taurine Upregulated gene 1; PANDA, P21-associated ncRNA DNA damage-activated.*

Table 4-2. P-value summary from statistical t-tests comparing mRNA gene expression between a group exposed to hypoxia (8% O_2) followed by normoxic reoxygenation (21% O_2) and a sham-operated control in a piglet model of neonatal hypoxia-ischemia. Five genes associated with or regulated by hypoxia were analyzed by qPCR in different regions of the brain; cortex, hippocampus, white matter and cerebellum.

	P values									
Brain region	**VEGFA**		**BDNF**		**HIF1α**		**p53**		**TNFα**	
Cortex	.002	**	.01	*	.12	ns	.32	ns	.37	ns
Hippocampus	<.0001	****	.09	ns	.35	ns	.85	ns	.91	ns
White matter	.051	ns	.33	ns	.71	ns	.21	ns	.91	ns
Cerebellum	<.0001	****	.49	ns	.90	ns	.21	ns	.019	*

Abbreviations: VEGFA, Vascular endothelial growth factor A; BDNF, Brain derived neurotrophic factor; HIF1α, Hypoxia-inducible factor α; p53, Tumor suppressor gene p53; TNFα, Tumor necrosis factor α.

4.2.2.2 Hyperoxic reoxygenation

Four of the lncRNAs were analyzed in samples taken from a piglet model of normoxic and hyperoxic reoxygenation to study the potential difference in gene expression between the latter groups. Samples from the cortex of these piglets representing four different treatment groups were investigated, including H1_Rox-21O_2(n´), H2_Rox-100O_2(30´), H3_Rox-100O_2(3´) and sham operated control (Figure 4-6). Ordinary One Way ANOVA or Kruskal Wallis, followed by post-hoc test Tukey´s or Dunn´s, were applied to the data for statistical analysis.

Quantitative real-time PCR

Analysis by qPCR revealed a significant increase in BDNF-AS expression relative to the control in H2_Rox-100O_2(30´) and H3_Rox-100O_2(3´), but not in the H1_Rox-21O_2(n´) group. Expression values between the treated groups were not significantly changed. Difference in H19 gene expression was determined as non-significant relative to the control, as well as between groups. However, the treated groups appear to be slightly increased relative to the control group, although it was determined as non-significant. MALAT1 and ANRIL were determined as neither in- nor decreased in all groups. However, compared to the controls, the treated groups had more within-treatment group variability.

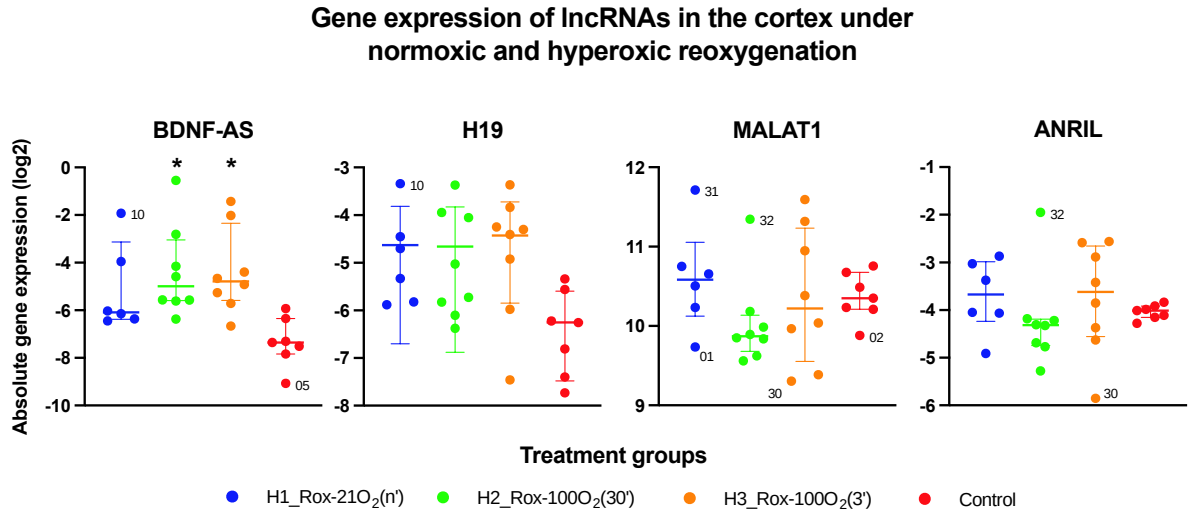

Figure 4-6 Absolute gene expression of hypoxia-associated lncRNA in the cortex (CX) of a neonatal hypoxia-ischemia piglet model. H1_Rox-21O2(n´) (n=6) was treated with hypoxia (8% O_2) followed by normoxic reoxygenation (21% O2). H2_Rox-100O_2(30´) (n=8) and H3_Rox-100O_2(3´) (n=8) were treated with hypoxia and then 30 and 3 minutes of hyperoxic reoxygenation (100% O_2), respectively, followed by normoxic reoxygenation. Sham-operated control (n=7) was treated with 21% O_2 the entire procedure. Data was normalized endogenous control TBP, and is shown on a logarithmic scale as $2^{-\Delta Ct}$. Each value represents one piglet. Values are expressed as either mean ± SD (H19) or median ± IQ-range (BDNF-AS; MALAT1; ANRIL). P<.05=. BDNF-AS, Brain derived neurotrophic factor antisense; H19, H19 Imprinted Maternally Expressed Transcript; MALAT1, metastasis associated lung adenocarcinoma transcript 1; ANRIL, Antisense Noncoding RNA in the INK4 Locus.*

Droplet Digital PCR

BDNF-AS and H19 RNA expression was analyzed using droplet Digital PCR (BioRad) to confirm and verify the results achieved by qPCR. Kruskal Wallis test determined the medians for BDNF-AS expression in samples from the H1_Rox-21O_2(n´), H2_Rox-100O_2(30´) and H3_Rox-100O_2(3´) groups being statistically different. Further post hoc analysis with Dunnett´s multiple comparison test revealed the lncRNA expression of hyperoxic reoxygenated groups to be significantly increased relative to the control group, with 30 minutes of reoxygenation to be even more enhanced (**Error! Reference source not found.**). Although values for the group treated with normoxic reoxygenation was determined as non-significant, gene expression seem to be slightly increased compared to the values of the control group. Neither normoxic or hyperoxic reoxygenation were significantly changed compared to each other. Ordinary One Way ANOVA determined means among H19 in all groups to be non-significant, and post-hoc test Tukey's multiple comparison test did not reveal any further significance among groups (**Error! Reference source not found.**). However, H19 in groups treated with hypoxia shows a tendency to be increased relative to the control group (Figure 4-7). The results from ddPCR (Figure 4-7) indicate a similar pattern of gene expression as presented from qPCR (Figure 4-6).

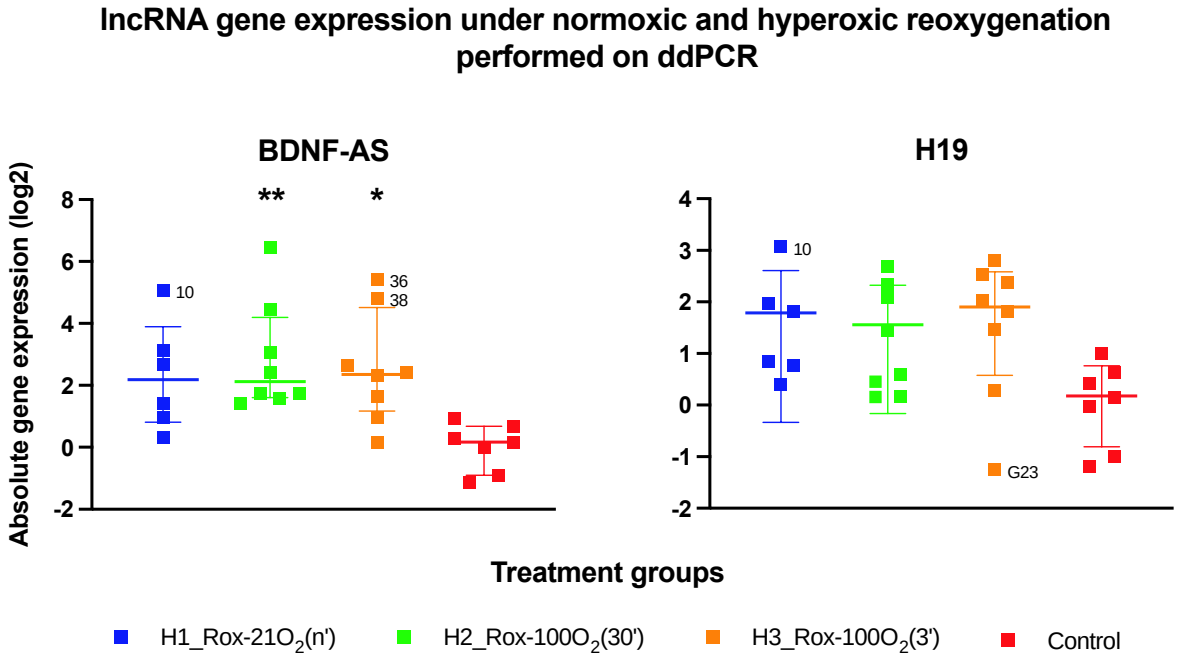

Figure 4-7. Gene expression of lncRNAs BDNF-AS (median± IQ-range) and H19 (mean ± SD) analyzed in the cortex of a piglet model of neonatal hypoxia-ischemia on droplet digital PCR. H1_Rox-21O2(n´) (n=6) was treated with hypoxia (8% O_2) followed by normoxic reoxygenation (21% O_2). H2_Rox-100O2(30´) (n=8) and H3_Rox-100O2(3´) (n=8) were treated with hypoxia and then 30 and 3 minutes of hyperoxic reoxygenation (100% O_2), respectively, followed by normoxic reoxygenation. Sham-operated control (n=7) was treated with 21% O2 the entire procedure. Data was normalized endogenous control TBP, and is shown on a logarithmic scale as 2-ΔCt. Each value represents one piglet. Data was normalized to endogenous control TBP. P<.05=; P<.01=**. BDNF-AS, Brain derived neurotrophic factor antisense; H19, H19 Imprinted Maternally Expressed Transcript.*

Adjusted P values							
Treatment groups	qPCR				ddPCR			
	BDNF-AS		H19		BDNF-AS		H19	
H2_Rox-100O2(30') vs. H3_Rox-100O2(3')	.99	ns	.95	ns	.99	ns	.86	ns
H2_Rox-100O2(30') vs. H1_Rox-21O2(n')	.99	ns	.99	ns	.99	ns	.97	ns
H2_Rox-100O2(30') vs. Control	.01	*	.25	ns	.005	**	.33	ns
H3_Rox-100O2(3') vs. H1_Rox-21O2(n')	.99	ns	.97	ns	.99	ns	.99	ns
H3_Rox-100O2(3') vs. Control	.01	*	.09	ns	.02	*	.09	ns
H1_Rox-21O2(n') vs. Control	.26	ns	.28	ns	.056	ns	.19	ns

Abbreviations: BDNF-AS, Brain derived neurotrophic factor antisense; H19, Imprinted Maternally Expressed Transcript. Ns, not significant; P<.05=; P<.01=**.*

Correlation analysis

Data from qPCR and ddPCR was compared using Pearson Correlation test. There was a positive correlation of values for both BDNF-AS (r=0,9781, n=29, P<.0001) and H19 (r=0,9862, n=29, P>.0001). Overall, there was a strong, positive correlation between gene expression results analyzed on qPCR and ddPCR (Figure 4-8).

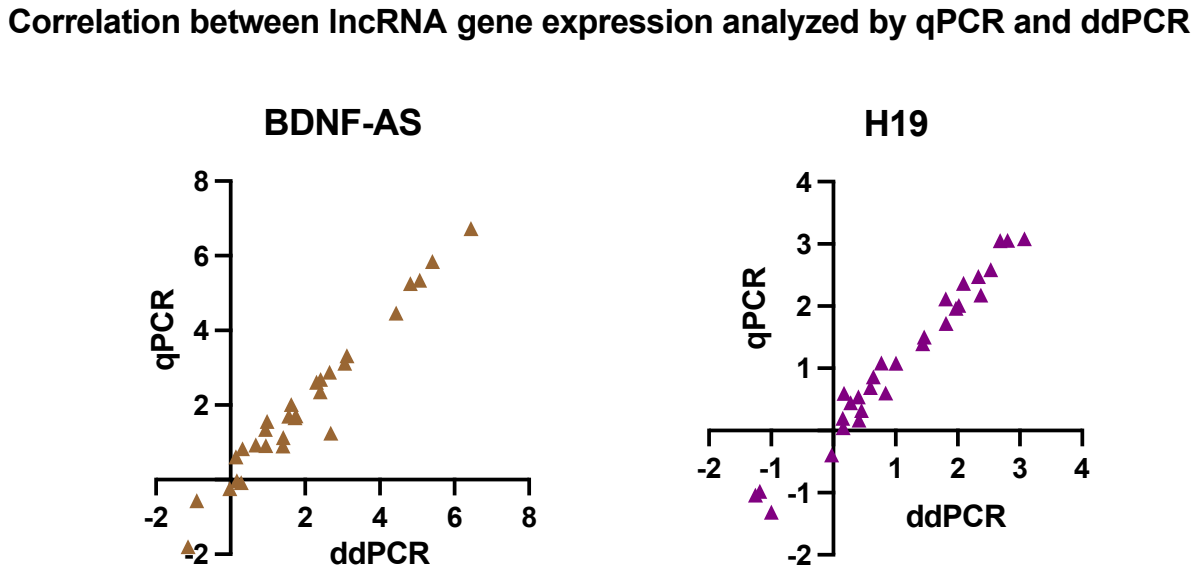

Figure 4-8. Correlation plot comparing qPCR and ddPCR gene expression results of BDNF (r=0,9781, n=29, P<.0001) and H19 (r=0,9862, n=29, P>.0001) in samples from the cortex analyzed in the normoxic (21% O_2), hyperoxic (30 and 3 minutes 100% O_2) and the control group. Correlation was determined as a strong positive correlation by Pearson correlation test. BDNF-AS, Brain derived neurotrophic factor antisense; H19, Imprinted Maternally Expressed Transcript.

5. Discussion

The aim of this study was to explore lncRNAs in neonatal hypoxia-ischemia and to investigate their potential as possible markers for the severity and overall outcome of the condition. To this end, a piglet model was facilitated to examine expression changes of selected protein coding genes and long non-coding RNAs associated with- or regulated by hypoxia. Samples were collected from diverse sections of the brain, including the cortex, hippocampus, white matter, and cerebellum. Assorted lncRNAs were further analyzed after hyperoxic reoxygenation exposure.

This is one of the first studies demonstrating the differential expression of lncRNA under neonatal hypoxic-ischemic conditions. The most striking result emerging from this study was the so far unknown up-regulation of BDNF-AS under a long or short period of hyperoxic reoxygenation. Our results indicate that 30 minutes of hyperoxic reoxygenation is sufficient for a significant increase in BDNF-AS expression. Importantly, even a short pulse of 3 minutes of hyperoxic reoxygenation is sufficient enough to cause a significant increase. We suggest that changes in the expression of BDNF-AS should be investigated further to test if this lncRNA could serve as a biomarker for oxidative stress damage and predict the severity of neonatal hypoxia-ischemia in the future.

5.1 Gene expression of protein-coding genes associated with hypoxia

Prior to the analysis of the lncRNAs, a collection of five different protein-coding genes (VEGFA, BDNF, HIF1α, TP53, and TNFα), known to be involved in oxidative stress reactions, were chosen as independent parameters to assess hypoxia-ischemia injury in sections of the piglet brains. The mRNA expression of the selected five genes were measured in tissue collected from the cortex, hippocampus, white matter, and cerebellum in piglets exposed to hypoxia and normoxic reoxygenation, hypoxia and 3 or 30 minutes of hyperoxic reoxygenation and a sham-operated control (Figure 3-1).

5.1.1 Tumor suppressor gene p53

The transcription factor p53 controls cellular responses through its transcription targets. Since p53 is known to activate in response to DNA and oxidative stress, we hypothesized that p53 would be altered after hypoxic exposure. Although the mRNA levels of the tumor suppressor

was neither up- nor down-regulated in samples from the various brain regions, we observed altered expression and high with-in group variability in the treated groups. A study on hypoxic stress in the MCF-7 cell line (breast cancer) reported up-regulation of p53 protein levels by hypoxic stress, but not p53 mRNA and mRNA levels of its downstream effector genes (64). Nevertheless, elevated p53 mRNA levels in hypoxic conditions in cell lines and cancer have been reported in other studies (163, 164). It should also be mentioned that gene expression between different cell lines, organisms and conditions are not necessarily comparable, and should be interpreted with caution. Additionally, a study on global gene expression reported altered gene expression over the time course of 2-72 hours in the brain of neonatal hypoxic-ischemic rats (165). Thus, the lack of significantly altered expression in our results may be explained by the time when our samples were collected (9,5 hours post HI) or reflect the cell- or tissue-specificity reported earlier (65).

5.1.2 Tumor necrosis factor α (TNFα)

TNFα is an important proinflammatory cytokine involved in HI-induced injury. Inflammation has been stated as one of the main causes of HI injury (72, 73), and elevated mRNA and protein levels of the cytokine have been reported in several studies concerning hypoxia and ischemia (68-71). In our study was TNFα mRNA only significantly up-regulated in samples from the cerebellum, although we observed an additional tendency of increased expression in the cortex samples. This might be explained by the high abundance of neurons in the cerebellum (149) and by reports of TNFα being involved in neuronal cell apoptosis (67). Furthermore, we observed high within-group variability in the treated groups, as well as in some of the control groups, potentially affecting the significance of altered expression. Also, hypoxia-induced up-regulation of TNFα has been suggested to increase over time in hypoxic osteoblastic cells, possibly explaining the lack of significant increase in the various brain regions (166).

5.1.3 Hypoxia-inducible factor 1 subunit α (HIF1α)

Studies have shown that HIF1α protein levels are elevated in response to hypoxia; however, HIF1α mRNA expression appears to be constitutively expressed in some cell types and up-regulated in others (31, 32). Here, we were able to show that the HIF1α gene expression in mRNA samples from a piglet model of neonatal hypoxia-ischemia is constitutively expressed in the brain regions, including cortex, hippocampus, white matter, and cerebellum. HIF1α gene expression was elevated in the cerebellum compared to other brain regions. This is

supported by Sjöstedt et al., who reported that the cerebellum, compared to other major brain regions, stands out with regard to the number of regionally enriched genes. The brain atlas database from their study also states that HIF1-α mRNA level is elevated in the cerebellum compared to the cerebral cortex and hippocampal formation (167).

5.1.4 Brain-derived neurotrophic factor

BDNF is critical for brain development, and has publicized with neuroprotective effects towards neonatal brain injury caused by hypoxia and/or ischemia (42, 45, 46). High levels of BDNF mRNA have been reported in samples generating from the cerebral cortex, hippocampus, and cerebellum of humans, rodents, and pigs (39, 40, 167). Highest amounts of BDNF mRNA samples were observed in the hippocampus (39, 40), which is in line with our results, indicating highest level in the hippocampus and cerebellum and lower gene expression in the cortex. Also consistent with our results are reports from animal studies describing an up-regulation of BDNF mRNA and protein level expression in the neonatal brain after hypoxia-ischemia (17). On the contrary, another study reported BDNF mRNA as down-regulated in response to hypoxia/ischemia in postnatal day 7 rats (86). However, their gene expression results were measured on day 5 and 7 after the insult, and our results were measured in samples collected 9,5 hours after HI. Xu et al (2016) reported that BDNF initially increased in response to ischemia, before slowly decreasing over time (54). This might explain the difference in measured BDNF mRNA in our studies. Moreover, studies have also shown that BDNF is inversely correlated with its antisense RNA BDNF-AS after hypoxic-ischemic insult (54), which is discussed in more detail in chapter 5.2.6.

5.1.5 Vascular Endothelial Growth Factor A (VEGFA)

VEGFA is an important growth factor and has shown to be involved in hypoxia-ischemia due to its protective features, including angiogenesis and the protection of cells against hypoxia by restoring blood supply (168). Publications have stated an increase in VEGFA mRNA and protein levels in response to HI and ischemic stroke (169-171). This is consistent with our results, indicating an increase in VEGFA mRNA in piglets exposed to hypoxia. VEGFA was significantly up-regulated in samples from the cortex, hippocampus, and cerebellum, with a similar pattern in white matter, indicated that the HI had heavily triggered the piglets.

Additionally, another study suggested that a further raise in VEGFA protein levels post-HI insult was associated with the development of HIE later on (37).

Based on the results of hypoxia-associated or -regulated protein-coding genes reported above, we conclude that the analyzed brain regions were clearly injured from the provoked insults, and consequently we proceeded with the study of various lncRNA candidates in samples collected from different brain regions after hypoxia-ischemia in newborn piglets.

5.2 LncRNA

This investigation of lncRNA expression changes started with measuring identified and selected candidate lncRNAs in various brain regions of piglets exposed to HI and normoxic reoxygenation (21% O_2), followed by a more specific survey investigating the selected lncRNAs after 3 or 30 minutes of exposure to hyperoxic reoxygenation (100% O_2) in samples from the cortex. The latter selection was evaluated based on the significant results from the normoxic reoxygenation, combined with which brain region we hypothesized would be affected the most.

5.2.1 p21-associated ncRNA DNA damage-activated (PANDA)

The lncRNA is a transcriptional target for p53, and has been reported to regulate apoptosis in response to DNA damage (98). Since p53 activity has been reported in hypoxia and ischemia, we hypothesized that PANDA expression could be altered in response to HI-induced injury. However, our results did not reveal a significant altered expression of PANDA in neither samples from the cortex nor the hippocampus. Although the reason for this is uncertain, it might be connected to the lncRNA tissue-specificity (87, 88) or p53 activity in hypoxic conditions. P53 activates p21 in response to stress, and PANDA is located and transcribed from the p21 locus (98). A study reported that both p21 protein levels and mRNA expression in humans and rodents were not affected in response to hypoxic stress (64), and another suggested that the activity of p53 is cell- and tissue specific (65). Nevertheless, this assumption is very vague and does not have enough evidence to support it.

5.2.2 Taurine Upregulated gene 1 (TUG1)

Hypoxia seriously damages the retina in humans and animals (172). The lncRNA TUG1 is important during retinal development (173) and consequently, we hypothesized that TUG1 could be altered in the neonatal brain during a HI event. Our results highlight that the expression of TUG1 in RNA samples from the hippocampus are significantly decreased relative to the control, and we observed the same pattern in the cortex, although not significant. A study reported that TUG1 expression was reduced in I/R induced mice and H/R induced HK-2 cells (130). On the contrary, TUG1 expression in Human umbilical vein endothelial cells (HUVEC) was significantly up-regulated in another study (174). However, the experimental set up was different and gene expression between different models and organs should be interpreted with caution.

5.2.3 Antisense Noncoding RNA in the INK4 Locus (ANRIL)

Normoxic reoxygenation

Increased expression of ANRIL has been demonstrated to promote angiogenesis via VEGFA activation (121) and its altered expression has been linked to pathological processes such as hypoxia and oxidative stress (81). Our result revealed a significant increase of ANRIL expression in samples from white matter and the cerebellum. Samples from the cortex and hippocampus did not show a significant increase; however, the observed values are more spread in the hypoxic group compared to the control group. Thus, the latter brain regions appear to have been affected by the hypoxia-ischemia, although not significant.

Hyperoxic reoxygenation

Expression of ANRIL was further studied in the hyperoxic groups in samples from the cortex using ANOVA and posthoc Dunn´s multiple comparison test, determining that the medians were not significantly different. Nevertheless, similar to the cortex in the normoxic reoxygenated group, the observed values are more spread compared to the control group. Moreover, the group exposed to 30 minutes of hyperoxia appears to be somewhat decreased compared to the other groups. A recent study reported that ANRIL expression in blood from patients suffering from acute ischemic stroke was inversely correlated with the severity (122). Taking together, these results indicate that the 30 minutes of hyperoxia could have led to a

more severe insult compared to the other groups, explaining the difference in expression. On the other hand, this is a very vague assumption based on studies using different materials and organisms and should therefore be evaluated with caution. Moreover, since ANRIL expression was determined as significantly increased in white matter and cerebellum, further analysis of ANRIL in the latter regions could give a more clear results. Thus, further tests should be carried out to investigate the gene expression of ANRIL in response to neonatal hypoxia-ischemia.

5.2.4 Metastasis associated lung adenocarcinoma transcript 1 (MALAT1)

Normoxic reoxygenation

The lncRNA MALAT1 has been reported as up-regulated in several cell lines and animal models treated with hypoxia (94). A study discovered that MALAT1 expression was increased in brain tissue derived from mice with hypoxic-ischemic brain damage (HIBD) and that the lncRNA was increased in hippocampal neurons from mice under oxidative and hypoxic stress (94). This is in agreement with our results revealing a significant increase in expression in samples from the hippocampus. However, the difference between the latter study (94) and our experimental setup is worth noting. Moreover, MALAT1 is one of the most abundant and conserved lncRNAs (93), and in mice has MALAT1 expression been reported as the most elevated in the cortex (175). This is consistent with our results, revealing MALAT1 as the most abundant out of all analyzed lncRNAs, further that samples from the cortex showed the uppermost expression.

Hyperoxic reoxygenation

MALAT1 expression was analyzed in samples from the cortex of piglets exposed to hyperoxic reoxygenation. Statistical tests did not reveal a significant difference between the groups. Nevertheless, MALAT1 expression appeared to be changed in a similar pattern like ANRIL. We observed a high with-in group variability and the expression between the treatment groups appear to be somewhat similar. Although it is a very rough assumption, this was also observed in the normoxic and control group between the different brain regions. Both lncRNAs are hypoxia-associated (HALs) with hypoxia response elements (HREs) in their promoter. The reason for their comparable expression patterns is uncertain; however, a recent study on the latter lncRNAs and their clinical potential in glaucoma patients demonstrated a similar

expression pattern between the two and reported their diagnostic value as higher combined than alone (176). The study also revealed that both ANRIL and MALAT1 expression was attenuated similarly in glaucoma patients and correlated with the pathological staging indicating a more severe progression. Taking these findings together, they might add support to the earlier, vaguely stated hypothesis that ANRIL is inversely correlated with the severity of hypoxia-ischemia reoxygenation, as well as MALAT1. On the other hand, the experimental protocol, conditions, and material between the latter studies, our results, and their correlation should be interpreted with caution. Thus, further tests with MALAT1 and ANRIL should be conducted to further investigate their connection and determine if it is related to the severity of neonatal hypoxia-ischemia.

5.2.5 H19 Imprinted Maternally Expressed Transcript (H19)

Normoxic reoxygenation

H19 might be one of the most well-studied lncRNAs to this date. Publications have related H19 expression variations to hypoxia and ischemic stroke (108, 110), suggesting a potential therapeutic role in the latter (177). Consistent with our results from samples taken from the cortex and white matter, several studies have observed an increase in H19 after HI and ischemia *in-vivo* and *in-vitro* (104, 106, 107). The lncRNA has been reported to induce hypoxia-reoxygenation injury in hepatoma carcinoma cells (178), as well as suggested to protect H9c2 cells against hypoxia-induced injury (179, 180). In patients suffering from ischemic stroke, H19 expression in plasma was positively correlated to the severity of the insult (177, 181) and inhibition of H19 in mice significantly decreased brain volume loss (181), brain edema, and infarct volume (177). A recent article stated that H19 expression was decreased in rats suffering from hypoxic-ischemic brain damage and that its over-expression resulted in VEGFA increase and repressed neuronal apoptosis and alleviated cognitive dysfunction (182). The various roles of H19 described here are also reflected in cancer, reporting contradictory features at the same time (105).

Hyperoxic reoxygenation

Performing ANOVA and posthoc test Tukey´s on the latter groups, the means of each group were not significantly different from each other or the control group. Nevertheless, we

observed a tendency to increased levels in the hypoxia groups. Therefore, the values from qPCR and ddPCR were analyzed again with post hoc test Dunnett´s to compare the means of expression in the hypoxia groups to only the mean of the control group. This test did not reveal a significant increase in H19 expression. However, the hypoxia group exposed to hyperoxic reoxygenation for 3 minutes was borderline significant in the results from both qPCR and ddPCR. Although the increase was not significant, the results are still interesting and might add additional support to the findings described above as well as other studies on hyperoxic reoxygenation.

Comparing the qPCR and ddPCR method

H19 expression was first analyzed in the normoxic, hyperoxic and control groups by qPCR and later on determined by a second, independent method (ddPCR) confirming the previous achieved results (a Pearson correlation test determined a strong positive correlation between the two techniques).

5.2.6 Brain-derived neurotrophic factor antisense (BDNF-AS)

BDNF-AS is the antisense to the target gene BDNF. A recent study demonstrated that knock-down of BDNF-AS increased BDNF, and thus improved neurological function (86). The molecule has been suggested to have an important role in the regulation of BDNF expression in humans (101) and to be a viable treatment target of hypoxia/ischemia-induced brain damage (86). Despite this interest, there has not been enough evidence to support the role of BDNF-AS in HI, and its exact function in this context has not yet been established.

Normoxic reoxygenation

Our data illustrate that BDNF-AS is significantly up-regulated in samples from the cortex, and a similar trend is observed in the hippocampus and cerebellum samples. Similar to our results of BDNF expression, BDNF-AS expression is elevated in the majority of probes from the hippocampus and the cerebellum. This is consistent with other studies demonstrating significant up-regulation of BDNF-AS (54, 86).

Hyperoxic reoxygenation

Based on the Pearson Correlation test, BDNF-AS expression in the normoxic, hyperoxic, and control groups, analyzed by both qPCR, and ddPCR, were strongly positively correlated. Thus, any further mentioning of BDNF-AS results is concerning the values obtained from ddPCR unless stated otherwise.

The expression patterns of BDNF-AS in the normoxic and hyperoxic groups were significantly increased compared to the control. Additionally, the enhancement in the group exposed to 30 minutes of hyperoxic reoxygenation was determined as being more significant compared to the other treatment groups. Since BDNF-AS has been shown to regulate BDNF expression in response to hypoxia-ischemia, including an inverse correlation (54, 86), our results are in line with Solberg et al. (2010). The latter study demonstrated that BDNF expression stepwise decreased when resuscitated with supplementary oxygen in a dose dependent manner (17), as we have demonstrated that BDNF-AS increase when resuscitated with supplementary oxygen. A decrease in BDNF expression has been associated with lower levels of protective mechanisms and an increase in hypoxic and oxidative stress (86). The effects of supplementary oxygen in the resuscitation of term infants have been widely studied in animal models, demonstrating an increase of oxidative stress resulting in DNA damage and epigenetic changes (3, 16-21). We suggest that the more significant increase of BDNF-AS expression in the latter group is due to increased oxidative and hypoxic stress levels, as demonstrated by Qiao et al (2020) in hippocampal neurons (86).

Even though ILCOR has since 2010 recommended resuscitation of newborns with an initial 21% oxygen, 100% oxygen is still recommended if there is a need for chest compressions. Since the antioxidant defense is immature in term newborns, and that brain tissue has been reported as particularly sensitive to oxidative stress, resuscitation with 100% oxygen in term newborns may results in severe short and long-term consequences as suggested by others.

In summary, we suggest that changes in the expression of BDNF-AS should be further investigated to verify if this lncRNA could serve as a biomarker for oxidative stress damage and predict the severity of neonatal hypoxia-ischemia in the future. These results also provide important additional support regarding oxidative brain injury caused by hyperoxic reoxygenation.

5.3 A comparison of gene expression across brain regions

The gene expression of coding and non-coding hypoxia-associated genes were analyzed in different regions of the brain (Table 5-1). The diversity in expression between the various lncRNAs and brain regions possibly reflects of their tissue specificity reported in other studies (87, 88). Moreover, while samples from the cortex, hippocampus and cerebellum are considered as clean and not contaminated with other brain regions, there is a possibility that tissue samples from white matter are slightly contaminated. This is caused by the collection procedure. Collecting samples from white matter is technically more difficult and requires more precision compared to tissue samples from the other brain regions. Thus, the results in this study associated with this brain region should be interpreted with caution.

Table 5-1. Gene expression comparison across brain regions in a neonatal hypoxia-ischemia piglet model, showing the total amount of tissues and mRNA/lncRNA with altered expression.

Gene expression in various brain regions after hypoxic exposure					
mRNA	**Cortex**	**Hippocampus**	**White Matter**	**Cerebellum**	**Total**
HIF1a	-	-	-	-	**0/4**
VEGFA	↑**	↑****	-	↑****	**3/4**
BDNF	↑*	↑	↑	-	**3/4**
p53	-	-	-	-	**0/4**
TNFa	↑	-	-	↑*	**2/4**
LncRNA					
BDNF-AS	↑*	-	-	↑	**2/4**
H19	↑*	↑	↑*	-	**3/4**
MALAT1	-	↑*	-	-	**1/4**
ANRIL	-	-	-	↑*	**1/4**
TUG1	↓	↓*	N/A	N/A	**2/4**
PANDA	-	-	N/A	N/A	**0/4**
Total	**6/11**	**5/11**	**2/9**	**4/9**	

Abbreviations: BDNF-AS, Brain-derived neurotrophic factor antisense; H19, H19 Imprinted Maternally Expressed Transcript; MALAT1, metastasis-associated lung adenocarcinoma transcript 1; ANRIL, Antisense Noncoding RNA in the INK4 Locus; ↑, observed increase in expression; P<.05=; P<.01=**; P<.0001=****.*

5.4 Methodological aspects

5.4.1 The neonatal hypoxia-ischemia piglet model

Pigs are very similar to humans on a genetic, brain developmental, physiological and organic matter. This evolutionary relationship comprises also other aspects, pigs show, like humans, genetic diversity among individuals, reflected in the variation of expression patterns (183-185). The observed variations are methodological challenging for molecular biology research,

requiring a high number of individuals and study ground to keep SD low, but thus the more realistic to the actual situation we are facing in the neonatal hypoxia-ischemia in the clinic. In contrast, rodent models used for research are often inbred, and therefore have little genetic diversity. Thus, new results achieved by using a piglet model may be transferred more easily to humans in comparison to outcome achieved by using a rodent model. However, the genetic diversity in this study can also be seen as a disadvantage. Its presence might be the results of underlying biological differences and thus more challenging to detect treatment effects, especially in cohort composed by a smaller population size. The number of animals is also a disadvantage when using a pigs model. Usually, in animal studies, a power analysis is used to determine the sample size needed to obtain the real effect in the experiment without wasting unnecessary resources and animals, which may lead to ethical issues. Here, we present an exploratory study, and consequently the sample size recommended by the power analysis has not been emphasized to such an extent. Instead, emphasis has been placed on resources, costs, and ethical issues. In this study, a total of 42 piglets were included for the experimental procedure, and six piglets were excluded from the study due to death or abnormalities observed within the piglets in the autopsy. This resulted in around 10 pigs per group, which is fewer piglets than the power analysis would recommend. However, this is more than the six animals per group that other studies have deemed sufficient (186). Furthermore, the use of pigs in research requires more resources and funding than smaller animals or cell cultures. The sample size used in this study was also influenced by the ethical issue of using a larger sample size for larger research animals.

5.4.2 Gene expression analysis

Quantitative real-time PCR

qPCR is described as the “golden standard” for gene expression measurements. Normalization in qPCR is essential to correct for variations between samples and applying three or more reference genes is commonly accepted as the most appropriate normalization strategy. However, here in this thesis, only one reference gene has been used. MIQE guidelines highlight that the use of a single reference gene should be avoided unless it is provided evidence that the expression of the reference gene is stable under the experimental condition (187). Nygard et al. (2007) conducted a study to investigate commonly used reference genes

in different pig tissues, such as the cerebral cortex, hippocampus, and cerebellum, using qPCR with SYBR Green. TBP was determined as a good reference gene in expression studies across different tissues, especially for low abundant transcripts (188), such as lncRNA. The results were also consistent with reports from Erkens et al. (2006) in different types of pig tissue (189). Consequently, only one reference gene was used in this study. In addition, the large number of samples and experiments, being expensive and time-consuming, restricted somehow the practical performance of many additional references. The number of replicates used was also limited to only two, which is common, although three replicates are often seen as standard. Nonetheless, we used an independent method (ddPCR) to validate our results and thus reinforce our findings. In future studies, one may consider to use additional reference genes and technical replicates. This will decrease the variations and variability, thus strengthen the results.

Droplet digital PCR

It is a high scientific standard to confirm achieved results by an independent method. We decided to validate our findings by measuring the same samples applying the ddPCR technique. Another advantage of the ddPCR technique is its principle to detect low abundant levels of RNA and to detect smaller gene expression differences and thus, more statistically significant results. The partitioning of samples and use of Poisson statistics allows a simplified quantification and do not require the use of technical replicates, standard curves, or normalization. However, for measuring gene expression, the use of normalization and technical replicates are recommended (155). In this thesis, normalization with endogenous control and two technical replicates were used to produce more precise and reproducible results. Although qPCR is regarded as the gold standard for the measurement of gene expression, the ddPCR technology offers several advantages and benefits. As mentioned above, ddPCR enables quantification of low abundant targets and can detect smaller gene expression differences. Since lncRNA is regarded being a low-abundant transcript, we hypothesized that ddPCR could better differentiate between normoxic and hyperoxic reoxygenation in gene expression compared to qPCR. Additionally, ddPCR has been demonstrated to show high resilience to PCR inhibitors (190). Since the RNA samples used in this thesis have been reversed transcribed for downstream analysis, it is possible that components from this reaction also can act as inhibitors of Taq polymerase. This could lead to

altered efficiency and artefactual qPCR data (191). By using ddPCR, we reduced the probability of this outcome as well as strengthened our results. Nevertheless, our results from qPCR and ddPCR were strongly correlated and did not appear to be affected by inhibitors.

5.4.3 Other aspects and limitations

The corona situation was a challenge for all of us, setting some limitations concerning distribution of chemicals and equipment, access to lab facilities and other resources. However, we were able to overcome or bypass these restrictions choosing alternative strategies and order of experiments, times in the lab, and zoom meetings.

Neonatal hypoxia-ischemia piglet model

The present study has investigated expression patterns in a neonatal hypoxic-ischemic piglet model 9,5 hours after the hypoxic insult. This strategy is common and the only available procedure with our lab facilities. However, we are aware that this shorter follow-up time has its limitations. Thus, we would like to suggest enlarging the current findings in other time frames in the context of perinatal hypoxia-ischemia using an additional model system like mice.

After note: At the final stage of the writing procedure, it was discovered that piglet nr. 22 had suffered an early death. It was not enough time to exclude the latter from the results and to rerun the entire analysis of the study. Nevertheless, we did not observe P22 as an outlier in our results, and do not believe the exclusion of this piglet would significantly affect the results in this thesis.

As previously mentioned in chapter 4.1.1, NanoDrop measurements from some of the samples were not within the acceptable A260/230 ratio determining relative amount of contaminants. Studies have shown that components used for RNA isolations are absorbed around 230 or 260 nm and may be the reason for this contamination; however, the samples were not excluded since we did not observe any outliers that would significantly alter our results. Additionally, cortex samples were assessed using RNA integrity assay determining

degradation and samples with a RIN-value below 5 were excluded. RNA integrity was not assessed in samples from the hippocampus, white matter and cerebellum.

6. Conclusion and future aspects

6.1 Conclusion

This comprehensive study combines multiple approaches, including the use of an established model system, applied bioinformatics, quality assessments, statistical methods and comparison of two independent methods (qPCR and ddPCR) in an attempt to ensure high quality research. The overall aim of this study was to explore specific lncRNAs as potential markers for the severity of neonatal hypoxia-ischemia, and the conclusion of this study is summarized with regard to the objectives.

1. We present one of the first studies demonstrating expression changes of selected hypoxia- and oxidative stress-associated lncRNAs in a neonatal hypoxic-ischemic setting. Also, to our best knowledge, this is the first time BDNF-AS, ANRIL, TUG1 and PANDA expression has been confirmed in pigs.
2. Using a neonatal hypoxic-ischemic piglet model, the selected lncRNAs BDNF-AS, H19, MALAT1, ANRIL, TUG1, and PANDA, were detected by qPCR in samples from the cortex, hippocampus, white matter, and cerebellum.
3. Exposure to hypoxia-ischemia caused significantly alteration in lncRNA expression (except for PANDA), mainly in the cortex and hippocampus.
4. However, expression levels and significance of altered expression varied for individual lncRNAs and among the various brain regions. MALAT1 was the most abundant lncRNA in all regions, followed by TUG1 and PANDA.
5. Interestingly, not only a decrease, but also an impulse of excess oxygen after the hypoxic event causes changes in the expression levels of BDNF-AS, H19, MALAT1, and ANRIL. Even for BDNF-AS in a time-dependent manner, providing further evidence for oxidative brain injury caused by hyperoxic reoxygenation in newborns. Our results suggest further investigations of the tested lncRNAs as potential novel biomarkers to predict the severity of neonatal hypoxia-ischemia in the future.

6.2 Future aspects

Despite extensive research concerning lncRNAs and hypoxic-ischemic encephalopathy during the last decade, several concerns about their relationship and therapeutic importance remain unanswered. To further our research, we intend to expand on the findings presented here and place them in a greater perspective:

1. Examine the differentiated expression of lncRNAs in other organs and related body fluids, such as blood, urine, and cerebrospinal fluid, in the same piglets as well as in other related cohorts. Additionally, we suggest to study lncRNA expression in a neonatal hypoxic-ischemic murine model.

2. Perform RNA FISH to investigate the localization and expression of lncRNA in the other brain halves of the same piglets.

3. Explore the potential relationship between lncRNA, miRNA, and cell-free DNA in association to neonatal hypoxia-ischemia.

4. Extend the methodological analyzes and investigate lncRNA expression in association with proteins, and perform whole transcriptome analyses to obtain a vaster insight into their pathways and mechanisms in a neonatal hypoxic-ischemic piglet model.

7. Contributions

Several collaborators have contributed with their field of expertise to this work. In a way, it is a prolongation of the ongoing hypoxia-reoxygenation work at the Department opening for a novel field, lncRNA regulation. The original idea to investigate lncRNA was generated by my supervisor, Lars O. Baumbusch, identifying the first lncRNA and deeply engaged with supervision and molecular expertise. Rønnaug Solberg conducted and supervised the piglet study, and greatly contributed with her knowledge on neonatal and perinatal hypoxia-ischemia. Ola Didrik Saugstad's engagement and research regarding resuscitation with room air versus supplementary oxygen in term and premature newborns was our inspiration for this thesis. Maria Melheim and Monica Atneosen-Åsegg conducted RNA extraction and primer testing of a pilot study prior to this thesis, and supported the thesis by general lab support. Weronika Przybyla, Sofie Strøm Andersen and Johanne Uthus Hermansen provided technical help in the lab. Finally, lab infrastructure, equipment and bench space was made available by the department head, Runar Almaas.

Reference list

1. Bryce J, Boschi-Pinto C, Shibuya K, Black RE, Group WHOCHER. WHO estimates of the causes of death in children. Lancet. 2005;365(9465):1147-52.
2. Perez M, Robbins ME, Revhaug C, Saugstad OD. Oxygen radical disease in the newborn, revisited: Oxidative stress and disease in the newborn period. Free Radic Biol Med. 2019;142:61-72.
3. Ramji S, Ahuja S, Thirupuram S, Rootwelt T, Rooth G, Saugstad OD. Resuscitation of asphyxic newborn infants with room air or 100% oxygen. Pediatr Res. 1993;34(6):809-12.
4. Ward DS, Karan SB, Pandit JJ. Hypoxia: developments in basic science, physiology and clinical studies. Anaesthesia. 2011;66 Suppl 2:19-26.
5. Douglas-Escobar M, Weiss MD. Hypoxic-ischemic encephalopathy: a review for the clinician. JAMA Pediatr. 2015;169(4):397-403.
6. Allen KA, Brandon DH. Hypoxic Ischemic Encephalopathy: Pathophysiology and Experimental Treatments. Newborn Infant Nurs Rev. 2011;11(3):125-33.
7. Woythaler M. Neurodevelopmental outcomes of the late preterm infant. Semin Fetal Neonatal Med. 2019;24(1):54-9.
8. Kleuskens DG, Goncalves Costa F, Annink KV, van den Hoogen A, Alderliesten T, Groenendaal F, et al. Pathophysiology of Cerebral Hyperperfusion in Term Neonates With Hypoxic-Ischemic Encephalopathy: A Systematic Review for Future Research. Front Pediatr. 2021;9:631258.
9. Saugstad OD. Oxidative stress in the newborn--a 30-year perspective. Biol Neonate. 2005;88(3):228-36.
10. Scarpato R, Testi S, Colosimo V, Garcia Crespo C, Micheli C, Azzara A, et al. Role of oxidative stress, genome damage and DNA methylation as determinants of pathological conditions in the newborn: an overview from conception to early neonatal stage. Mutat Res. 2020;783:108295.
11. Davalli P, Mitic T, Caporali A, Lauriola A, D'Arca D. ROS, Cell Senescence, and Novel Molecular Mechanisms in Aging and Age-Related Diseases. Oxid Med Cell Longev. 2016;2016:3565127.
12. Pizzino G, Irrera N, Cucinotta M, Pallio G, Mannino F, Arcoraci V, et al. Oxidative Stress: Harms and Benefits for Human Health. Oxid Med Cell Longev. 2017;2017:8416763.
13. Ozsurekci Y, Aykac K. Oxidative Stress Related Diseases in Newborns. Oxid Med Cell Longev. 2016;2016:2768365.
14. Cobley JN, Fiorello ML, Bailey DM. 13 reasons why the brain is susceptible to oxidative stress. Redox Biol. 2018;15:490-503.
15. Andresen JH, Saugstad OD. Oxygen metabolism and oxygenation of the newborn. Semin Fetal Neonatal Med. 2020;25(2):101078.
16. Saugstad OD, Ramji S, Irani SF, El-Meneza S, Hernandez EA, Vento M, et al. Resuscitation of newborn infants with 21% or 100% oxygen: follow-up at 18 to 24 months. Pediatrics. 2003;112(2):296-300.

17. Solberg R, Loberg EM, Andresen JH, Wright MS, Charrat E, Khrestchatisky M, et al. Resuscitation of newborn piglets. short-term influence of FiO2 on matrix metalloproteinases, caspase-3 and BDNF. PLoS One. 2010;5(12):e14261.
18. Solberg R, Andresen JH, Escrig R, Vento M, Saugstad OD. Resuscitation of hypoxic newborn piglets with oxygen induces a dose-dependent increase in markers of oxidation. Pediatr Res. 2007;62(5):559-63.
19. Vento M, Asensi M, Sastre J, Lloret A, Garcia-Sala F, Vina J. Oxidative stress in asphyxiated term infants resuscitated with 100% oxygen. J Pediatr. 2003;142(3):240-6.
20. Vento M, Asensi M, Sastre J, Garcia-Sala F, Pallardo FV, Vina J. Resuscitation with room air instead of 100% oxygen prevents oxidative stress in moderately asphyxiated term neonates. Pediatrics. 2001;107(4):642-7.
21. Vento M, Asensi M, Sastre J, Garcia-Sala F, Vina J. Six years of experience with the use of room air for the resuscitation of asphyxiated newly born term infants. Biol Neonate. 2001;79(3-4):261-7.
22. Madar J, Roehr CC, Ainsworth S, Ersdal H, Morley C, Rudiger M, et al. European Resuscitation Council Guidelines 2021: Newborn resuscitation and support of transition of infants at birth. Resuscitation. 2021;161:291-326.
23. Wyckoff MH, Aziz K, Escobedo MB, Kapadia VS, Kattwinkel J, Perlman JM, et al. Part 13: Neonatal Resuscitation: 2015 American Heart Association Guidelines Update for Cardiopulmonary Resuscitation and Emergency Cardiovascular Care. Circulation. 2015;132(18 Suppl 2):S543-60.
24. Escobedo MB, Aziz K, Kapadia VS, Lee HC, Niermeyer S, Schmolzer GM, et al. 2019 American Heart Association Focused Update on Neonatal Resuscitation: An Update to the American Heart Association Guidelines for Cardiopulmonary Resuscitation and Emergency Cardiovascular Care. Circulation. 2019;140(24):e922-e30.
25. Jacobs SE, Berg M, Hunt R, Tarnow-Mordi WO, Inder TE, Davis PG. Cooling for newborns with hypoxic ischaemic encephalopathy. Cochrane Database Syst Rev. 2013(1):CD003311.
26. Sabir H, Scull-Brown E, Liu X, Thoresen M. Immediate hypothermia is not neuroprotective after severe hypoxia-ischemia and is deleterious when delayed by 12 hours in neonatal rats. Stroke. 2012;43(12):3364-70.
27. Davidson JO, Wassink G, van den Heuij LG, Bennet L, Gunn AJ. Therapeutic Hypothermia for Neonatal Hypoxic-Ischemic Encephalopathy - Where to from Here? Front Neurol. 2015;6:198.
28. Pugh CW, Ratcliffe PJ. New horizons in hypoxia signaling pathways. Exp Cell Res. 2017;356(2):116-21.
29. Semenza GL. Hypoxia-inducible factor 1 (HIF-1) pathway. Sci STKE. 2007;2007(407):cm8.
30. Salceda S, Caro J. Hypoxia-inducible factor 1alpha (HIF-1alpha) protein is rapidly degraded by the ubiquitin-proteasome system under normoxic conditions. Its stabilization by hypoxia depends on redox-induced changes. J Biol Chem. 1997;272(36):22642-7.

31. Minet E, Ernest I, Michel G, Roland I, Remacle J, Raes M, et al. HIF1A gene transcription is dependent on a core promoter sequence encompassing activating and inhibiting sequences located upstream from the transcription initiation site and cis elements located within the 5'UTR. Biochem Biophys Res Commun. 1999;261(2):534-40.
32. Galban S, Kuwano Y, Pullmann R, Jr., Martindale JL, Kim HH, Lal A, et al. RNA-binding proteins HuR and PTB promote the translation of hypoxia-inducible factor 1alpha. Mol Cell Biol. 2008;28(1):93-107.
33. Forsythe JA, Jiang BH, Iyer NV, Agani F, Leung SW, Koos RD, et al. Activation of vascular endothelial growth factor gene transcription by hypoxia-inducible factor 1. Mol Cell Biol. 1996;16(9):4604-13.
34. English WR, Lunt SJ, Fisher M, Lefley DV, Dhingra M, Lee YC, et al. Differential Expression of VEGFA Isoforms Regulates Metastasis and Response to Anti-VEGFA Therapy in Sarcoma. Cancer Res. 2017;77(10):2633-46.
35. Kuo NT, Benhayon D, Przybylski RJ, Martin RJ, LaManna JC. Prolonged hypoxia increases vascular endothelial growth factor mRNA and protein in adult mouse brain. J Appl Physiol (1985). 1999;86(1):260-4.
36. Kaur C, Sivakumar V, Ang LS, Sundaresan A. Hypoxic damage to the periventricular white matter in neonatal brain: role of vascular endothelial growth factor, nitric oxide and excitotoxicity. J Neurochem. 2006;98(4):1200-16.
37. Aly H, Hassanein S, Nada A, Mohamed MH, Atef SH, Atiea W. Vascular endothelial growth factor in neonates with perinatal asphyxia. Brain Dev. 2009;31(8):600-4.
38. Huang EJ, Reichardt LF. Neurotrophins: roles in neuronal development and function. Annu Rev Neurosci. 2001;24:677-736.
39. Hofer M, Pagliusi SR, Hohn A, Leibrock J, Barde YA. Regional distribution of brain-derived neurotrophic factor mRNA in the adult mouse brain. EMBO J. 1990;9(8):2459-64.
40. Timmusk T, Palm K, Metsis M, Reintam T, Paalme V, Saarma M, et al. Multiple promoters direct tissue-specific expression of the rat BDNF gene. Neuron. 1993;10(3):475-89.
41. Schinder AF, Poo M. The neurotrophin hypothesis for synaptic plasticity. Trends Neurosci. 2000;23(12):639-45.
42. Bruna B, Lobos P, Herrera-Molina R, Hidalgo C, Paula-Lima A, Adasme T. The signaling pathways underlying BDNF-induced Nrf2 hippocampal nuclear translocation involve ROS, RyR-Mediated Ca(2+) signals, ERK and PI3K. Biochem Biophys Res Commun. 2018;505(1):201-7.
43. Kim J, Yang JH, Ryu IS, Sohn S, Kim S, Choe ES. Interactions of Glutamatergic Neurotransmission and Brain-Derived Neurotrophic Factor in the Regulation of Behaviors after Nicotine Administration. Int J Mol Sci. 2019;20(12).
44. Liu Y, Sun L, Huan Y, Zhao H, Deng J. Application of bFGF and BDNF to improve angiogenesis and cardiac function. J Surg Res. 2006;136(1):85-91.
45. Halade GV, Ma Y, Ramirez TA, Zhang J, Dai Q, Hensler JG, et al. Reduced BDNF attenuates inflammation and angiogenesis to improve survival and cardiac function

following myocardial infarction in mice. Am J Physiol Heart Circ Physiol. 2013;305(12):H1830-42.
46. Nakamura K, Martin KC, Jackson JK, Beppu K, Woo CW, Thiele CJ. Brain-derived neurotrophic factor activation of TrkB induces vascular endothelial growth factor expression via hypoxia-inducible factor-1alpha in neuroblastoma cells. Cancer Res. 2006;66(8):4249-55.
47. Zhao R, Wang X, Wang H, Yu T, Wang Q, Yang X, et al. Inhibition of long noncoding RNA BDNF-AS rescues cell death and apoptosis in hypoxia/reoxygenation damaged murine cardiomyocyte. Biochimie. 2017;138:43-9.
48. Coull JA, Beggs S, Boudreau D, Boivin D, Tsuda M, Inoue K, et al. BDNF from microglia causes the shift in neuronal anion gradient underlying neuropathic pain. Nature. 2005;438(7070):1017-21.
49. Connor B, Dragunow M. The role of neuronal growth factors in neurodegenerative disorders of the human brain. Brain Res Brain Res Rev. 1998;27(1):1-39.
50. Murer MG, Yan Q, Raisman-Vozari R. Brain-derived neurotrophic factor in the control human brain, and in Alzheimer's disease and Parkinson's disease. Prog Neurobiol. 2001;63(1):71-124.
51. Almeida LE, Roby CD, Krueger BK. Increased BDNF expression in fetal brain in the valproic acid model of autism. Mol Cell Neurosci. 2014;59:57-62.
52. Almli CR, Levy TJ, Han BH, Shah AR, Gidday JM, Holtzman DM. BDNF protects against spatial memory deficits following neonatal hypoxia-ischemia. Exp Neurol. 2000;166(1):99-114.
53. Cheng Y, Gidday JM, Yan Q, Shah AR, Holtzman DM. Marked age-dependent neuroprotection by brain-derived neurotrophic factor against neonatal hypoxic-ischemic brain injury. Ann Neurol. 1997;41(4):521-9.
54. Xu L, Zhang Z, Xie T, Zhang X, Dai T. Inhibition of BDNF-AS Provides Neuroprotection for Retinal Ganglion Cells against Ischemic Injury. PLoS One. 2016;11(12):e0164941.
55. Lane DP. Cancer. p53, guardian of the genome. Nature. 1992;358(6381):15-6.
56. Levine AJ. p53, the cellular gatekeeper for growth and division. Cell. 1997;88(3):323-31.
57. Vousden KH, Prives C. Blinded by the Light: The Growing Complexity of p53. Cell. 2009;137(3):413-31.
58. Levine AJ. The many faces of p53: something for everyone. J Mol Cell Biol. 2019;11(7):524-30.
59. Muller PA, Vousden KH, Norman JC. p53 and its mutants in tumor cell migration and invasion. J Cell Biol. 2011;192(2):209-18.
60. Liu J, Zhang C, Hu W, Feng Z. Tumor suppressor p53 and metabolism. J Mol Cell Biol. 2019;11(4):284-92.
61. Zhang C, Liu J, Xu D, Zhang T, Hu W, Feng Z. Gain-of-function mutant p53 in cancer progression and therapy. J Mol Cell Biol. 2020;12(9):674-87.
62. Hu W. The role of p53 gene family in reproduction. Cold Spring Harb Perspect Biol. 2009;1(6):a001073.

63. Levine AJ, Oren M. The first 30 years of p53: growing ever more complex. Nat Rev Cancer. 2009;9(10):749-58.
64. Koumenis C, Alarcon R, Hammond E, Sutphin P, Hoffman W, Murphy M, et al. Regulation of p53 by hypoxia: dissociation of transcriptional repression and apoptosis from p53-dependent transactivation. Mol Cell Biol. 2001;21(4):1297-310.
65. Cosse JP, Sermeus A, Vannuvel K, Ninane N, Raes M, Michiels C. Differential effects of hypoxia on etoposide-induced apoptosis according to the cancer cell lines. Mol Cancer. 2007;6:61.
66. Mahdavi Sharif P, Jabbari P, Razi S, Keshavarz-Fathi M, Rezaei N. Importance of TNF-alpha and its alterations in the development of cancers. Cytokine. 2020;130:155066.
67. Lau LT, Yu AC. Astrocytes produce and release interleukin-1, interleukin-6, tumor necrosis factor alpha and interferon-gamma following traumatic and metabolic injury. J Neurotrauma. 2001;18(3):351-9.
68. Walberer M, Rueger MA, Simard ML, Emig B, Jander S, Fink GR, et al. Dynamics of neuroinflammation in the macrosphere model of arterio-arterial embolic focal ischemia: an approximation to human stroke patterns. Exp Transl Stroke Med. 2010;2(1):22.
69. Chen CY, Sun WZ, Kang KH, Chou HC, Tsao PN, Hsieh WS, et al. Hypoxic Preconditioning Suppresses Glial Activation and Neuroinflammation in Neonatal Brain Insults. Mediators Inflamm. 2015;2015:632592.
70. Li X, Zhang J, Zhu X, Hou R, Li X, Dong X, et al. Effects of progesterone on hippocampal ultrastructure and expression of inflammatory mediators in neonatal rats with hypoxic-ischemic brain injury. Exp Ther Med. 2014;7(5):1311-6.
71. Bonestroo HJ, Nijboer CH, van Velthoven CT, Kavelaars A, Hack CE, van Bel F, et al. Cerebral and hepatic inflammatory response after neonatal hypoxia-ischemia in newborn rats. Dev Neurosci. 2013;35(2-3):197-211.
72. Liu F, McCullough LD. Inflammatory responses in hypoxic ischemic encephalopathy. Acta Pharmacol Sin. 2013;34(9):1121-30.
73. Kasdorf E, Perlman JM. Hyperthermia, inflammation, and perinatal brain injury. Pediatr Neurol. 2013;49(1):8-14.
74. Clamp M, Fry B, Kamal M, Xie X, Cuff J, Lin MF, et al. Distinguishing protein-coding and noncoding genes in the human genome. Proc Natl Acad Sci U S A. 2007;104(49):19428-33.
75. Boland CR. Non-coding RNA: It's Not Junk. Dig Dis Sci. 2017;62(11):3260.
76. Sun M, Kraus WL. From discovery to function: the expanding roles of long noncoding RNAs in physiology and disease. Endocr Rev. 2015;36(1):25-64.
77. Kour S, Rath PC. Age-Related Expression of a Repeat-Rich Intergenic Long Noncoding RNA in the Rat Brain. Mol Neurobiol 2017;54:639–60.
78. Grammatikakis I, Panda AC, Abdelmohsen K, M. G. Long noncoding RNAs (lncRNAs) and the molecular hallmarks of aging. Aging (Albany NY). 2014;6(12):992-1009.
79. Frankish A, Diekhans M, Jungreis I, Lagarde J, Loveland JE, Mudge JM, et al. Gencode 2021. Nucleic Acids Res. 2021;49(D1):D916-D23.

80. Kim C, Kang D, Lee EK, Lee J-S. Long Noncoding RNAs and RNA-Binding Proteins in Oxidative Stress, Cellular Senescence, and Age-Related Diseases. Oxidative Medicine and Cellular Longevity. 2017;2017:21.
81. Kuo TC, Kung HJ, Shih JW. Signaling in and out: long-noncoding RNAs in tumor hypoxia. J Biomed Sci. 2020;27(1):59.
82. Shih J-W, Kung H-J. Long non-coding RNA and tumor hypoxia: new players ushered toward an old arena. Journal of Biomedical Science. 2017;24(53):19.
83. Fuschi P, Maimone B, Gaetano C, Martelli F. Noncoding RNAs in the Vascular System Response to Oxidative Stress. Antioxid Redox Signal. 2019;30(7):992-1010.
84. Yin KJ, Hamblin M, Chen YE. Non-coding RNAs in cerebral endothelial pathophysiology: emerging roles in stroke. Neurochem Int. 2014;77:9-16.
85. Xin JW, Jiang YG. Long noncoding RNA MALAT1 inhibits apoptosis induced by oxygen-glucose deprivation and reoxygenation in human brain microvascular endothelial cells. Exp Ther Med. 2017;13(4):1225-34.
86. Qiao LX, Zhao RB, Wu MF, Zhu LH, Xia ZK. Silencing of long noncoding antisense RNA brainderived neurotrophic factor attenuates hypoxia/ischemiainduced neonatal brain injury. Int J Mol Med. 2020;46(2):653-62.
87. Ravasi T, Suzuki H, Pang KC, Katayama S, Furuno M, Okunishi R, et al. Experimental validation of the regulated expression of large numbers of non-coding RNAs from the mouse genome. Genome Res. 2006;16(1):11-9.
88. Garberg HT, Huun MU, Baumbusch LO, Asegg-Atneosen M, Solberg R, Saugstad OD. Temporal Profile of Circulating microRNAs after Global Hypoxia-Ischemia in Newborn Piglets. Neonatology. 2017;111(2):133-9.
89. Kung JT, Colognori D, Lee JT. Long noncoding RNAs: past, present, and future. Genetics. 2013;193(3):651-69.
90. Wang X, Shen C, Zhu J, Shen G, Li Z, Dong J. Long Noncoding RNAs in the Regulation of Oxidative Stress. Oxid Med Cell Longev. 2019;2019:1318795.
91. Gabory A, Jammes H, Dandolo L. The H19 locus: role of an imprinted non-coding RNA in growth and development. Bioessays. 2010;32(6):473-80.
92. Li X, Wang H, Yao B, Xu W, Chen J, Zhou X. lncRNA H19/miR-675 axis regulates cardiomyocyte apoptosis by targeting VDAC1 in diabetic cardiomyopathy. Sci Rep. 2016;6:36340.
93. Ji P, Diederichs S, Wang W, Boing S, Metzger R, Schneider PM, et al. MALAT-1, a novel noncoding RNA, and thymosin beta4 predict metastasis and survival in early-stage non-small cell lung cancer. Oncogene. 2003;22(39):8031-41.
94. Fang H, Li HF, He MH, Yan JY, Yang M, Zhang FX, et al. Long non-coding RNA MALAT1 sponges microRNA-429 to regulate apoptosis of hippocampal neurons in hypoxic-ischemic brain damage by regulating WNT1. Brain Res Bull. 2019;152:1-10.
95. Li X, Song Y, Liu F, Liu D, Miao H, Ren J, et al. Long Non-Coding RNA MALAT1 Promotes Proliferation, Angiogenesis, and Immunosuppressive Properties of Mesenchymal Stem Cells by Inducing VEGF and IDO. J Cell Biochem. 2017;118(9):2780-91.

96. Wei X, Wang C, Ma C, Sun W, Li H, Cai Z. Long noncoding RNA ANRIL is activated by hypoxia-inducible factor-1alpha and promotes osteosarcoma cell invasion and suppresses cell apoptosis upon hypoxia. Cancer Cell Int. 2016;16:73.
97. Su S, Liu J, He K, Zhang M, Feng C, Peng F, et al. Overexpression of the long noncoding RNA TUG1 protects against cold-induced injury of mouse livers by inhibiting apoptosis and inflammation. FEBS J. 2016;283(7):1261-74.
98. Hung T, Wang Y, Lin MF, Koegel AK, Kotake Y, Grant GD, et al. Extensive and coordinated transcription of noncoding RNAs within cell-cycle promoters. Nature Genetics. 2011;43(7):621-9.
99. Li Y, Xu F, Xiao H, Han F. Long noncoding RNA BDNF-AS inversely regulated BDNF and modulated high-glucose induced apoptosis in human retinal pigment epithelial cells. J Cell Biochem. 2018;119(1):817-23.
100. Burgess S. Antisense National Human Genome Research Institute, NIH, Available from: https://www.genome.gov/genetics-glossary/antisense.
101. Pruunsild P, Kazantseva A, Aid T, Palm K, Timmusk T. Dissecting the human BDNF locus: bidirectional transcription, complex splicing, and multiple promoters. Genomics. 2007;90(3):397-406.
102. Genome Browser. UCSC Genomics Institute. 2013 [cited 16.05.21]. Available from: https://genome.ucsc.edu/cgi-bin/hgTracks?db=hg38&lastVirtModeType=default&lastVirtModeExtraState=&virtModeType=default&virtMode=0&nonVirtPosition=&position=chr11%3A27506845%2D27694128&hgsid=1108987361_oIIfevVyOXzAeYYa6AjMlAaMNPk1.
103. Modarresi F, Faghihi MA, Lopez-Toledano MA, Fatemi RP, Magistri M, Brothers SP, et al. Inhibition of natural antisense transcripts in vivo results in gene-specific transcriptional upregulation. Nat Biotechnol. 2012;30(5):453-9.
104. Matouk IJ, DeGroot N, Mezan S, Ayesh S, Abu-lail R, Hochberg A, et al. The H19 non-coding RNA is essential for human tumor growth. PLoS One. 2007;2(9):e845.
105. Tsang WP, Ng EK, Ng SS, Jin H, Yu J, Sung JJ, et al. Oncofetal H19-derived miR-675 regulates tumor suppressor RB in human colorectal cancer. Carcinogenesis. 2010;31(3):350-8.
106. Matouk IJ, Mezan S, Mizrahi A, Ohana P, Abu-Lail R, Fellig Y, et al. The oncofetal H19 RNA connection: hypoxia, p53 and cancer. Biochim Biophys Acta. 2010;1803(4):443-51.
107. Wu W, Hu Q, Nie E, Yu T, Wu Y, Zhi T, et al. Hypoxia induces H19 expression through direct and indirect Hif-1alpha activity, promoting oncogenic effects in glioblastoma. Sci Rep. 2017;7:45029.
108. Wang J, Zhao H, Fan Z, Li G, Ma Q, Tao Z, et al. Long Noncoding RNA H19 Promotes Neuroinflammation in Ischemic Stroke by Driving Histone Deacetylase 1-Dependent M1 Microglial Polarization. Stroke. 2017;48(8):2211-21.
109. Yuan Y, Li X, Chu Y, Ye G, Yang L, Dong Z. Long Non-coding RNA H19 Augments Hypoxia/Reoxygenation-Induced Renal Tubular Epithelial Cell Apoptosis and Injury by the miR-130a/BCL2L11 Pathway. Front Physiol. 2021;12:632398.

110. Xiao Z, Qiu Y, Lin Y, Medina R, Zhuang S, Rosenblum JS, et al. Blocking lncRNA H19-miR-19a-Id2 axis attenuates hypoxia/ischemia induced neuronal injury. Aging (Albany NY). 2019;11(11):3585-600.
111. Eissmann M, Gutschner T, Hammerle M, Gunther S, Caudron-Herger M, Gross M, et al. Loss of the abundant nuclear non-coding RNA MALAT1 is compatible with life and development. RNA Biol. 2012;9(8):1076-87.
112. Zhang X, Hamblin MH, Yin KJ. The long noncoding RNA Malat1: Its physiological and pathophysiological functions. RNA Biol. 2017;14(12):1705-14.
113. Goyal B, Yadav SRM, Awasthee N, Gupta S, Kunnumakkara AB, Gupta SC. Diagnostic, prognostic, and therapeutic significance of long non-coding RNA MALAT1 in cancer. Biochim Biophys Acta Rev Cancer. 2021;1875(2):188502.
114. Fouad YA, Aanei C. Revisiting the hallmarks of cancer. Am J Cancer Res. 2017;7(5):1016-36.
115. Patel NA, Moss LD, Lee JY, Tajiri N, Acosta S, Hudson C, et al. Long noncoding RNA MALAT1 in exosomes drives regenerative function and modulates inflammation-linked networks following traumatic brain injury. J Neuroinflam. 2018;15(1):204.
116. Zhang X, Tang X, Liu K, Hamblin MH, Yin KJ. Long Noncoding RNA Malat1 Regulates Cerebrovascular Pathologies in Ischemic Stroke. J Neurosci. 2017;37(7):1797-806.
117. Yang L, Xu F, Zhang M, Shang XY, Xie X, Fu T, et al. Role of LncRNA MALAT-1 in hypoxia-induced PC12 cell injury via regulating p38MAPK signaling pathway. Neurosci Lett. 2018;670:41-7.
118. Cardamone G, Paraboschi EM, Solda G, Cantoni C, Supino D, Piccio L, et al. Not only cancer: the long non-coding RNA MALAT1 affects the repertoire of alternatively spliced transcripts and circular RNAs in multiple sclerosis. Hum Mol Genet. 2019;28(9):1414-28.
119. Aguilo F, Zhou MM, Walsh MJ. Long noncoding RNA, polycomb, and the ghosts haunting INK4b-ARF-INK4a expression. Cancer Res. 2011;71(16):5365-9.
120. Liu P, Zhang M, Niu Q, Zhang F, Yang Y, Jiang X. Knockdown of long non-coding RNA ANRIL inhibits tumorigenesis in human gastric cancer cells via microRNA-99a-mediated down-regulation of BMI1. Braz J Med Biol Res. 2018;51(10):e6839.
121. Zhang B, Wang D, Ji TF, Shi L, Yu JL. Overexpression of lncRNA ANRIL up-regulates VEGF expression and promotes angiogenesis of diabetes mellitus combined with cerebral infarction by activating NF-kappaB signaling pathway in a rat model. Oncotarget. 2017;8(10):17347-59.
122. Feng L, Guo J, Ai F. Circulating long noncoding RNA ANRIL downregulation correlates with increased risk, higher disease severity and elevated pro-inflammatory cytokines in patients with acute ischemic stroke. J Clin Lab Anal. 2019;33(1):e22629.
123. Lewandowski JP, Dumbovic G, Watson AR, Hwang T, Jacobs-Palmer E, Chang N, et al. The Tug1 lncRNA locus is essential for male fertility. Genome Biol. 2020;21(1):237.
124. Yu X, Hu L, Li S, Shen J, Wang D, Xu R, et al. Long non-coding RNA Taurine upregulated gene 1 promotes osteosarcoma cell metastasis by mediating HIF-1alpha via miR-143-5p. Cell Death Dis. 2019;10(4):280.

125. Zhou H, Sun L, Wan F. Molecular mechanisms of TUG1 in the proliferation, apoptosis, migration and invasion of cancer cells. Oncol Lett. 2019;18(5):4393-402.
126. Wang X, Chen X, Zhang D, Yang G, Yang Z, Yin Z, et al. Prognostic and clinicopathological role of long non-coding RNA taurine upregulated 1 in various human malignancies: A systemic review and meta-analysis. Tumour Biol. 2017;39(7):1010428317714361.
127. Shan W, Chen W, Zhao X, Pei A, Chen M, Yu Y, et al. Long noncoding RNA TUG1 contributes to cerebral ischaemia/reperfusion injury by sponging mir-145 to up-regulate AQP4 expression. J Cell Mol Med. 2020;24(1):250-9.
128. Lin PC, Huang HD, Chang CC, Chang YS, Yen JC, Lee CC, et al. Long noncoding RNA TUG1 is downregulated in non-small cell lung cancer and can regulate CELF1 on binding to PRC2. BMC Cancer. 2016;16:583.
129. Yang L, Lin C, Liu W, Zhang J, Ohgi KA, Grinstein JD, et al. ncRNA- and Pc2 methylation-dependent gene relocation between nuclear structures mediates gene activation programs. Cell. 2011;147(4):773-88.
130. Chen L, Xu JY, Tan HB. LncRNA TUG1 regulates the development of ischemia-reperfusion mediated acute kidney injury through miR-494-3p/E-cadherin axis. J Inflamm. 2021;18(1):12.
131. Kotake Y, Goto T, Naemura M, Inoue Y, Okamoto H, Tahara K. Long Noncoding RNA PANDA Positively Regulates Proliferation of Osteosarcoma Cells. Anticancer Res. 2017;37(1):81-5.
132. Permuth JB, Chen DT, Yoder SJ, Li J, Smith AT, Choi JW, et al. Linc-ing Circulating Long Non-coding RNAs to the Diagnosis and Malignant Prediction of Intraductal Papillary Mucinous Neoplasms of the Pancreas. Sci Rep. 2017;7(1):10484.
133. Goureau A, Garrigues A, Tosser-Klopp G, Lahbib-Mansais Y, Chardon P, Yerle M. Conserved synteny and gene order difference between human chromosome 12 and pig chromosome 5. Cytogenet Cell Genet. 2001;94(1-2):49-54.
134. Dobbing J, Sands J. Comparative aspects of the brain growth spurt. Early Hum Dev. 1979;3((1)):79-83.
135. Conrad MS, Dilger RN, Johnson RW. Brain growth of the domestic pig (Sus scrofa) from 2 to 24 weeks of age: a longitudinal MRI study. Dev Neurosci. 2012;34(4):291-8.
136. Conrad MS, Johnson RW. The domestic piglet: an important model for investigating the neurodevelopmental consequences of early life insults. Annu Rev Anim Biosci. 2015;3:245-64.
137. Schachtschneider KM, Madsen O, Park C, Rund LA, Groenen MA, Schook LB. Adult porcine genome-wide DNA methylation patterns support pigs as a biomedical model. BMC Genomics. 2015;16:743.
138. Thibault KL, Margulies SS. Age-dependent material properties of the porcine cerebrum: effect on pediatric inertial head injury criteria. J Biomech. 1998;31(12):1119-26.
139. Dickerson JW, Dobbing J. Prenatal and postnatal growth and development of the central nervous system of the pig. Proc R Soc Lond B Biol Sci. 1967;166(1005):384-95.

140. Kyng KJ, Skajaa T, Kerrn-Jespersen S, Andreassen CS, Bennedsgaard K, Henriksen TB. A Piglet Model of Neonatal Hypoxic-Ischemic Encephalopathy. J Vis Exp. 2015(99):e52454.
141. Rezai K, Andreasen NC, Alliger R, Cohen G, Swayze V, 2nd, O'Leary DS. The neuropsychology of the prefrontal cortex. Arch Neurol. 1993;50(6):636-42.
142. Jose RG, Samuel AS, Isabel MM. Neuropsychology of executive functions in patients with focal lesion in the prefrontal cortex: A systematic review. Brain Cogn. 2020;146:105633.
143. Morecraft RJ, H.Yeterian E. Prefrontal Cortex. In: Ramachandran VS, editor. Encyclopedia of the Human Brain. Academic Press: Elsevier; 2002. p. 11-26.
144. Anand KS, Dhikav V. Hippocampus in health and disease: An overview. Ann Indian Acad Neurol. 2012;15(4):239-46.
145. Cooper JM, Gadian DG, Jentschke S, Goldman A, Munoz M, Pitts G, et al. Neonatal hypoxia, hippocampal atrophy, and memory impairment: evidence of a causal sequence. Cereb Cortex. 2015;25(6):1469-76.
146. Neves K. White Matter Expansion. 2017. In: Evolution of Nervous Systems [Internet]. Elsevier: Academic Press; [291-308]. Available from: https://www.sciencedirect.com/science/article/pii/B9780128040423000476.
147. Fields RD. Neuroscience. Change in the brain's white matter. Science. 2010;330(6005):768-9.
148. Torres-Cuevas I, Corral-Debrinski M, Gressens P. Brain oxidative damage in murine models of neonatal hypoxia/ischemia and reoxygenation. Free Radic Biol Med. 2019;142:3-15.
149. Walsh K, L.Parker K. The Role of the Cerebellum in Cognitive and Affective Processes. Reference Module in Biomedical Sciences [Internet]. 2018. Available from: https://www.sciencedirect.com/science/article/pii/B9780128012383998052.
150. Bouet V, Dijk F, Ijkema-Paassen J, Wubbels RJ, van der Want JJ, Gramsbergen A. Early hypergravity exposure effects calbindin-D28k and inositol-3-phosphate expression in Purkinje cells. Neurosci Lett. 2005;382(1-2):10-5.
151. Wang VY, Zoghbi HY. Genetic regulation of cerebellar development. Nat Rev Neurosci. 2001;2(7):484-91.
152. Welsh JP, Yuen G, Placantonakis DG, Vu TQ, Haiss F, O'Hearn E, et al. Why do Purkinje cells die so easily after global brain ischemia? Aldolase C, EAAT4, and the cerebellar contribution to posthypoxic myoclonus. Adv Neurol. 2002;89:331-59.
153. Quan PL, Sauzade M, Brouzes E. dPCR: A Technology Review. Sensors (Basel). 2018;18(4).
154. Svec D, Tichopad A, Novosadova V, Pfaffl MW, Kubista M. How good is a PCR efficiency estimate: Recommendations for precise and robust qPCR efficiency assessments. Biomol Detect Quantif. 2015;3:9-16.
155. Taylor SC, Laperriere G, Germain H. Droplet Digital PCR versus qPCR for gene expression analysis with low abundant targets: from variable nonsense to publication quality data. Sci Rep. 2017;7(1):2409.

156. Hindson BJ, Ness KD, Masquelier DA, Belgrader P, Heredia NJ, Makarewicz AJ, et al. High-throughput droplet digital PCR system for absolute quantitation of DNA copy number. Anal Chem. 2011;83(22):8604-10.
157. Dube S, Qin J, Ramakrishnan R. Mathematical analysis of copy number variation in a DNA sample using digital PCR on a nanofluidic device. PLoS One. 2008;3(8):e2876.
158. Zmienko A, Samelak-Czajka A, Goralski M, Sobieszczuk-Nowicka E, Kozlowski P, Figlerowicz M. Selection of reference genes for qPCR- and ddPCR-based analyses of gene expression in Senescing Barley leaves. PLoS One. 2015;10(2):e0118226.
159. Heredia NJ, Belgrader P, Wang S, Koehler R, Regan J, Cosman AM, et al. Droplet Digital PCR quantitation of HER2 expression in FFPE breast cancer samples. Methods. 2013;59(1):S20-3.
160. Benterud T, Pankratov L, Solberg R, Bolstad N, Skinningsrud A, Baumbusch L, et al. Perinatal Asphyxia May Influence the Level of Beta-Amyloid (1-42) in Cerebrospinal Fluid: An Experimental Study on Newborn Pigs. PLoS One. 2015;10(10):e0140966.
161. Gupta SK, Haigh BJ, Griffin FJ, Wheeler TT. The mammalian secreted RNases: mechanisms of action in host defence. Innate Immun. 2013;19(1):86-97.
162. Morrison TB, Weis JJ, Wittwer CT. Quantification of low-copy transcripts by continuous SYBR Green I monitoring during amplification. Biotechniques. 1998;24(6):954-8, 60, 62.
163. Madan E, Parker TM, Pelham CJ, Palma AM, Peixoto ML, Nagane M, et al. HIF-transcribed p53 chaperones HIF-1alpha. Nucleic Acids Res. 2019;47(19):10212-34.
164. Wang Y, Pakunlu RI, Tsao W, Pozharov V, Minko T. Bimodal effect of hypoxia in cancer: role of hypoxia inducible factor in apoptosis. Mol Pharm. 2004;1(2):156-65.
165. Hedtjarn M, Mallard C, Eklind S, Gustafson-Brywe K, Hagberg H. Global gene expression in the immature brain after hypoxia-ischemia. J Cereb Blood Flow Metab. 2004;24(12):1317-32.
166. Xing Y, Wang R, Chen D, Mao J, Shi R, Wu Z, et al. COX2 is involved in hypoxia-induced TNF-alpha expression in osteoblast. Sci Rep. 2015;5:10020.
167. Sjostedt E, Zhong W, Fagerberg L, Karlsson M, Mitsios N, Adori C, et al. An atlas of the protein-coding genes in the human, pig, and mouse brain. Science. 2020;367(6482).
168. Gao C, Zhang CC, Yang HX, Hao YN. MALAT1 Protected the Angiogenesis Function of Human Brain Microvascular Endothelial Cells (HBMECs) Under Oxygen Glucose Deprivation/re-oxygenation (OGD/R) Challenge by Interacting with miR-205-5p/VEGFA Pathway. Neuroscience. 2020;435:135-45.
169. Ma IT, McConaghy S, Namachivayam K, Halloran BA, Kurundkar AR, MohanKumar K, et al. VEGF mRNA and protein concentrations in the developing human eye. Pediatr Res. 2015;77(4):500-5.
170. Meng H, Song Y, Zhu J, Liu Q, Lu P, Ye N, et al. LRG1 promotes angiogenesis through upregulating the TGFbeta1 pathway in ischemic rat brain. Mol Med Rep. 2016;14(6):5535-43.

171. Navarro-Sobrino M, Rosell A, Hernandez-Guillamon M, Penalba A, Boada C, Domingues-Montanari S, et al. A large screening of angiogenesis biomarkers and their association with neurological outcome after ischemic stroke. Atherosclerosis. 2011;216(1):205-11.
172. Shahulhameed S, Swain S, Jana S, Chhablani J, Ali MJ, Pappuru RR, et al. A Robust Model System for Retinal Hypoxia: Live Imaging of Calcium Dynamics and Gene Expression Studies in Primary Human Mixed Retinal Culture. Front Neurosci. 2019;13:1445.
173. Young TL, Matsuda T, Cepko CL. The noncoding RNA taurine upregulated gene 1 is required for differentiation of the murine retina. Curr Biol. 2005;15(6):501-12.
174. Michalik KM, You X, Manavski Y, Doddaballapur A, Zornig M, Braun T, et al. Long noncoding RNA MALAT1 regulates endothelial cell function and vessel growth. Circ Res. 2014;114(9):1389-97.
175. Zhang B, Arun G, Mao YS, Lazar Z, Hung G, Bhattacharjee G, et al. The lncRNA Malat1 is dispensable for mouse development but its transcription plays a cis-regulatory role in the adult. Cell Rep. 2012;2(1):111-23.
176. Zheng M, Zheng Y, Gao M, Ma H, Zhang X, Li Y, et al. Expression and clinical value of lncRNA MALAT1 and lncRNA ANRIL in glaucoma patients. Exp Ther Med. 2020;19(2):1329-35.
177. Wang J, Cao B, Zhao H, Gao Y, Luo Y, Chen Y, et al. Long noncoding RNA H19 prevents neurogenesis in ischemic stroke through p53/Notch1 pathway. Brain Res Bull. 2019;150:111-7.
178. Cui C, Li Z, Wu D. The long non-coding RNA H19 induces hypoxia/reoxygenation injury by up-regulating autophagy in the hepatoma carcinoma cells. Biol Res. 2019;52(1):32.
179. Gong LC, Xu HM, Guo GL, Zhang T, Shi JW, Chang C. Long Non-Coding RNA H19 Protects H9c2 Cells against Hypoxia-Induced Injury by Targeting MicroRNA-139. Cell Physiol Biochem. 2017;44(3):857-69.
180. Yuan L, Yu L, Zhang J, Zhou Z, Li C, Zhou B, et al. Long noncoding RNA H19 protects H9c2 cells against hypoxiainduced injury by activating the PI3K/AKT and ERK/p38 pathways. Mol Med Rep. 2020;21(4):1709-16.
181. Wang J, Cao B, Han D, Sun M, Feng J. Long Non-coding RNA H19 Induces Cerebral Ischemia Reperfusion Injury via Activation of Autophagy. Aging Dis. 2017;8(1):71-84.
182. Fang H, Li HF, Pan Q, Yang M, Zhang FX, Wang RR, et al. Long Noncoding RNA H19 Overexpression Protects against Hypoxic-Ischemic Brain Damage by Inhibiting miR-107 and Up-Regulating Vascular Endothelial Growth Factor. Am J Pathol. 2021;191(3):503-14.
183. Benterud T, Ystgaard MB, Manueldas S, Pankratov L, Alfaro-Cervello C, Florholmen G, et al. N-Acetylcysteine Amide Exerts Possible Neuroprotective Effects in Newborn Pigs after Perinatal Asphyxia. Neonatology. 2017;111(1):12-21.
184. de Lange C, Solberg R, Holtedahl JE, Tulipan A, Barlinn J, Trigg W, et al. Dynamic TSPO-PET for assessing early effects of cerebral hypoxia and resuscitation in new born pigs. Nucl Med Biol. 2018;66:49-57.

185. Huun MU, Garberg H, Loberg EM, Escobar J, Martinez-Orgado J, Saugstad OD, et al. DHA and therapeutic hypothermia in a short-term follow-up piglet model of hypoxia-ischemia: Effects on H+MRS biomarkers. PLoS One. 2018;13(8):e0201895.
186. Charan J, Kantharia ND. How to calculate sample size in animal studies? J Pharmacol Pharmacother. 2013;4(4):303-6.
187. Bustin SA, Benes V, Garson JA, Hellemans J, Huggett J, Kubista M, et al. The MIQE guidelines: minimum information for publication of quantitative real-time PCR experiments. Clin Chem. 2009;55(4):611-22.
188. Nygard AB, Jorgensen CB, Cirera S, Fredholm M. Selection of reference genes for gene expression studies in pig tissues using SYBR green qPCR. BMC Mol Biol. 2007;8:67.
189. Erkens T, Van Poucke M, Vandesompele J, Goossens K, Van Zeveren A, Peelman LJ. Development of a new set of reference genes for normalization of real-time RT-PCR data of porcine backfat and longissimus dorsi muscle, and evaluation with PPARGC1A. BMC Biotechnol. 2006;6:41.
190. Racki N, Dreo T, Gutierrez-Aguirre I, Blejec A, Ravnikar M. Reverse transcriptase droplet digital PCR shows high resilience to PCR inhibitors from plant, soil and water samples. Plant Methods. 2014;10(1):42.
191. Suslov O, Steindler DA. PCR inhibition by reverse transcriptase leads to an overestimation of amplification efficiency. Nucleic Acids Res. 2005;33(20):e181.

Appendix A: Detailed protocols

A1: Isolation of RNA from Animal Tissue – E.Z.N.A Total RNA kit (Omega Bio-tek, Inc)

1. 10-30 mg of tissue was transferred to a 2 ml Precellys homogenization tube (Bertin Technologies)
2. 1 ml RNA-Solv Reagent was added to the Precellys tube and homogenized using Minilys (Bertin Technologies) at max speed for 20 seconds
3. Samples incubated at room temperature for 5 minutes
4. 200 µl chloroform was added, and the samples was vortexed thoroughly for 20 seconds
5. Samples incubated at room temperature for 2-3 minutes
6. Samples were centrifuge at maximum speed (12 000xg) at 4°C for 15 minutes to separate the aqueous and organic phase
7. The upper aqueous phase (500 µl) was transferred into a new 1,5 ml tube
8. 500 µl of 70% ethanol was added and vortexed to mix thoroughly
9. 700 µl sample was transferred to HiBind RNA column
10. Samples were centrifuged at 10 000xg for 1 minute
11. The filtrate was discarded and the collection tube was reused
12. 250 µl RNA Wash Buffer I was added to the HiBind Mini Column
13. Samples were centrifuged at 10 000xg for 1 minute
14. DNase I was made quickly in room temperature (Table A-1). Samples were not vortexed, but mixed gently by reverting the tube.

Table A-1. Components for DNase I Digestion used for RNA isolation from animal tissue.

DNase I Digestion	**Volume per sample (µl)**
E.Z.N.A DNase I Digestion Buffer	73,5
E.Z.N.A RNase-free DNase I	1,5
Total volume	75,0

15. 75 µl of DNase I Digestion was added onto the membrane of the column and incubated for 15 minutes
16. 250 µl RNA Wash Buffer I was added
17. Incubated for 2 minutes
18. Centrifuged at 10 000xg for 1 minute

19. Filtrate was discarded and the collection tube was reused
20. 500 µl RNA Wash Buffer II was added
21. Centrifuged at 10 000xg for 1 minute
22. Filtrate was discarded and the collection tube was reused
23. Steps 20-22 was repeated
24. Empty HiBind RNA Mini Column was centrifuged at maximum speed (12 000xg) for 2 minutes to dry the column to remove trace of ethanol that may interfere downstream applications
25. HiBind column was placed in a clean 1,5 ml Eppendorf tube
26. 40 µl of nuclease free water (NFW) was added to the HiBind column and samples were centrifuge at maximum speed (12 000xg) for 2 minutes. Eluted RNA was measured using Nanodrop® ND-1000 Spectrophotometer (NanoDrop Technologies, Inc.) and stored at -80°C until further use.

A2: RNA ScreenTape Assay for TapeStation Systems (Agilent)

1. RNA sample buffer (Agilent) was equilibrated at room temperature for 30 minutes, and RNA samples were thawed on ice
2. RNA ScreenTape was inserted to the ScreenTape instrument (Agilent)
3. Reagents and samples were vortexed and then spun down
4. 5 ul RNA sample buffer and 1 ul RNA sample was transferred to a 96-well plate (Agilent)
5. Caps were applied to tube strips
6. Samples were spun down for 1 minute
7. Samples were heated at 72°C for 3 minutes, and then placed on ice for 2 minutes before the sample was spun down for 1 min
8. Samples were loaded into the TapeStation instrument, and caps were removed before the analysis started

Appendix B: Primer sequences

Table B-0-1. Primer sequences of endogenous controls, mRNAs, and lncRNAs used for qPCR and ddPCR for reference with their melting point.

Working name	Gene name	(F/R)	Primer sequence (5´-3´)	Tm°C
Endogenous controls				
RLP0	Ribosomal protein, large, P0	F	ACAATGTGGGCTCCAAGCA	58,1
		R	CATCAGCACCACGGCTTTC	57,8
TBP	TATA-box binding Protein	F	GACCATTGCACTTCGTGCC	58,7
		R	CTGGACTGTTCTTCACTCTTGGC	59,0
mRNAs				
VEGFA	Vascular Endothelial Growth Factor A	F	ACGAAGTGGTGAAGTTCATGGA	57,5
		R	CACCAGGGTCTCGATTGGA	56,9
BDNF	Brain-derived neurotrophic factor	F	GTGACTGAAAAGTTCCACCAGGT	58,4
		R	CCTCGGACGTTGGCTTCTT	58,3
HIF1α	Hypoxia-inducible factor 1 subunit α	F	TGGCAGCAATGACACAGAAAC	58,4
		R	TGATTGAGTGCAGGGTCAGC	58,4
p53	tumor suppressor gene p53	F	AGCACTAAGCGAGCACTGCC	59,4
		R	CAGCTCTCGGAACATCTCGAA	59,2
TNFα	tumor necrosis factor α	F	CAAGGACTCAGATCATCGTCTCA	57,1
		R	CATACCCACTCGCCATTGGA	57,8
lncRNAs				
BDNF-AS	Brain-derived neurotrophic factor antisense	F	GGACAGAACAGTGGACTCTCAGACT	60,6
		R	CCCAGGTGTATGTTCTGCATCA	58,0
H19	Imprinted Maternally Expressed Transcript	F	CCTGAACACTCTCGGCTGG	58,0
		R	GCTGGGTAGCACCATCTCTTG	58,4
MALAT1	Metastasis Associated Lung Adenocarcinoma Transcript 1	F	CTGAAGCCTTTAGTCTTTTCCAGATG	59,8
		R	TTACTGGGTCTGGCTTCTCTGG	59,4
ANRIL	The antisense non-coding RNA in the INK4 locus	F	TGCTCTATCCGCCAATCAGG	59,8
		R	ACTCAGTGTCCAGATGTCGCAG	59,0
TUG1	Taurine Upregulated gene 1	F	CCCTGTCACTCCCAGATGTAGC	59,6
		R	AGCCAGGCTATGATCTGGAAGA	58,9
PANDA	P21 Associated ncRNA DNA damage Activated	F	GCTCTGATGTTTTCTTTGCCTTC	58,2
		R	ACATGACGAAGGGCCTTGTT	58,1

Abbreviations: BDNF, Brain-derived neurotrophic factor; HIF1α, Hypoxia-inducible factor α; p53, Tumor suppressor gene p53; BDNF-AS, Brain-derived neurotrophic factor antisense; H19, H19 Imprinted Maternally Expressed Transcript; MALAT1, metastasis-associated lung adenocarcinoma transcript 1; ANRIL, Antisense Noncoding RNA in the INK4 Locus; TUG1, Taurine Upregulated gene 1; PANDA, p21-associated ncRNA DNA damage-activated. F/R, Forward/Reverse primer; F, Forward; R, Reverse; Tm, melting temperature

Appendix C: Products and manufacturers

Table C-0-1. List of products used in the study with the respective manufacturer and country.

Product	Manufacturer	Country
2x QX200 ddPCR EvaGreen Supermix	BioRad	USA
4200 TapeStation System	Agilent Technologies, Inc.	USA
96-Well ddPCR Plate, Semi skirted	BioRad	USA
AB-1170 Optically Clear Adhesive Seal Sheets	Thermo Scientific	USA
Absolute ethanol (100%)	VWR Chemicals	France
Biofuge fresco	Kendro Laboratory Products	Germany
Chloroform	Sigma Aldrich	USA
DG8™ Cartridge	BioRad	USA
Droplet Generation Oil for EvaGreen®	BioRad	USA
Droplet Generator DG8™ Gasket	BioRad	USA
E.Z.N.A® Total RNA kit II – Animal Tissue Protocol	Omega Bio-tek, Inc	USA
Gene specific primers	Thermo Scientific	UK
High Capacity cDNA reverse transcription kit	Applied Biosystems by Thermo Fisher Scientific	Lithuania
MicroAMP® Optical 96-Well Reaction Plate	Applied Biosystems by life technologies	China
Minilys	Bertin Technologies	France
Nanodrop® ND-1000 Spectrophotometer	NanoDrop Technologies, Inc.	USA
Nuclease free water	Ambion	USA
Pierceable Foil Heat Seal	BioRad	USA
PowerSYBR® Green PCR Master Mix	Applied Biosystems by Thermo Fisher Scientific	UK
Precellys Lysing Kit, Tissue homogenizing Ckmix	Bertin Technologies	France
PTC-100™ Programmable Thermo Controller	MJ Research, Inc.	USA
PX1 plate sealer	BioRad	USA
QX200 Droplet Reader	BioRad	Singapore
QX200™ Droplet Generator	BioRad	Singapore
RNA ScreenTape Assay	Agilent Technologies, Inc.	Germany
RNA ScreenTape Sample Buffer	Agilent Technologies, Inc.	Germany
RNA Solv® reagent	Omega Bio-tek, Inc	USA
RNase free DNase I set	Omega Bio-tek, Inc	USA
Veriti™ 96-well Thermal Cycler	Applied Biosystems	Singapore
ViiA 7 Real-Time system	Applied Biosystems by life technologies	USA
VWR® Microcentrifuge Tubes	avantor™ delivered by VWR™	

Appendix D: Additional results and raw data

D1: QQ-plots displaying distribution of mRNA and RNA expression

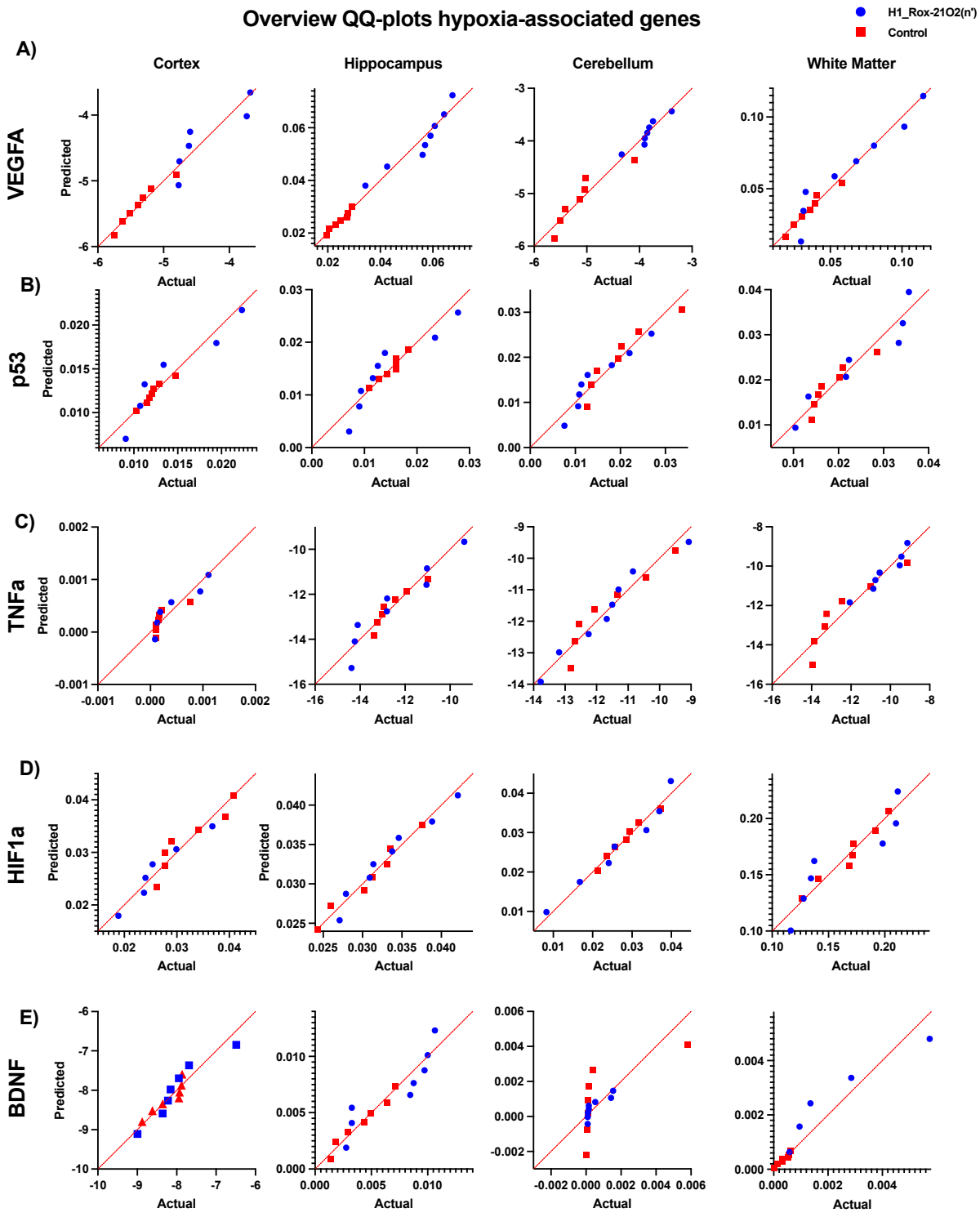

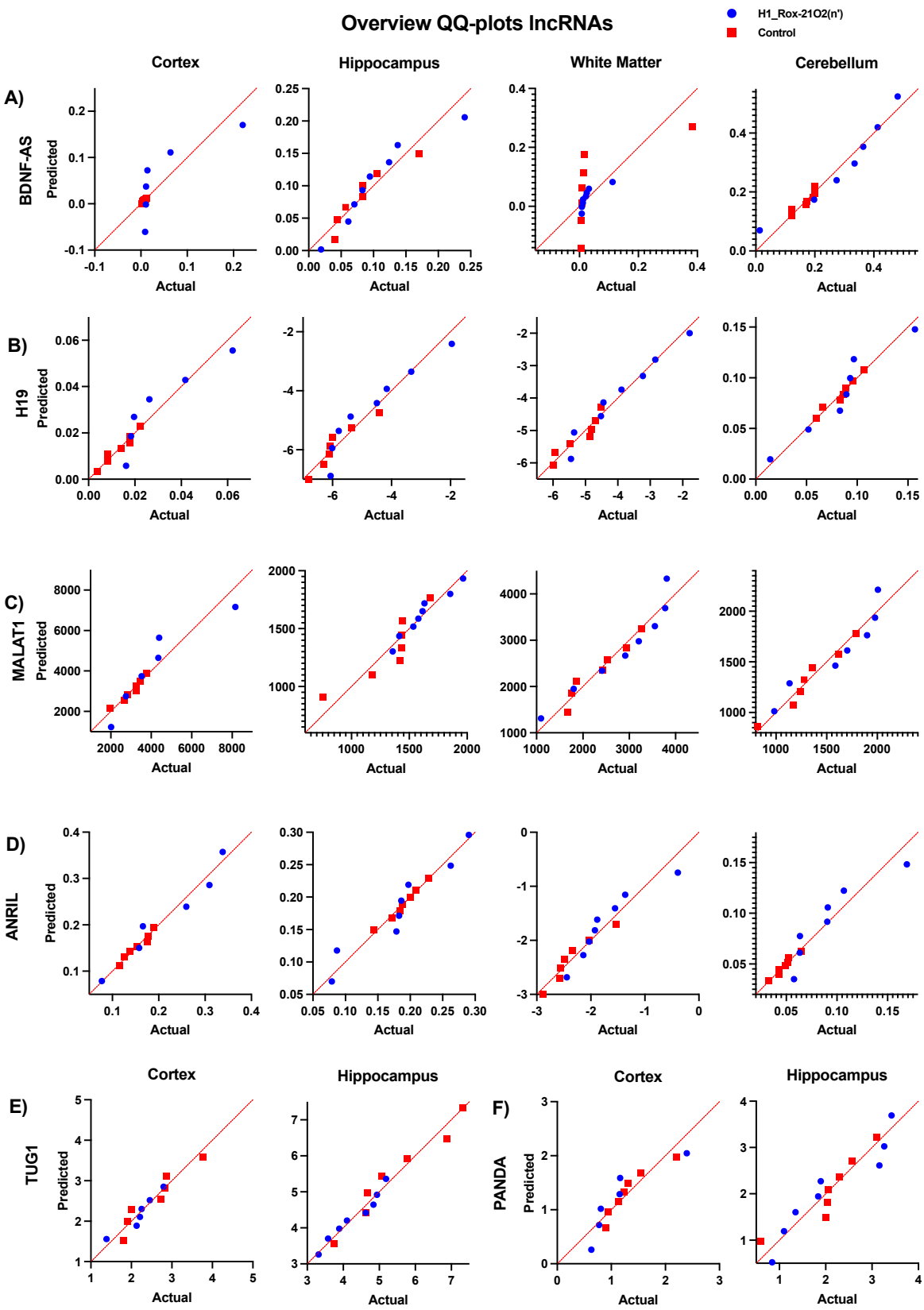
Overview QQ-plots lncRNAs
H1_Rox-21O2(n')
Control
Cortex
Hippocampus
White Matter
Cerebellum
A)
BDNF-AS
B)
H19
C)
MALAT1
D)
ANRIL
E)
TUG1
F)
PANDA
Predicted
Actual

D2: Nanodrop values from RNA quality measurements

Table D-2-0-1. NanoDrop values measured in samples from the cortex of piglets exposed to hypoxia, hyperoxic reoxygenation and control group.

Cortex				
Treatment group	Piglet	ng/ul	260/280	260/230
H1_Rox-21O2(n')	P01	310	2,03	1,84
	P08	193	2,10	2,44
	P10	199	2,07	2,13
	P20	274	2,09	1,74
	P31	221	2,02	2,02
	P39	164	1,96	1,81
H2_Rox-100O2(30')	P03	354	2,08	2,21
	P09	197	2,08	2,21
	P11	166	2,10	2,21
	P16	185	2,05	2,01
	P17	118	2,08	0,59
	P19	197	2,02	2,01
	P32	232	2,04	2,07
	P40	265	2,05	2,13
H3_Rox-100O2(3')	P22	236	2,06	2,03
	P23	267	2,06	2,13
	P26	284	2,07	2,06
	P27	122	2,02	1,89
	P30	179	2,03	2,07
	P33	199	2,02	1,98
	P36	313	2,04	1,92
	P38	226	2,02	1,97
Control	P02	255	2,08	2,25
	P05	246	2,12	2,37
	P07	432	2,09	2,11
	P12	237	2,08	1,96
	P21	251	2,11	2,50
	P24	257	2,04	2,14
	P25	454	1,98	1,85

Table D-0-2-2. NanoDrop values measured in samples from the hippocampus, white matter and cerebellum of piglets exposed to hypoxia and the control group.

		Hippocampus			White Matter			Cerebellum		
Treatment group	Piglet	ng/ul	260/280	260/230	ng/ul	260/280	260/230	ng/ul	260/280	260/230
H1_Rox-21O2(n')	P01	209	2,10	1,76	164	2,13	2,43	342	1,90	2,27
	P08	334	2,00	2,03	225	2,12	2,37	270	2,02	2,20
	P10	225	2,09	2,35	83	2,06	2,13	381	2,03	2,10
	P13	74	2,05	2,11	231	2,07	2,26	229	2,02	2,18
	P20	204	2,10	1,53	110	2,09	1,12	N/A	N/A	N/A
	P31	146	2,05	2,25	268	2,07	2,22	172	2,09	2,17
	P35	130	2,07	2,51	69	2,07	0,89	241	2,12	1,73
	P39	207	2,05	2,40	146	2,09	1,19	166	2,13	1,15
Control	P02	180	1,99	2,00	83	2,14	2,56	453	1,93	2,21
	P05	205	2,00	1,89	262	2,13	2,27	301	1,95	2,13
	P07	243	2,08	2,43	193	2,14	2,37	303	1,94	2,29
	P12	128	2,01	2,16	185	2,12	2,41	348	2,04	1,94
	P21	151	2,03	2,10	184	2,09	1,68	310	2,06	1,55
	P24	130	2,08	2,33	107	2,08	1,45	579	2,04	2,19
	P25	240	2,02	1,74	175	2,08	1,18	504	2,14	2,35

D3: P-values and statistical tests used for mRNA and RNA expression

Table D-3-1. P-values and descriptive statistics from qPCR

Hypoxia-regulated genes	Tissue	H1_Rox-21O2(n')				Control				P-value		Remarks
		Mean	Median	SD	n	Mean	Median	SD	n			
	Cx	0,051	0,041	0,01952	6	0,0247	0,0238	0,0058	7	0,0021	**	3
	Hc	0,055	0,058	0,0111	8	0,028	0,025	0,007	7	<0,0001	****	2
	Wm	0,064	0,061	0,0331	8	0,041	0,036	0,013	7	0,0514	ns	2
VEGFA	Cb	-3,847	-3,851	0,2797	7	-5,116	-5,136	0,510	7	<0,0001	****	1, 2,
	Cx	0,002	0,001	0,0022	6	0,000	0,000	0,000	7	0,014	**	3
	Hc	0,007	0,009	0,0034	8	0,004	0,004	0,002	7	0,0939	ns	3
	Wm	0,001	0,000	0,0006	8	0,001	0,000	0,002	7	0,3357	ns	3
BDNF	Cb	-7,977	-8,153	0,7725	7	-8,207	-7,940	0,410	7	0,4999	ns	1, 2,
	Cx	0,026	0,025	0,006155	6	0,032	0,029	0,006	7	0,1214	ns	2
	Hc	0,033	0,033	0,0052	8	0,031	0,031	0,005	7	0,3492	ns	2
	Wm	0,026	0,026	0,0113	7	0,028	0,029	0,005	7	0,7143	ns	2
HIF1a	Cb	0,162	0,137	0,0422	7	0,168	0,171	0,027	7	0,9015	ns	3
	Cx	0,014	0,012	0,0053	6	0,012	0,012	0,001	7	0,3207	ns	2
	Hc	0,014	0,013	0,0074	8	0,015	0,016	0,002	7	0,8465	ns	2
	Wm	0,015	0,012	0,0066	8	0,020	0,020	0,007	7	0,2125	ns	2
p53	Cb	0,024	0,022	0,01027	7	0,019	0,016	0,005	7	0,206	ns	2
	Cx	0,0005	0,0003	0,0004	6	0,000	0,000	0,000	7	0,366	ns	3
	Hc	-12,47	-12,81	1,8250	8	-12,560	-12,930	0,855	7	0,9056	ns	1, 2,
	Wm	-11,70	-11,59	1,4440	8	-11,620	-12,060	1,266	7	0,9136	ns	1, 2,
TNFa	Cb	-10,33	-10,54	1,0310	7	-12,420	-13,250	1,773	7	0,0194	*	1, 2,

Abbreviations: BDNF, Brain-derived neurotrophic factor; HIF1α, Hypoxia-inducible factor α; p53, Tumor suppressor gene p53; BDNF-AS. Cx, Cortex; Hc, Hippocampus; Wm, White matter; Cb, Cerebellum; SD, Standard deviation.Remarks: 1: Log2 transformation;, 2: Unpaired t-test; 3. Mann Whitney test

Table D-3-2. P-values and descriptive statistics from qPCR

Hypoxia-associated lncRNAs	Tissue	H1_Rox-21O2(n')				Control				P-value		Remarks
		Mean	Median	STDEV	n	Mean	Median	STDEV	n			
	Cx	0,055	0,013	0,084	6	0,006	0,006	0,004	7	0,0140	*	3
	Hc	0,104	0,089	0,066	8	0,083	0,083	0,045	7	0,5073		2
	Wm	0,029	0,017	0,035	8	0,063	0,008	0,141	7	0,1893		3
BDNF-AS	Cb	0,297	0,335	0,155	7	0,169	0,172	0,034	7	0,0538		2
	Cx	0,031	0,023	0,018	6	0,013	0,014	0,007	7	0,0348	*	2
	Hc	-4,648	-4,940	1,460	8	-5,869	-6,090	0,769	7	0,0695		1, 2
	Wm	-3,937	-4,165	1,264	8	-5,181	-4,872	0,609	7	0,0341	*	1, 2
H19	Cb	0,084	0,089	0,044	7	0,084	0,087	0,016	7	0,9870		2
	Cx	4197	3936	2145	6	3030	3247	593	7	0,1927		2
	Hc	1618	1596	205	8	1334	1430	293	7	0,0465	*	2
	Wm	2821	3060	984	8	2348	2425	619	7	0,2939		2
MALAT1	Cb	1613	1703	409	7	1324	1278	313	7	0,1645		2
	Cx	0,218	0,213	0,101	6	0,153	0,153	0,028	7	0,1297		2
	Hc	0,183	0,185	0,074	8	0,189	0,188	0,027	7	0,8336		2
	Wm	-1,715	-1,902	0,631	8	-2,346	-2,493	0,441	7	0,0454	*	1, 2
ANRIL	Cb	0,092	0,090	0,039	7	0,048	0,050	0,010	7	0,0136	*	2
	Cx	2,204	2,231	0,468	6	2,552	2,727	0,705	7	0,3262		2
TUG1	Hc	4,310	4,365	0,685	8	5,443	5,064	1,289	7	0,0494	*	2
	Cx	2,456	1,986	1,404	6	2,619	2,356	0,947	7	0,2949		3
PANDA	Hc	2,108	1,866	1,033	8	2,094	2,051	0,766	7	0,9765		1, 2

MALAT1; ANRIL; TUG1; PANDA: HC) or median ± IQ-range (PANDA: CX). P<.05=. MALAT1, metastasis associated lung adenocarcinoma transcript 1; ANRIL, Antisense Noncoding RNA in the INK4 Locus; TUG1, Taurine Upregulated gene 1; PANDA, P21-associated ncRNA DNA damage-activated. Remarks: 1: Log2 transformation;, 2: Unpaired t-test; 3. Mann Whitney test*

Table D-3-3. P-values and descriptive statistics from qPCR

lncRNA	Treatment group		Tissue	Kruskal Wallis			Dunn´s Multiple comparisons test				
				P-value		n	Mean rank diff.	n1	n2	Adjusted P-value	
BDNF-AS	H2_Rox-100O2(30')	H3_Rox-100O2(3')	Cx	0,005	**	29	0,125	8	8	>0,9999	ns
	H2_Rox-100O2(30')	H1_Rox-21O2(n')					4,25	8	6	>0,9999	ns
	H2_Rox-100O2(30')	Control					13,8	8	7	0,0103	*
	H3_Rox-100O2(3')	H1_Rox-21O2(n')					4,13	8	6	>0,9999	ns
	H3_Rox-100O2(3')	Control					13,7	8	7	0,0113	*
	H1_Rox-21O2(n')	Control					9,57	6	7	0,2600	ns
H19	H2_Rox-100O2(30')	H3_Rox-100O2(3')	Cx	0,043	*	29	-2,38	8	8	>0,9999	ns
	H2_Rox-100O2(30')	H1_Rox-21O2(n')					-1,42	8	6	>0,9999	ns
	H2_Rox-100O2(30')	Control					9,11	8	7	0,2326	ns
	H3_Rox-100O2(3')	H1_Rox-21O2(n')					0,958	8	6	>0,9999	ns
	H3_Rox-100O2(3')	Control					11,5	8	7	0,0550	ns
	H1_Rox-21O2(n')	Control					10,5	6	7	0,1579	ns
MALAT1	H1_Rox-21O2(n')	H2_Rox-100O2(30')	Cx	0,215	ns	29	9,00	6	8	0,3020	ns
	H1_Rox-21O2(n')	H3_Rox-100O2(3')					3,75	6	8	>0,9999	ns
	H1_Rox-21O2(n')	Control					2,00	6	7	>0,9999	ns
	H2_Rox-100O2(30')	H3_Rox-100O2(3')					-5,25	8	8	>0,9999	ns
	H2_Rox-100O2(30')	Control					-7,00	8	7	0,6731	ns
	H3_Rox-100O2(3')	Control					-1,75	8	7	>0,9999	ns
ANRIL	H1_Rox-21O2(n')	H2_Rox-100O2(30')	Cx	0,266	ns	29	7,83	6	8	0,5309	ns
	H1_Rox-21O2(n')	H3_Rox-100O2(3')					0,83	6	8	>0,9999	ns
	H1_Rox-21O2(n')	Control					1,83	6	7	>0,9999	ns
	H2_Rox-100O2(30')	H3_Rox-100O2(3')					-7,00	8	8	0,6008	ns
	H2_Rox-100O2(30')	Control					-6,00	8	7	>0,9999	ns
	H3_Rox-100O2(3')	Control					1,00	8	7	>0,9999	ns

Abbreviations: Cx, Cortex; Brain-derived neurotrophic factor antisense; H19, H19 Imprinted Maternally Expressed Transcript; MALAT1, metastasis-associated lung adenocarcinoma transcript 1; ANRIL, Antisense Noncoding RNA in the INK4 Locus.

Table D-3-4. P-values and descriptive statistics from qPCR

lncRNA	Treatmentgroup		Tissue	Kruskal Wallis P-value		n	Dunn´s Multiple comparisons test Mean rank diff.	n1	n2	Adjusted P-value	
BDNF-AS	H2_Rox-100O2(30')	H3_Rox-100O2(3')	Cx	0,004	**	29	0,13	8	8	>0,9999	ns
	H2_Rox-100O2(30')	H1_Rox-21O2(n')					4,25	8	6	>0,9999	ns
	H2_Rox-100O2(30')	Control					13,82	8	7	0,0053	**
	H3_Rox-100O2(3')	H1_Rox-21O2(n')					4,13	8	6	>0,9999	ns
	H3_Rox-100O2(3')	Control					13,70	8	7	0,0206	*
	H1_Rox-21O2(n')	Control					9,57	6	7	0,0562	ns
				One-way ANOVA			**Mean diff**			**Tukey´s multiple comparisons test**	
H19	H2_Rox-100O2(30')	H3_Rox-100O2(3')	Cx	0,093	ns	29	-0,79	8	8	0,8603	ns
	H2_Rox-100O2(30')	H1_Rox-21O2(n')					-0,50	8	6	0,9669	ns
	H2_Rox-100O2(30')	Control					1,81	8	7	0,3280	ns
	H3_Rox-100O2(3')	H1_Rox-21O2(n')					0,29	8	6	0,9932	ns
	H3_Rox-100O2(3')	Control					2,61	8	7	0,0856	ns
	H1_Rox-21O2(n')	Control					2,31	6	7	0,1937	ns

Abbreviations: Cx, Cortex; Brain-derived neurotrophic factor antisense; H19, H19 Imprinted Maternally Expressed Transcript.

D5: Gene expression measurements

Table D-5-1. ΔCt Mean values of MRNA expression in piglets exposed to hypoxia-normoxic reoxygenation in various regions of the piglet brain,, obtained from gene expression analysis by qPCR.

	CORTEX					HIPPOCAMPUS				
	VEGFA	p53	TNFα	HIFα	BDNF	VEGFA	p53	TNFα	HIFα	BDNF
P01	3,682	5,687	9,820	5,396	8,45	4,081	5,415	11,05	5,016	6,836
P08	4,771	6,544	12,89	5,064	10,73	3,959	6,166	12,80	4,888	8,503
P10	4,597	5,485	10,04	5,300	10,04	4,157	5,168	9,371	4,571	6,644
P20	4,616	6,785	12,39	5,379	10,94	4,553	6,428	11,03	5,164	6,554
P31	4,759	6,476	13,45	5,726	9,527	4,864	6,738	14,11	5,206	6,685
P39	3,736	6,223	11,29	4,766	7,444	4,132	7,138	12,81	4,994	6,887
P02	5,632	6,379	13,18	5,109	10,64	5,678	6,529	13,38	5,363	7,129
P05	5,317	6,439	13,12	4,616	15,09	5,102	6,287	12,94	4,999	7,843
P07	4,800	6,275	13,12	5,257	10,84	5,182	5,957	13,25	5,266	7,291
P12	5,518	6,406	12,75	5,173	11,60	5,596	6,126	13,03	4,735	8,406
P21	5,748	6,355	12,58	4,674	11,55	5,330	5,963	11,93	4,917	7,667
P24	5,392	6,607	12,15	5,168	10,80	5,434	5,958	12,45	5,046	9,505
P25	5,193	6,086	10,35	4,875	12,78	5,192	5,765	10,98	4,897	9,128
	WHITE MATTER					CEREBELLUM				
	VEGFA	p53	TNFα	HIFα	BDNF	VEGFA	p53	TNFα	HIFα	BDNF
P01	3,299	6,459	11,30	N/A	12,58	3,851	4,91	9,44	2,86	8,22
P08	4,929	5,787	11,50	4,649	13,14	4,336	5,53	10,54	2,25	7,94
P10	3,635	5,505	9,075	4,759	10,88	3,900	4,81	9,52	2,34	6,49
P20	5,081	5,216	10,84	5,289	13,43	N/A	N/A	N/A	N/A	N/A
P31	4,237	6,555	13,19	6,916	12,62	3,740	5,483	10,86	2,241	8,995
P39	3,122	6,296	12,25	4,893	9,450	3,387	4,867	9,136	3,101	7,686
P02	5,353	5,673	12,54	5,280	13,99	5,618	5,631	13,88	2,567	8,875
P05	4,626	6,205	12,68	4,747	11,26	5,025	6,143	13,93	2,382	7,925
P07	5,042	6,078	12,83	5,405	13,43	5,040	6,003	13,31	2,299	7,861
P12	5,737	6,315	12,06	5,087	12,66	5,136	6,096	13,24	2,540	7,880
P21	4,108	5,626	10,43	5,128	7,431	4,085	5,131	9,116	2,546	8,356
P24	4,660	5,380	11,33	5,559	13,33	5,406	5,937	12,48	2,979	8,614

Table D-5-2. ΔCt mean values of lncRNA expression in piglets exposed to hypoxia-normoxic reoxygenation in various regions of the piglet brain, obtained from gene expression analysis by qPCR.

Normoxic reoxygenation

	CORTEX					
	BDNF-AS	H19	MALAT	ANRIL	TUG1	PANDA
P01	3,97	4,582	-10,979	2,665	-0,470	-1,165
P08	6,80	5,771	-11,425	3,694	-1,170	-0,631
P10	2,19	4,008	-12,087	1,564	-1,296	-2,396
P20	6,49	5,671	-11,782	2,591	-1,144	-0,806
P31	6,53	5,254	-12,993	1,945	-1,089	-1,153
P39	6,16	5,947	-12,099	1,693	-1,483	-0,774
P02	7,33	6,137	-10,951	2,859	-0,997	-0,941
P05	9,01	8,066	-11,877	3,122	-1,913	-0,894
P07	7,36	6,903	-11,665	2,494	-0,846	-1,136
P12	7,91	6,912	-11,673	2,987	-0,922	-1,311
P21	6,62	5,819	-11,458	2,515	-1,494	-1,542
P24	6,28	5,826	-11,386	2,705	-1,448	-1,236
P25	8,12	5,479	-11,761	2,406	-1,519	-2,205
	HIPPOCAMPUS					
P01	2,863	3,330	-10,465	2,452	-1,961	-0,843
P08	3,405	6,061	-10,584	1,930	-2,274	-3,157
P10	4,034	1,957	-10,671	1,785	-2,304	-3,264
P20	2,055	4,159	-10,405	2,485	-2,210	-1,838
P31	3,826	5,385	-10,856	2,425	-2,376	-3,420
P39	5,719	5,788	-10,624	2,343	-1,840	-1,349
P02	2,552	6,102	-9,562	2,323	-1,909	-2,296
P05	3,244	4,419	-10,482	2,545	-2,340	-0,599
P07	3,585	6,814	-10,487	2,129	-2,209	-2,010
P12	4,131	6,090	-10,712	2,410	-2,528	-2,051
P21	3,591	6,296	-10,493	2,797	-2,783	-2,034
P24	4,620	5,993	-10,471	2,259	-2,873	-2,565
P25	4,502	5,368	-10,203	2,441	-2,227	-3,101

Table D-5-3. ΔCt mean values of lncRNA expression in piglets exposed to hypoxia-normoxic reoxygenation in various regions of the piglet brain, obtained from gene expression analysis by qPCR.

	NORMOXIC REOXYGENATION							
	WHITE MATTER				CEREBELLUM			
	BDNF-AS	H19	MALAT	ANRIL	BDNF-AS	H19	MALAT	ANRIL
P01	6,924	3,226	-10,10	2,138	1,869	3,426	-10,15	3,467
P08	6,975	3,887	-11,24	2,444	2,336	3,591	-10,73	3,979
P10	4,965	1,785	-10,81	1,880	1,056	3,370	-10,63	3,978
P20	6,427	5,347	-11,65	2,028	N/A	N/A	N/A	N/A
P31	5,330	2,845	-11,79	0,389	6,259	6,134	-9,94	3,227
P39	6,330	4,443	-11,88	1,363	1,579	2,671	-10,95	2,564
P02	6,983	4,506	-10,70	2,493	3,041	3,386	-10,32	4,270
P05	5,835	5,930	-11,24	2,882	2,363	3,529	-10,66	4,949
P07	7,282	5,984	-10,77	2,582	2,553	3,915	-10,41	4,549
P12	7,390	5,476	-10,86	2,557	2,326	3,225	-10,80	4,540
P21	1,387	4,872	-11,31	2,344	2,538	4,066	-10,19	3,956
P24	6,101	4,682	-11,67	2,033	3,036	3,581	-9,68	4,254
P25	7,007	4,820	-11,52	1,533	2,324	3,497	-10,28	4,337

Table D-5-4. ΔCt mean values (qPCR) and Normalized expression (ddPCR) of lncRNA in piglets exposed to hyperoxic-normoxic reoxygenation in the cortex of the piglet brain.

Hyperoxic reoxygenation

	BDNF-AS	H19	TBP		H19			BDNF		
Piglet	ΔCт Mean	ΔCт Mean	Conc.	RQ	Conc.	RQ	NE	Conc	RQ	NE
P03	5,611	6,376	226,1	0,829	3,178	0,9238	1,114	2,276	2,741	3,306
P09	0,549	5,825	276,3	1,013	3,923	1,1404	1,125	73,54	88,57	87,41
P11	2,810	3,943	234,3	0,859	14,88	4,3256	5,034	15,46	18,62	21,67
P16	6,367	6,101	134,7	0,494	2,323	0,6753	1,368	1,084	1,306	2,644
P17	5,560	5,728	179,9	0,660	3,439	0,9995	1,515	1,849	2,227	3,377
P19	5,567	5,027	219,7	0,806	7,520	2,1857	2,713	1,972	2,375	2,949
P32	4,586	4,053	361,1	1,324	19,40	5,6374	4,258	5,851	7,047	5,322
P40	4,150	3,368	169,9	0,623	13,78	4,0057	6,429	4,312	5,193	8,334
P22	4,922	5,976	55,28	0,203	0,846	0,2459	1,213	0,890	1,072	5,291
P23	4,399	7,460	124,4	0,456	0,658	0,1913	0,419	2,388	2,875	6,305
P26	4,664	3,834	229,4	0,841	16,76	4,8703	5,790	3,450	4,154	4,939
P27	5,714	4,921	164,3	0,602	5,720	1,6626	2,760	0,984	1,186	1,968
P30	6,662	4,247	85,69	0,314	5,597	1,6267	5,178	0,289	0,348	1,107
P33	5,260	4,408	274,1	1,005	14,02	4,0760	4,055	2,583	3,111	3,095
P36	1,433	3,365	251,2	0,921	22,14	6,4353	6,988	32,58	39,23	42,60
P38	2,018	4,303	240,2	0,881	10,60	3,0810	3,498	20,71	24,94	28,32
P01	3,952	4,702	229,2	0,840	10,17	2,9550	3,516	6,081	7,324	8,714
P08	6,444	5,332	270,4	0,991	5,820	1,6915	1,706	1,028	1,239	1,249
P10	1,926	3,341	232,3	0,852	24,66	7,1663	8,414	23,74	28,59	33,57
P20	6,363	5,880	281,1	1,031	4,689	1,3627	1,322	1,650	1,987	1,928
P31	6,030	4,454	23,79	0,087	1,180	0,3429	3,931	0,468	0,563	6,457
P39	6,142	5,821	133,5	0,490	3,018	0,8771	1,791	1,083	1,305	2,665
P02	7,352	6,812	280,2	1,027	3,463	1,0067	0,980	1,040	1,253	1,219
P05	9,070	7,399	315,3	1,156	1,751	0,5090	0,440	0,436	0,525	0,454
P07	7,300	7,732	361,7	1,326	2,287	0,6647	0,501	1,240	1,493	1,126
P12	7,512	5,561	250,7	0,919	4,930	1,4329	1,559	0,751	0,904	0,984
P21	6,345	6,225	269,9	0,990	3,780	1,0988	1,110	1,312	1,580	1,597
P24	5,930	6,254	228,5	0,838	3,833	1,1141	1,330	1,330	1,602	1,912
P25	7,835	5,340	227,3	0,833	5,759	1,6738	2,009	0,370	0,445	0,534

Abbreviations: TBP, TATA-Box binding protein; BDNF-AS, Brain derived neurotrophic factor antisense; H19, Imprinted Maternally Expressed Transcript. Conc, Copies/µl; RQ, relative quantity; NE, normalized relative expression.

D6: Background data from the piglet study

Pig	Weight	Sex	Hb start	Hb end	BE end Hypoxia	MABP end Hypoxia	MABP end
1	2025g	Female	7,9	7,4	-12,4	19,7	43
2	2190g	Male	6,9	7,8	-2,2	58	57
3	2230g	Male	8,4	7,6	-21,6	21	37
5	1920g	Female	8,1	7,5	6,7	1,7	59
6	1990g	Male	9,2	8	-6,4	-22	44
7	1965g	Female	8,7	8,2	5,3	60	48
8	1980g	Female	6,5	5	-11,7	32	32
9	2120g	Female	7,8	8,1	0,3	44,4	61
10	2165g	Male	7,5	6,6	-20,3	31,4	81
11	1900g	Male	6	4,3	-17	19,9	61
12	1980g	Male	8,3	8,1	0,5	53	70
13	1900g	Female	9,1	4,8	-20,7	31,7	29
14	2090g	Male	9,5	8,4	4,4	56	21
16	2020g	Male	7,6	7	-21,2	22,3	41
17	2020g	Male	9	8,4	-21,1	29,2	42
18	2085g	Female	9,1	7,5	-1,6	59	67
19	2065g	Female	8,9	8,1	-15,5	19,5	45
20	2050g	Female	8,8	8,1	-9,2	19,9	67
21	2020g	Female	7,7	7,7	-3,3	59	47
23	1960g	Female	7	5,7	-22,3	31,5	46,9
24	1805g	Male	6,9	6,2	0,7	54	54
25	1870g	Female	5,3	5,5	5,9	50	41
26	1910g	Female	6,1	4,8	-13,7	18,8	55
27	2050g	Male	5,7	5,5	-14,1	24,9	24,9
28	2050g	Male	6,4	6,6	-17,6	19,4	25,6
29	1930g	Female	8,4	7,3	-18,6	20,3	42,6
30	1940g	Male	6,6	6,7	-19,7	19,86	47,5
31	1890g	Female	6,8	6,1	-23,8	19,1	28,3
32	1995g	Female	7,4	6,8	-10,7	19,8	50,6
33	1910g	Female	6,5	6,4	-19,2	32	57
35	1830g	Male	7,5	5,7	-20	19,6	57
36	1950g	Male	7,2	5,8	-25,2	27,2	57
38	2085g	Male	6,3	5,2	-10,7	19,5	49,7
39	1950g	Male	9,2	6,2	-17,6	19,7	60,1
40	1975g	Male	5,2	5	-15,8	19,1	57,8
42	1870g	Female	8	8,2	-21,7	22,3	28,5